

Forschungszentrum Karlsruhe

in der Helmholtz-Gemeinschaft

Wissenschaftliche Berichte

FZKA 6894

**GAS CHROMATOGRAPHY
AT THE TRITIUM LABORATORY KARLSRUHE**

R. Lässer and S. Grünhagen

Hauptabteilung Versuchstechnik

Impressum der Print-Ausgabe:

**Als Manuskript gedruckt
Für diesen Bericht behalten wir uns alle Rechte vor**

**Forschungszentrum Karlsruhe GmbH
Postfach 3640, 76021 Karlsruhe**

**Mitglied der Hermann von Helmholtz-Gemeinschaft
Deutscher Forschungszentren (HGF)**

ISSN 0947-8620

GASCHROMATOGRAPHIE IM TRITIUMLABOR KARLSRUHE

ZUSAMMENFASSUNG

Die Kenntnis der genauen Zusammensetzung von Gasen in einer Prozessierungsanlage ist von fundamentaler Bedeutung für die Qualität und die Charakterisierung der erzeugten Produkte. In Tritiumprozessierungsanlagen ist die permanente Kontrolle der Gasgemische sogar noch wichtiger, da sich deren Zusammensetzung nicht nur allein auf Grund des radioaktiven Zerfalls des Tritium in Helium-3 verändert, sondern auch durch radiochemische Prozesse, die durch die beim Tritiumzerfall freiwerdende Energie induziert werden können. Thermodynamisch stabile Gasmoleküle können in Ionen, Radikale, Bruchstücke und angeregte Teilchen umgewandelt werden und als Endprodukt können neue Gase entstehen, die zu Anbeginn im Gasgemisch nicht vorhanden waren.

Unter den analytischen Methoden wie Massenspektrometrie, Gaschromatographie, Laser Raman Spektroskopie, Verwendung von Ionisationskammern, die auch im Tritiumlabor Karlsruhe (TLK) angewendet werden, spielt Gaschromatographie eine spezielle Rolle. Die wesentlichen Gründe hierfür sind die Einfachheit des gaschromatographischen Trennprozesses, der geringe Bedarf an Platz, die geringen Investitionskosten im Vergleich zu anderen Methoden, die geringe Störanfälligkeit der Apparatur, die einfache Analyse der Messdaten und die Tatsache, dass alle Gase von Interesse (bis auf Wasserdampf) mittels Gaschromatographie nachgewiesen werden können. Dies ist zum Beispiel nicht der Fall bei der Laser Raman Spektroskopie, denn einatomige Gase wie Edelgase können nicht charakterisiert werden und komplexere Moleküle wie höhere Kohlenwasserstoffe sind quantitative nur schwer zu erfassen, speziell wenn die drei Wasserstoffisotope präsent sind. Auch Analysen mittels Massenspektrometrie können nur mit größerem Aufwand durchgeführt werden, wenn verschiedene Kohlenwasserstoffe und Wasserstoffisotope im Gasgemisch vorliegen, da dann die Zuordnung der verschiedenen, zum Teil überlappenden Massen zu den Gasen oder den Crackingprodukten fragwürdig werden kann. Die Situation kann noch komplizierter werden, falls zusätzlich noch Trimere berücksichtigt werden müssen.

Drei spezielle, konventionelle Gaschromatographen sind gegenwärtig in ständiger Verwendung im TLK, zwei davon (GC1 and GC2) sind die Hauptkomponenten der Tritiummesstechnik (TMT), während der dritte Gaschromatograph (GC3) im wesentlichen die analytischen Aufgaben innerhalb des Experimentes CAPER übernimmt. Diese drei Gaschromatographen, ihre Fließbilder, die wesentlichen Bestandteile der Apparaturen, die ermittelten Gaschromatogramme sowie mögliche Verbesserungen werden im Detail präsentiert und diskutiert. Ein wesentlicher Nachteil der konventionellen Gaschromatographie liegt in den langen Retentionszeiten, die für die Trennung der Wasserstoffmoleküle erforderlich sind. Deshalb wurde die Mikrogaschromatographie weiter entwickelt. Durch die Verwendung von externen kapillaren Säulen, die gekühlt werden können, konnten die erforderlichen Retentionszeiten um eine Größenordnung verkürzt werden. Weiters wurde auch der Nutzen der Mikrogaschromatographie für den Nachweis von Verunreinigungen demonstriert, wie sie in zukünftigen Fusionsanlagen erwartet werden. Alle Details der verwendeten Mikrogaschromatographen sowie die gewonnenen Erfahrungen und Ergebnisse werden beschrieben.

Auch das Design der analytischen Geräte des **analytischen Systems (ANS)** für die Tritiumprozessierungsanlage von ITER wird kurz beschrieben, da es zu einem erheblichen Anteil auf der Erfahrung im Umgang mit den Gaschromatographen des TLK

und auf der Entwicklungsarbeit in der Mikrogaschromatographie in den letzten Jahren beruht.

Schließlich werden noch ein paar mögliche Verbesserungen für den Gaschromatographen GC1 kurz erwähnt.

Die Aufgabe dieses Berichtes ist es, die Erkenntnisse und Erfahrungen, die im Umgang mit Gaschromatographie in den letzten Jahren im TLK gewonnen worden sind, wiederzugeben sowie die verschiedenen Komponenten und die gemessenen Chromatogramme in einer einfachen und umfassenden Weise darzustellen.

Daher hoffen die Autoren, dass der vorliegende Bericht unter anderem auch von Nutzen für Wissenschaftler ist, die an analytischen Problemen interessiert sind, oder für Designer von zukünftigen gaschromatographischen Apparaturen.

GAS CHROMATOGRAPHY AT THE TRITIUM LABORATORY KARLSRUHE

ABSTRACT

The knowledge of the gas composition in any gas processing plant is a fundamental pre-condition for the high quality of the products to be achieved and for their characterisation. In tritium processing plants the continuous control of the various product streams is even more important because the composition of gases containing tritium may change not only because of the tritium decay to helium-3, but also because of the radiochemical processes which are induced by the energy released during the tritium decay. Thermodynamically stable gas species may be converted into ions, radicals, fragments and excited species. Finally even new gas species may be generated which were not present before in the gas mixture.

Among the analytical techniques (mass spectrometry, laser Raman spectroscopy, gas chromatography, use of ionisation chambers) employed at the Tritium Laboratory Karlsruhe (TLK), gas chromatography plays a prominent role. The main reasons for that are the simplicity of the gas chromatographic separation process, the small space required for the equipment, the low investment costs in comparison to other methods, the robustness of the equipment, the simple and straightforward analysis and the fact that all gas species of interest (with the exception of water) can easily be detected by gas chromatographic means. This is, for example, not the case in laser Raman spectroscopy where noble gases can not be characterised by means of vibrational excitations or where the quantitative analysis of even simple gas species such as methane becomes already almost too difficult to perform. Higher hydrocarbons with their even larger possibility of vibrational excitations, especially when all three hydrogen isotopes are present, are even more difficult. Also mass spectrometry can become too complex for a quantitative analysis when too many hydrocarbons are present. Peaks of gas species may start to overlap with the cracking products other gases. The situation becomes even worse when trimers have to be considered and three hydrogen isotopes are present in the gas mixture and in the hydrogen containing molecules.

The conventional gas chromatographs GC1 and GC2 used in the Tritium Measurement Techniques (TMT) System of the TLK and the gas chromatograph GC3 of the experiment CAPER are presented in detail, by discussing their flow diagrams, their major components, the chromatograms measured by means of various detectors, shortcomings and possible improvements. One of the main disadvantages of the

conventional gas chromatography is the long retention times required for the analysis of hydrogen gas mixtures. To overcome this disadvantage, micro gas chromatography for hydrogen analysis was developed. Reduction of the retention times by one order of magnitude was achieved. This development requires the modification of conventional micro gas chromatographs. The installation of a special external analytical capillary column is necessary to cool the column to the low temperatures required for the separation of the hydrogen molecules. Furthermore, the usefulness of conventional micro gas chromatography for the detection of impurities in gas mixtures similar to the ones to be processed in future power producing fusion devices is demonstrated by the analysis of different impurity gas mixtures. The necessary enhancements, the special flow diagrams, the obtained micro gas chromatograms for various helium-hydrogen and impurity mixtures are also discussed in detail.

The design of the analytical tools of the Analytical System (ANS) of the ITER Tritium Plant is briefly mentioned because it is based to a large extent on the experience gained during the frequent use of gas chromatography at the TLK and on the development of micro gas chromatography in the last years.

Finally, because most analytical equipment can be improved, a few possible enhancements for GC1 are briefly mentioned.

The purpose of this report is to summarise the experience gained with gas chromatography at the TLK during the last years, to explain the design of the gas chromatographs in detail and to present the collected information of major components and of the obtained chromatograms in a simple and comprehensive way. Therefore, the authors hope that the present report may be of use for any scientist interested in analytical problems or for designers of future analytical tools such as conventional or micro gas chromatography.

Contents

1) Introduction.....	1
2) General statements	2
3) Experimental details of the gas chromatographs used at the TLK	3
3.1) The gas chromatograph GC1 of the TMT.....	3
3.1.1) The flow diagram of GC1	3
3.1.2) Compression stage of GC1.....	4
3.1.3) Injection stage of GC1	4
3.1.4) Operation of GC1	4
System 1 of GC1: Analysis of ^3He and of the six hydrogen molecules.....	4
System 1 of GC1: Analysis of N_2 , O_2 , CO , ΣCQ_4 , CO_2 , and higher hydrocarbons	5
System 2 of GC1: Analysis of $^3\text{He}+^4\text{He}$, ΣQ_2 , O_2 , CO and ΣCQ_4	5
Intermediate summary of GC1	6
3.1.5) Treatment of the exhaust gases of GC1.....	6
3.1.6) Columns and detectors used in GC1.....	6
3.2) The gas chromatograph GC2 of TMT.....	11
3.2.1) The flow diagram of GC2.....	11
3.2.2) Compression stage of GC2.....	11
3.2.3) Injection stage of GC2	12
3.2.4) Operation of GC2.....	12
Analysis of ^3He , ΣQ_2 , O_2 , N_2 , CO and ΣCQ_4	12
Analysis of CO_2 , ΣNQ_3 , $\Sigma\text{Q}_2\text{O}$ and higher hydrocarbons.....	13
3.2.5) Treatment of the exhaust gases of GC2.....	13
3.2.6) Columns and detectors used in GC2.....	13
3.2.7) Photos of the gas chromatographs GC1 and GC2.....	15
3.3) The gas chromatograph GC3 of CAPER.....	17
3.3.1) The flow diagram of GC3.....	17
3.3.2) Preparation of sample for GC3	17
3.3.3) Injection stage of GC3	18
3.3.4) Operation of GC3.....	18
Analysis of ^3He and of the six hydrogen molecules.....	18
Analysis of O_2 , N_2 and CO	18
Analysis of methane, CO_2 , water and higher hydrocarbons.....	18
General remarks	18
3.3.5) Treatment of the exhaust gases of GC3.....	20
3.3.6) The columns and detectors used in GC3	20
3.3.7) Photos of the gas chromatograph GC3	20
3.4) The micro gas chromatograph μGC1	22
3.4.1) Flow diagram of μGC1	22
3.4.2) Operation of μGC1	22
3.5) The micro gas chromatograph μGC2	25
3.5.1) Flow diagram of μGC2	25
3.5.2) Operation of μGC2	25
3.5.3) Photos of the micro gas chromatographs μGC1 and μGC2	25
3.6) Major components of the gas chromatographs GC1, GC2 and GC3.....	29
3.6.1) Thermal Conductivity Detectors (TCDs).....	29
3.6.2) Helium ionisation Detector (HeD)	29
3.6.3) Ionisation Chambers (ICs)	29
3.6.4) Columns used in the various gas chromatographs.....	30
3.6.5) Use of Valco valves.....	30
3.6.6) Carrier gases and flows used in GC1 and GC2.....	30
3.6.7) Pipe work and valves	31
3.7) Injection of calibrated gas mixtures into GC1, GC2, GC3, μGC1 and μGC2	32
3.7.1) Injection of calibrated gas mixtures into GC1 and GC2.....	32
3.7.2) Injection of calibrated gas mixtures into GC3	33
3.7.3) Injection of gas mixtures into μGC1 and μGC2	33
4) Analysis by means of conventional gas chromatography	35
4.1) Determination of the compression pressures in the injection loops of GC1 and GC2.....	35
4.1.1) The compression pressures in the injection volumes of GC1	35
4.1.2) The compression pressure in the injection volume of GC2.....	36

4.2) Minimum pressures in the compression loops required for full compression in GC1 and GC2	37
4.3) Analysis of protium by thermal conductivity detectors with He as carrier gas	39
4.4) Analysis of ³ He, hydrogen gas and hydrocarbon mixtures	41
4.4.1) Observation of hydrogen gas mixtures with GC1	41
Inactive hydrogen gas mixtures observed with TCD-B of GC1	41
Hydrogen gas mixtures with tritium observed with TCD-B of GC1	44
4.4.2) Observation of hydrocarbon mixtures with GC1, GC2 and GC3	47
HeD chromatogram of GC1	48
TCD-A chromatogram of GC2	48
TCD-A chromatogram of GC3	49
Comparison of the HeD chromatogram of GC1 with the TCD chromatograms of GC2	50
Additional TCD-A chromatogram of GC2	51
4.4.3) Observation of ³ He and low concentrations of hydrocarbons in tritiated gas mixtures by means of GC1	51
4.4.4) Observation of ³ He and highly tritiated hydrogen mixtures by means of GC1	55
4.5) Comparative study of GC1, GC2 and GC3 by means of a special gas mixture	59
4.5.1) Use of gas chromatograph GC1	59
System 1 of GC1	59
System 2 of GC1	60
4.5.2) Use of gas chromatograph GC2	63
4.5.3) Use of gas chromatograph GC3	65
4.6) Calibration factors for the gas chromatographs GC1 and GC2	68
5) Analysis by means of micro gas chromatography	71
5.1) Analysis of helium and hydrogen isotope mixtures by means of μ GC1	71
5.2) Analysis of gas mixtures in fusion fuel cycle by means of μ GC2	78
5.3) Comparison of chromatograms measured with GC2 and μ GC2	82
5.3.1) Chromatograms of a 1 vol% gas mixture in H ₂	82
5.3.2) Chromatograms of a 2 vol% gas mixture in H ₂	84
5.4) Use of further capillary columns for micro gas chromatography	86
5.5) Use of Helium and Neon as carrier gases in micro gas chromatography	89
5.6) Influence of the head pressure on the retention time	92
6) Gas chromatography proposed for ITER	93
6.1) Operation of the micro gas chromatographs used in ANS	93
6.2) The operation of the special gas chromatographs used in ANS	96
6.2.1) The compression loops	96
6.2.2) Injection of gas in the sampling volume	96
6.2.3) Separation and detection of He, the six hydrogen molecules and of impurities	97
6.2.4) Separation and detection of impurities	97
7) Possible enhancements for GC1 and GC2 used in TMT	99
8) Conclusions	101
Acknowledgement	102
List of Figures	103
List of Tables	107
References	108

GAS CHROMATOGRAPHY AT THE TRITIUM LABORATORY KARLSRUHE

1) Introduction

Knowledge of the chemical composition of gases in any processing plant is of fundamental importance for safe operation and achievement of well characterised product streams. This is particularly relevant in tritium handling plants regardless of whether they are used for basic research, preparation of products for industrial applications or constituents of the fuel cycle of fusion reactors. The composition of tritium-containing mixtures changes not only due to the radioactive decay of tritium (T) to ^3He , but also because of radiation induced reactions. Thermodynamically stable gas species may be converted into ions, radicals, fragments and excited species by the energy released during the tritium decay creating eventually new molecules previously not present. It is well known that tritium reacts with gases adsorbed on inner walls of containments or dissolved in steel such as carbon yielding hydrocarbons and other species.

One of the major tasks of the Tritium Laboratory Karlsruhe (TLK) /1.1/ is the enhancement or development of effective and new methods for the analysis of tritium-containing gas mixtures. A further goal is their technical and practical demonstration in the daily applications of a tritium processing plant. The main methods /1.2/ used for the analysis of gas mixtures handled at the TLK are mass spectrometry (Quadrupoles and Omegatrons /1.3, 1.4/), gas chromatography /1.5-1.7/ and laser Raman spectroscopy /1.8-1.11/. In addition, for the characterisation of tritium, calorimetry /1.12, 1.13/ and ionisation chambers are employed. Among these techniques, gas chromatography plays a prominent role. Three gas chromatographs are in operation at the TLK, two for routine applications (such as the determination of the composition of tritium gas mixtures from the Infrastructure Systems or from research activities) in the Tritium Measurement Techniques (TMT) System and one dedicated to the experiment CAPER /1.14, 1.15/. In CAPER the processing of fusion exhaust gases is simulated on a semi-technical scale by in situ-mixing of relevant impurities with tritium, processing of these gas mixtures with the main emphasis to regain the tritium and then measurement of the detritiation factors of the various installed processes. One of the main goals of CAPER is the demonstration that a detritiation factor of 10^8 is possible. In addition, micro gas chromatographs /1.16/ are used for the analysis of hydrogen and impurity gas mixtures.

This paper discusses the specific design of the gas chromatographs employed at the TLK and summarises the experience gained in the last years. Details of flow diagrams, columns, detectors used and chromatograms measured for specific gas mixtures are presented and possible enhancements are mentioned.

2) General statements

Gas chromatography is a well established analytical tool with high accuracy and very low detection limits for the determination of a large variety of different gas compositions. Commercial separation columns and special detectors are available for almost any gas analytical application.

For the separation of hydrogen isotope mixtures special gas chromatographs have been developed capable of separating and analysing quantitatively the six hydrogen molecules /1.5-1.7, 1.17-1.30/.

The separation of the six hydrogen molecules is achieved at temperatures below 150 K, in most cases at 77 K. At these low temperatures (77K) most of the gases to be analysed with the exception of He, Q₂ (Q₂ stand for any of the six hydrogen molecules, Q for any of the three isotopes H, D, T) and Ne are partly trapped in the column at low temperatures. This can lead to an increase in flow resistance and finally to total clogging of the column, but in any case the detectors are measuring too small amounts for most gases. These difficulties at low temperatures can be avoided by a simple two stage process where the gases which are normally trapped at these low temperatures are separated from the other ones before reaching the low temperature column, and only ³He, ⁴He, Ne and Q₂ are injected into the low temperature column. This principle is also used in the TLK gas chromatographs GC1 and GC3 where pre-columns are used to separate helium and Q₂ from the other gases. This is possible because helium and Q₂ pass faster through this column than any other gas of interest. After the exit of He and Q₂, the later eluting gases are prevented from entering the low temperature column by switching e.g. a Valco valve. Only He and Q₂ enter and pass through the low temperature column. Whereas He also passes quickly through the low temperature column, the interaction between the hydrogen species and the internal material of the low temperature column is stronger, dependent on the various hydrogen molecules and in this way the separation between the six hydrogen molecules is achieved.

3) Experimental details of the gas chromatographs used at the TLK

At the TLK five different gas chromatographic systems are in use. Two (GC1 and GC2) are the heart of the subsystem Tritium Measurement Technique (TMT) /1.7/, a third one (GC3) is part of the subsystem CAPER /1.14, 1.15/ to study the detritiation of simulated fusion exhaust gases and the fourth and the fifth are special and conventional micro gas chromatographs (μ GC1 and μ GC2) /1.16/.

In the following the five gas chromatographs are discussed in detail.

3.1) The gas chromatograph GC1 of the TMT

3.1.1) The flow diagram of GC1

Fig. 3.1.1 shows the flow diagram of the gas chromatograph GC1 which is located within the glove box of TMT.

GC1 can be split into the following sections:

- the compression stage with the main components of capillary-A, capillary-C and the two injection volumes connected to the Valco-A and Valco-C,
- System 1 for detection of ^3He and of the six hydrogen molecules with a thermal conductivity detector (TCD-B) and of the three tritiated Q_2 molecules with an ionisation chamber (IC-B) and for the determination of ppm levels of impurities with a helium ionisation detector (HeD-A) and of their tritiated fractions with IC-A,
- System 2 for detection of helium, hydrogen, oxygen and methane in the 0.1% to 100% range with TCD-C and of the tritiated components with IC-C.

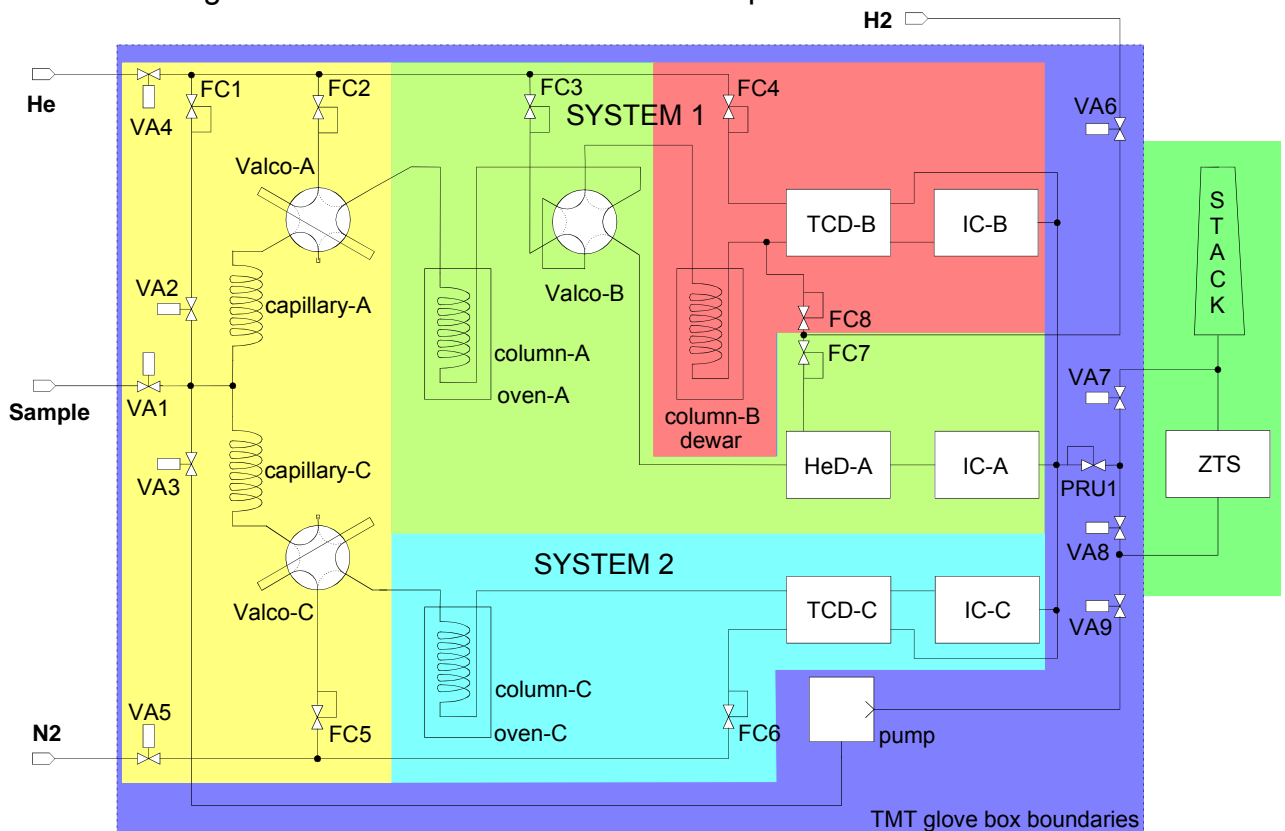


Fig. 3.1.1: Flow diagram of GC1.

In the following the various parts of GC1 briefly mentioned above will be discussed in more details.

3.1.2) Compression stage of GC1

The purpose of the compression loop is to compress gases of low pressure to higher pressures to increase the gas amounts which are injected into System 1 and System 2. Larger injected gas amounts mean greater chromatogram peaks, larger peak areas and lower detection limits. Furthermore, the compression to the same final pressure allows easy comparison of the peak areas between different chromatograms. The whole compression loop during the compression is highlighted in the top of Fig. 3.1.2.

Gas mixtures in the pressure range between 2.5 kPa and 0.15 MPa can be compressed in GC1 without any detection of the gas used for compression (see also Sections 4.1 and 4.2). Helium is used for compression as well as carrier gas.

The compression is performed in the following way: After repeated compression cycles with He via opening and closing VA-2 and evacuation of the compression loop via opening valve VA-3 by means of a combination of Normetex- and metal bellows pumps (schematically presented in Fig. 3.1.1 by a single pump symbol) valve VA-1 is opened, the gas to be analysed expands into the capillary-A and capillary-C and is compressed by helium after closing VA-1 and opening valve VA-2.

Naturally also un-compressed samples can be analysed. During this sample preparation process valve VA-2 is kept closed. This method is used when the injection of large amounts of tritium into the analytical columns and finally into the TLK Central Tritium Retention System (ZTS /1.31/) is to be reduced because there tritium is oxidised to water which is trapped on dry molecular sieve beds.

3.1.3) Injection stage of GC1

The small injection volumes shown in the top of Fig. 3.1.2 between two ports of Valco-A and of Valco-C are part of the compression loops. The injection volume is 0.2 cm³ and 0.1 cm³ for Valco-A and Valco-C, respectively. These volumes were chosen to be large enough to detect small concentrations and small enough to reduce the injection of too large quantities of tritium or of too large amounts of gas which can lead to highly asymmetrical peak forms due to overloading effects of the separation columns.

The carrier gas flows through the other ports of the Valvo-A and Valco-C when the gas chromatograph is in standby mode as shown in the top of Fig. 3.1.2 or a sample is compressed. At the start of an analysis the Valco-A and Valco-C are switched. Then the carrier gas passes through the small injection volumes and injects the un-compressed or compressed samples into System 1 and System 2 of GC1. This carrier gas flow is highlighted in the middle section of Fig. 3.1.2.

3.1.4) Operation of GC1

System 1 of GC1: Analysis of ³He and of the six hydrogen molecules

After the injection of the sample from the injection volume into System 1 by switching Valco-A, the sample is transported by the carrier gas to column-A where the first separation occurs. ³He and ΣQ₂ pass faster through column-A than other gases. No separation into the six hydrogen molecules occurs in column-A. The Valco-B at the outlet of column-A transfers ³He and Q₂ directly into column-B where the separation of Q₂ into the six molecules H₂, HD, HT, D₂, DT, T₂ occurs at liquid nitrogen

temperature. ^3He and the six hydrogen molecules are detected well separated with TCD-B, the tritiated hydrogen molecules are also observed by the ionisation chamber IC-B. The tritiated gas species HT, DT, T_2 are seen with very similar retention times by both detectors because IC-B is mounted directly after TCD-B. The bold lines of System 1 in the middle of Fig. 3.1.2 show exactly the path of the carrier gas required for the analysis of ^3He and hydrogen gas species.

Protium is added to the carrier gas helium just in front of the TCD-B. This is necessary because of the anomaly in the thermal conductivity of He- H_2 gas mixtures which shows a minimum at low protium concentrations of a few percents /1.32/. Two mixtures with different He- H_2 concentrations on both sides of the minimum have the same thermal conductivity and therefore the interpretation of the peak areas is not any more unique. It is necessary that the added H_2 quantity is so large that further addition of H_2 from the sample to be analysed will lead only to increases of the thermal conductivity of the He- Q_2 gas mixture. See also Section 4.3.

System 1 of GC1: Analysis of N_2 , O_2 , CO , ΣCQ_4 , CO_2 , and higher hydrocarbons

After the passage of ΣQ_2 through Valco-B it is switched to transfer the other gases of the gas mixture, which are eluting in the sequence N_2 , O_2 , CO , ΣCQ_4 , CO_2 and higher hydrocarbons from column-A, to the HeD-A and IC-A for analysis. The path of the carrier gas through the various valves, columns and detectors is shown for System 1 in the bottom of Fig. 3.1.2 by the thicker lines. Now the carrier gas controlled by the mass flow controller FC3 pushes Q_2 through column-B, TCD-B and IC-B, whereas the carrier stream passing through FC2 moves the impurities through column-A, TCD-A and IC-A. Protium is added to the carrier gas He just in front of the HeD-A to achieve a stable baseline of the HeD-A.

The purpose of column-A is twofold: i) to cause a large enough difference in the retention times between Q_2 and the impurities to allow switching of the Valco-B at a time when no gas species passes through it and ii) to separate the impurities well enough for direct measurement by the HeD-A.

The purpose of Valco-B is to avoid injection of the impurities from column-A into column-B because there they would be trapped at 77 K and could therefore not be analysed.

Disadvantages of the so far discussed gas chromatograph are i) that helium is not detected because it is used as carrier gas and ii) that only very low impurity concentrations smaller than approximately 200 ppm can be analysed quantitatively by the HeD-A. For the determination of helium and higher impurity concentrations a further analytical system is required, System 2.

System 2 of GC1: Analysis of $^3\text{He}+^4\text{He}$, ΣQ_2 , O_2 , CO and ΣCQ_4

At the start of an analysis the sample of the gas mixture present in the injection volume of Valco-C is injected into System 2 by switching Valvo-C. The sample is transported with the carrier gas stream N_2 which is controlled by FC5, through column-C filled with molecular sieve where the separation into the gases $^3\text{He}+^4\text{He}$, ΣQ_2 , O_2 , CO and ΣCQ_4 occurs. The TCD-C is used for the determination of the integral concentration of the gas species and IC-C for their tritiated parts. N_2 is not observed due to the use of N_2 as carrier gas in System 2. Column-C can not separate the hydrogen isotopes and the TCD-C sees only one hydrogen peak ΣQ_2 . Due to the fact that the six hydrogen molecules show slightly different thermal conductivities it is in general not possible to determine from the ΣQ_2 -peak the total hydrogen concentrations. Only when it is known that the ΣQ_2 peak is caused by one type of hydrogen molecules can its concentration be calculated. In principle this is

also true for the sum peak of ^3He and ^4He , but due to the presence of only two helium isotopes and very similar calibration factors the contribution of ^4He can be calculated by subtracting the relevant ^3He area from the common peak with the knowledge of the ^3He concentration obtained by System 1.

Intermediate summary of GC1

GC1 allows the determination of the concentrations of ^3He and the six hydrogen molecules with TCD-B in the range above 200 ppm, of N_2 , O_2 , CO , ΣCQ_4 , CO_2 , and higher hydrocarbons with the HeD-A in the range from 0.1 to 200 ppm and of $^3\text{He}+^4\text{He}$, ΣQ_2 , O_2 , CO and ΣCQ_4 with TCD-C in the range above 500 ppm. The ΣQ_2 peak can only be used for analysis if it is known that either only protium or deuterium or tritium is present. Tritiated species can be detected with IC-A, IC-B and IC-C when their concentrations exceed 0.1 ppm in the compressed sample.

With GC1 nitrogen can only be determined quantitatively if its concentration is between 0.1 and 200 ppm. If its concentration is higher an overflow of the HeD-A signal is observed which means that N_2 can only be determined qualitatively. In a similar way concentrations of higher hydrocarbons above 200 ppm are also not observed quantitatively because HeD-A allows only determinations up to 200 ppm and with TCD-C higher hydrocarbons are not seen because column-C traps these gases. On the other hand, IC-A allows the determination of the tritiated fractions of all concentrations of higher hydrocarbons.

3.1.5) Treatment of the exhaust gases of GC1

The exhaust gases of System 1 and System 2 are collected in a common manifold and transferred to the Central Tritium Retention System (ZTS). An up-stream pressure regulator is mounted into the connecting line (see Fig. 3.1.1) inside the TMT glove box because part of ZTS is operated in the pressure range between 75 and 90 kPa (a). In the absence of these upstream pressure gauges the TCD baselines would be far noisier as pressure changes within the ZTS would cause base line fluctuations.

3.1.6) Columns and detectors used in GC1

The columns and detectors of GC1 can be divided into three parts which fulfil different objects:

- column-A, HeD-A and IC-A for the separation and detection of impurities of low concentrations by the HeD-A, but of any concentrations by IC-A,
- column-B, TCD-B and IC-B for the separation and determination of ^3He , the six hydrogen molecules by TCD-B and of their tritiated contents by IC-B,
- column-C, TCD-C and IC-C for the separation and detection of the sum of ^3He and ^4He , the ΣQ_2 , impurities at higher concentrations by TCD-C and of the sum of $\text{HT}+\text{DT}+\text{T}_2$ as well as of the tritium concentrations in impurities by IC-C. The ΣQ_2 peak can only be used for analysis if it is known that either only protium or deuterium or tritium is present.

Details of the used columns, detectors, carrier flows, the gas species to be detected and the concentration ranges to be analysed are listed in Tables 3.1, 3.2, 3.3 and 3.4.

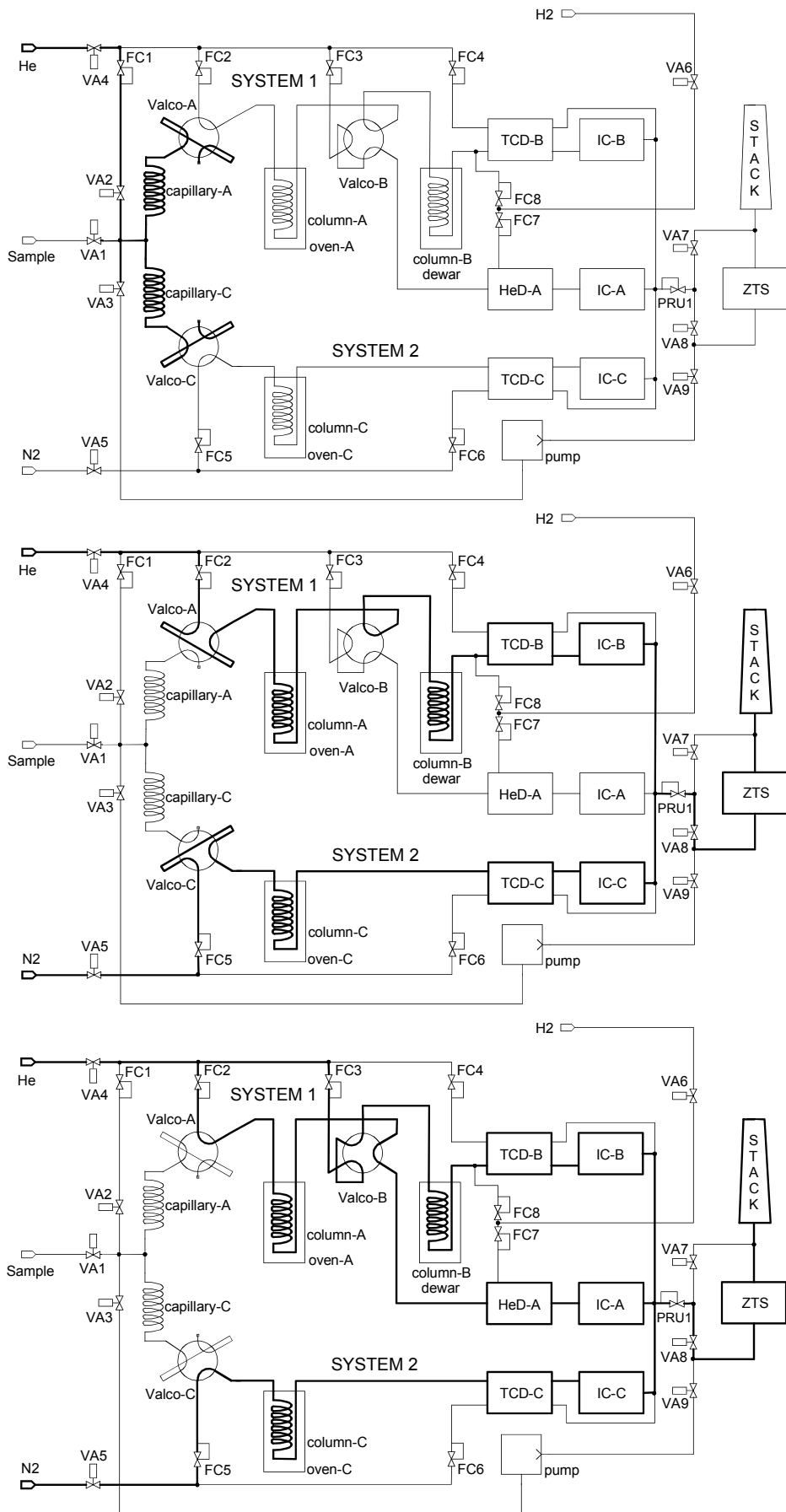


Fig. 3.1.2: Compression of a sample (top) and carrier flows during/after the injection of the sample into System 1 and System 2, transfer of He and ΣQ_2 into Col-B (middle) and analysis of impurities with Valco-B switched (bottom).

Table 3.1: The columns employed in GC1, GC2 and GC3.

Tag of Column	Type	Outer Diameter, Length	Temperature used/K	Maximum Temperature/K
GC1				
Column-A	PORAPAK Q	3 mm, 6 m	243 – 373	383
Column-B	Al ₂ O ₃ doped with Fe	3 mm, 2 m	77	393
Column-C	Molecular sieve 5Å	3 mm, 6 m	333	573
GC2				
Column-A	PORAPAK QS + CHROMOSORB 104	3 mm, 3 m 3 mm, 2 m	393 393	550 550
Column-B	Molecular sieve 5Å	3 mm, 3 m	373	573
GC3				
Column-A	HayeSep R	3 mm, 2.4 m	343	523
Column-B	Molecular sieve 5Å	3 mm, 2.1 m	433	673
Column-C	Al ₂ O ₃ doped with Fe	3 mm, 2.0 m	77	393

For column-A of GC1 sometimes temperature programs are used for the analysis of hydrocarbons: e.g. the temperature of column-A is kept at 313 K for 20 minutes and is then increased by a rate of 10°K per minute to 373 K.

In the case of GC2 temperature programs are also used for the analysis of hydrocarbons, e.g. the temperatures of column-A and column-B are kept at 393 K and 373 K, respectively, for 8 minutes and are then increased by a rate of 10 K per minute to the same final temperature of 423 K.

Table 3.2: Bridge currents of the thermal conductivity detectors (TCD) and temperature of the TCDs employed in GC1, GC2 and GC3.

Tag of Detector	Normal Bridge Current / mA	Maximum Bridge Current / mA	Temperature / K
GC1			
HeD-A	-	-	333
TCD-B	240.5	275	393
TCD-C	125.0	140	353
GC2			
TCD-A	200.3	270.0	393
TCD-B	200.4	270.0	393
GC3			
TCD-A	150	270	393
TCD-B	150	270	393
TCD-C	150	230	473

Table 3.3: Carrier gas flows through the thermal conductivity detectors (TCDs) and helium ionisation detector (HeD-A), the purge flows through the Valco valves and supply pressure of these gases.

Tag of Equipment	Flow / (cm ³ /min)	Type of Gas	Pressure /MPa	Further Remark
GC-1				
HeD-A ¹	45.7	He	0.48	
TCD-B ¹	25.5	He	0.33	analysis side
TCD-B	25.4	He	0.33	reference side
TCD-C	18.2	N ₂	0.63	analysis side
TCD-C	24.7	N ₂	0.63	reference side
Valco valve-A	7.4	He	0.15	0.2 cm ³
Valco valve-B	7.5	He	0.15	
Valco valve-C	43.0	N ₂	0.21	0.1 cm ³
GC-2				
TCD-A	30.0	He	0.76	analysis side
TCD-A	30.0	He	0.76	reference side
TCD-B	30.0	He	0.62	analysis side
TCD-B	30.0	He	0.62	reference side
Valco valve-A	20.0	He	0.20	0.2 cm ³
Valco valve-B	20.0	He	0.20	
GC-3				
TCD-A	30.0	He	0.48	analysis side
TCD-A	30.0	He	0.48	reference side
TCD-B	30.0	He	0.33	analysis side
TCD-B	30.0	He	0.33	reference side
TCD-C	30.0	He	0.63	analysis side
TCD-C	30.0	He	0.63	reference side

¹ Small amounts of hydrogen are added in front of the HeD-A and of the TCD-B.

Table 3.4: Details (detectors and columns used, gas species and concentration ranges) of GC1, GC2 and GC3. Abbreviations: HeD: helium ionisation detector, TCD: thermal conductivity detector, IC: ionisation chamber, Col: column, Detec: detector.

GC1			
Detec	Col-X	Gas species observed	Range
HeD-A	X=A: Porapak, 6 m, 40°C	N ₂ , O ₂ , CO, CQ ₄ , CO ₂ , Q ₂ O, C _n Q _m (n≥2, m≥2)	0.1 – 200 ppm
IC-A		CQ ₄ , Q ₂ O, C _n Q _m (n≥2, m≥2)	≥ 0.1 ppm
TCD-B	X=B: Al ₂ O ₃ with Fe, 2 m, 77 K	³ He, H ₂ , HD, HT, D ₂ , DT, T ₂	≈ 0.02 – 100%
IC-B		HT, DT, T ₂	≥ 0.1 ppm
TCD-C	X=C: molecular sieve, 6 m, 60°C	³ He+ ⁴ He, ΣQ ₂ ¹ , O ₂ , CQ ₄ , CO	≈ 0.05 – 100%
IC-C		HT+DT+T ₂ , CQ ₄	≥ 0.1 ppm
GC2			
Detec	Col-X	Gas species observed	Range
TCD-A	X=A: Porapak, 3 m, 120°C + Chromosorb, 2 m, 120°C	CO ₂ , NQ ₃ , Q ₂ O, C _n Q _m (n≥2, m≥2)	≈ 0.05 – 100%
IC-A		NQ ₃ , Q ₂ O, C _n Q _m (n≥2, m≥2)	≥ 0.1 ppm
TCD-B	X=B: molecular sieve 5A, 3 m, 100°C	³ He, ΣQ ₂ , O ₂ , N ₂ , CQ ₄ , CO	≈ 0.05 – 100%
IC-B		HT+DT+T ₂ , CQ ₄	≥ 0.1 ppm
GC3			
Detec	Col-X	Gas species observed	Range
TCD-A	X=A: Hayesep R, 2.4 m, 70°C	CQ ₄ , CO ₂ , Q ₂ O, C _n Q _m (n≥2, m≥2)	≈ 0.05 – 100%
IC-A		CQ ₄ , Q ₂ O, C _n Q _m (n≥2, m≥2)	≥ 0.1 ppm
TCD-B	X=B: molecular sieve, 2.1 m, 160°C	O ₂ , N ₂ , CO	≈ 0.05 – 100%
IC-B		---	---
TCD-	X=C: Al ₂ O ₃ with Fe, 2 m, 77 K	³ He, H ₂ , HD, HT, D ₂ , DT, T ₂	≈ 0.05 – 100%
IC-C		HT, DT, T ₂	≥ 0.1 ppm

¹ The ΣQ₂ peak (see TCD-C of GC1) can only be used for analysis if it is known that either only protium or deuterium or tritium is present.

3.2) The gas chromatograph GC2 of TMT

3.2.1) The flow diagram of GC2

Fig. 3.2.1 presents the schematic flow diagram of the gas chromatograph GC2 which is located in the glove box of TMT /1.7/ next to GC1.

GC2 can be divided into

- the compression stage with the capillary and the injection volume of Valco-A,
- system-A for the detection of CO₂, NH₃, H₂O and higher hydrocarbons by means of column-A and TCD-A and of their tritiated fractions by IC-A,
- system-B for the determination of ³He, ΣQ₂, O₂, N₂, CH₄ and CO by means of column-B and TCD-B and of their tritiated parts such as HT+DT+T2 and methane with IC-B.

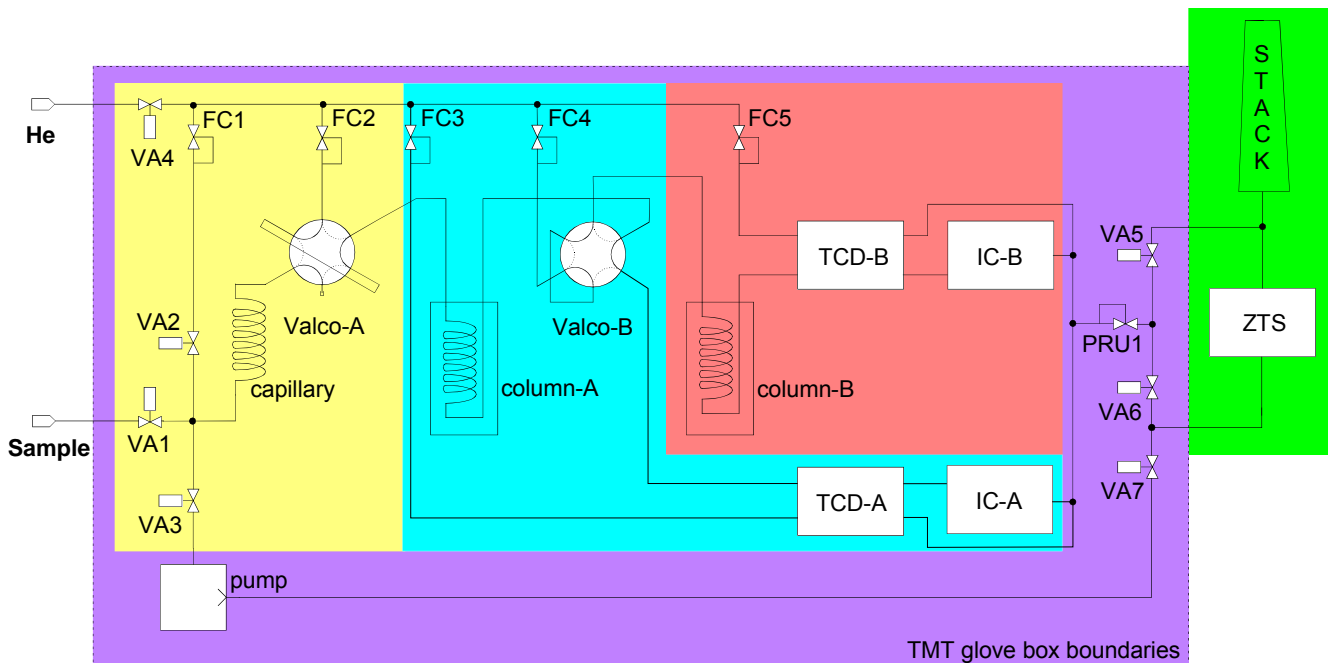


Fig. 3.2.1: Flow diagram of GC2.

In the following the various parts of GC2 briefly mentioned above will be discussed in more details.

3.2.2) Compression stage of GC2

The purpose of the compression loop is to compress gases of low pressure to a higher pressure to increase the gas amounts to be injected. Larger gas amounts introduced into GCs mean larger chromatogram peaks and lower detection limits. Furthermore the compression to the same final pressure allows easier comparison between different chromatograms. The position of Valco-A during the compression is given in the top of Fig. 3.2.2.

Gas mixtures in the pressure range between 3 kPa and 0.21 MPa can be compressed in GC2 without any detection of the gas used for compression (see also Sections 4.1 and 4.2). Helium is used as carrier gas and as the compression medium.

A compression is performed in the following way: After a few compression cycles with He via opening and closing VA-2 and evacuation of the capillary by means of a combination of Normetex- and metal bellows pumps (schematically presented in Fig. 3.2.1 by a single pump symbol) through VA-3, valve VA-1 is opened, the gas sample to be analysed expands into the evacuated capillary and is compressed by helium via opening valve VA-2.

Also un-compressed samples can be analysed. During the compression and injection process valve VA-2 is kept closed. This reduces the injection of large amounts of tritium into the columns and finally into the Central Tritium Retention System (ZTS) where tritium after oxidation to water is trapped as water on dry molecular sieve because the injected activities are proportional to the gas pressure in the compression loop.

3.2.3) Injection stage of GC2

The small injection volume shown in the top of Fig. 3.2.2 between two ports of Valco-A is part of the compression loop. The injection volume is 0.2 cm^3 .

The carrier gas flows through the other ports of the Valvo-A when the gas chromatograph is in standby mode or a sample is compressed. At the start of an analysis the Valco-A is switched. The carrier gas passes now through the small injection volume and injects the sample into column-A. This position of Valco-A is shown in the middle section of Fig. 3.2.2.

3.2.4) Operation of GC2

Analysis of ^3He , ΣQ_2 , O_2 , N_2 , CO and ΣCQ_4

After compression the sample in the injection volume is introduced by means of Valco-A into column-A of GC2. In column-A the gas species ^3He , ΣQ_2 , O_2 , N_2 , CO , ΣCQ_4 are not completely separated, but elute in the shape of a sum peak. The gas species CO_2 , ΣNQ_3 , $\Sigma\text{Q}_2\text{O}$ and higher hydrocarbons are well separated and the time between the last part of the multicomponent-peak and the start of the CO_2 peak is long enough to allow switching of the gas flow by Valco-B. A not complete separation means that the eluting peaks overlap and form a multicomponent-peak. A further column is necessary to achieve full separation. The purpose of Valco-B is to inject the multicomponent-peak directly into column-B for final separation. At the outlet of column-B the gases ^3He , ΣQ_2 , O_2 , N_2 , CO , ΣCQ_4 are well separated and measured by TCD-B. IC-B determines their tritiated parts. The corresponding carrier flows are highlighted in middle picture of Fig. 3.2.2.

In the case of GC2 no protium is added in front of TCD-B. Only when pure deuterium or pure tritium were injected, can the hydrogen peak be analysed. It must be stated that especially hydrogen mixtures and pure protium can not be analysed, protium mainly due to the already mentioned anomaly of the thermal conductivity of helium-protium mixtures. Very unusual forms of the ΣQ_2 peak are produced in the chromatograms by the presence of higher protium concentrations. These shapes are caused by the resulting thermal conductivity of the gas mixtures which pass through TCD-B and which have thermal conductivities either smaller or larger than the corresponding value of pure helium dependent on the protium concentration. The concentrations of O_2 , CO , ΣCQ_4 can also be obtained with System 2 of GC1, but due to the larger difference between their thermal conductivities and the thermal conductivity of the carrier gas helium in comparison to N_2 the chromatograms of GC2 are easier to analyse. In addition, lower detection limits can be achieved with GC2 in comparison to System 2 of GC1 (not mentioning here the very low detection limit of

the HeD-A in System 1 of GC1). The only truly new information obtained with GC2 in comparison to GC1 is the determination of the amount of nitrogen, CO₂ and of higher hydrocarbons in the sample when their concentration is larger than 200 ppm. Also IC-B of GC2 functions mainly as a further check of the results of GC1. Differences in the peak areas of impurities between IC-B of GC2 and IC-C of GC1 are expected due to the different carrier gases. The IC-B, when tritium contaminated on the inner surfaces, functions very similarly to a helium ionisation chamber (only with a far smaller total tritium activity). Nontritiated gas species can be detected after their ionisation by metastable helium which is produced by the high energy electrons of the tritium decay.

Analysis of CO₂, ΣNQ₃, ΣQ₂O and higher hydrocarbons

After the multicomponent-peak has moved through Valco valve-B the valve is switched and the gas species CO₂, ΣNQ₃, ΣQ₂O and higher hydrocarbons well separated in column-A are transferred to the TCD-A and IC-A for analysis. The use of Valco-B is important because otherwise the gas species CO₂, ΣNQ₃, ΣQ₂O and higher hydrocarbons would be trapped in the molecular sieve of column-B and not detected by TCD-B or IC-B. The carrier flows are highlighted in the bottom flow diagram of Fig. 3.2.2.

The exhaust gases of system-A and system-B are collected in a common manifold and then transferred to ZTS.

3.2.5) Treatment of the exhaust gases of GC2

The exhaust gases of GC2 are collected in a common manifold and transferred to ZTS. An up-stream pressure regulator is mounted into the connecting line inside the TMT glove box because part of ZTS is operated in the pressure range between 75 and 90 kPa (a). In the absence of these upstream pressure gauges the TCD baselines would be far noisier as the pressure changes within the ZTS would cause base line fluctuations.

3.2.6) Columns and detectors used in GC2

The columns and detectors of GC2 can be divided into the following different functional areas similarly to GC1:

- column-A, TCD-A and IC-A,
- column-B, TCD-B and IC-B.

The main differences in comparison to GC1 are that other columns are used, that the HeD-A is replaced by a TCD and that no system similar to System 2 of GC1 exists.

Details of the used columns, detectors, the gas species to be detected and the concentration ranges to be measured are listed in Tables 3.1, 3.2, 3.3 and 3.4.

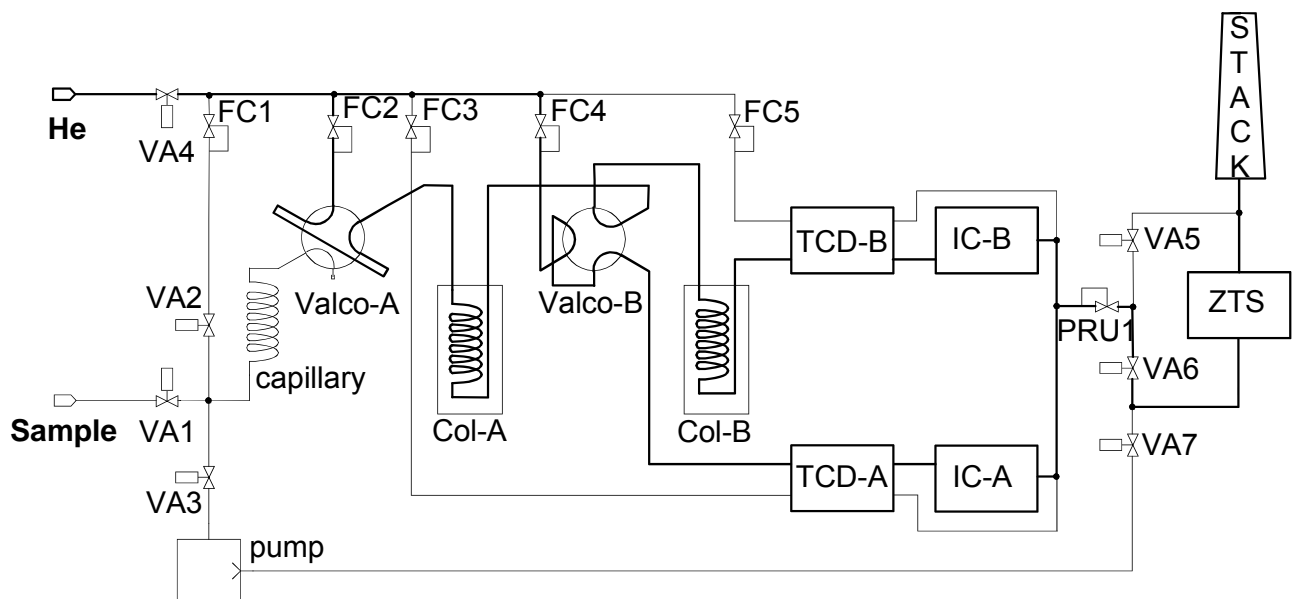
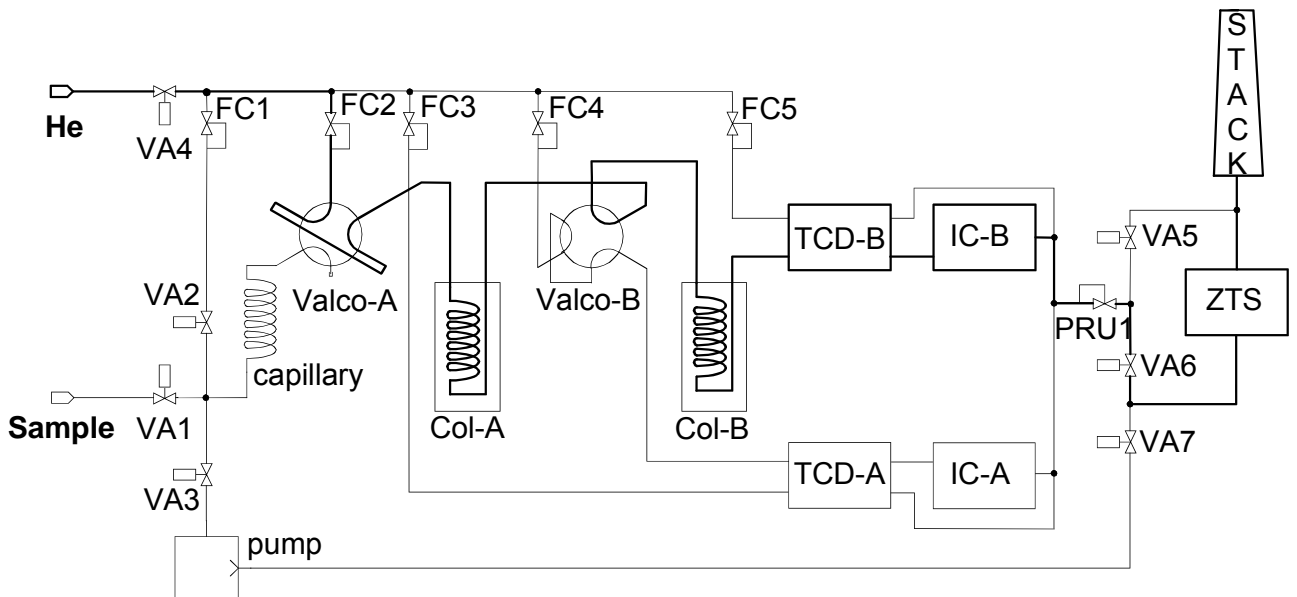
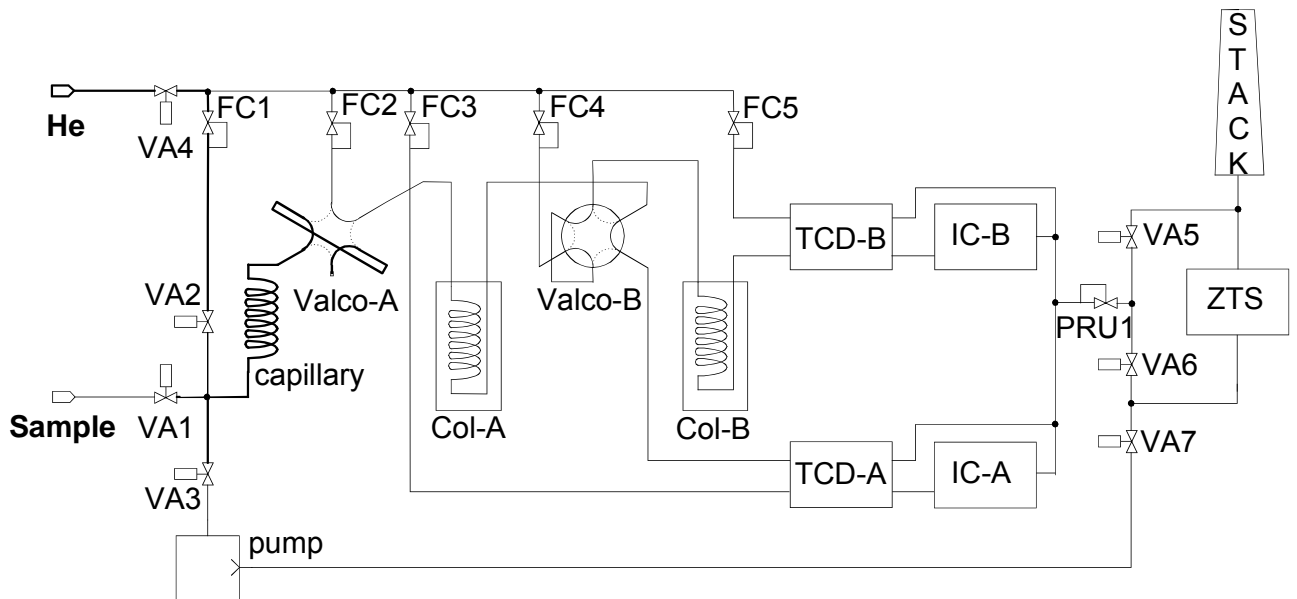


Fig. 3.2.2: Compression of a sample (top) and carrier flows during transfer of the sample to column-A and column-B (middle) and bypassing column-B (bottom).

3.2.7) Photos of the gas chromatographs GC1 and GC2

The following equipment is visible in Fig. 3.2.3:

- GC1 and GC2 behind the upper window of the TMT glove box,
- the lower section of the liquid nitrogen dewar behind the lower window of the TMT glove box,
- the control unit of the TMT glove box in its yellow housing in the left upper corner,
- one of the two control units of the two Siemens Sichromats,
- two Keithley electronic units to measure the currents of the ionisation chambers,
- the visual display for the chromatograms of GC1 and GC2,
- the transfer unit for equipment into and out of the glove box.

The ports of the TMT glove box are closed either by bungs or gloves. Gloves are only placed at locations which are frequently used by the operator.



Fig. 3.2.3: View on a large section of the TMT glove box: On the left side the main electronic equipment is visible, whereas GC1 and GC2 are seen on the left and right side behind the upper window of the TMT glove box.



Fig. 3.2.4: View on the upper part of the TMT glove box with GC1 on the left and GC2 on the right side.

Fig. 3.2.4 shows more clearly the two GCs GC1 and GC2 behind the upper window of the TMT glove box. On top of the two GCs one can recognise the actuators of Valco valves and in the front, installed in the GCs, simple pressure gauges with needle indication.

Fig. 3.2.5 shows the mechanical structure of one side of the TMT glove box. One can see that especially the upper section of the glove box is overfilled with equipment which makes handling or replacement of any components difficult. In future enough space needs to be foreseen around equipment to allow access for maintenance and modifications.



Fig. 3.2.5: View on one side of the TMT glove box.

3.3) The gas chromatograph GC3 of CAPER

3.3.1) The flow diagram of GC3

Fig. 3.3.1 presents the flow diagram of the gas chromatograph GC3 which is located in the glove box A belonging to the CAPER system [1.14, 1.15]. The pipe work between the exit of GC3 and the stack is presented in a simplified way.

GC3 can be split into different sections

- the injection system with Valco-A,
- system-A with column-A and TCD-A and IC-A for the detection of CO₂, methane and higher hydrocarbons and their tritiated fractions,
- a further Valco-B to transfer the gas stream either to column-B or to the TCD-A,
- system-B with column-B and TCD-B and IC-B for the detection of O₂, N₂ and CO,
- a further Valco-C to transfer the gas stream either to column-C or to the TCD-B,
- system-C with column-C and TCD-C and IC-C for the detection of ³He, the six hydrogen molecules and of the tritiated molecules HT, DT and T₂.

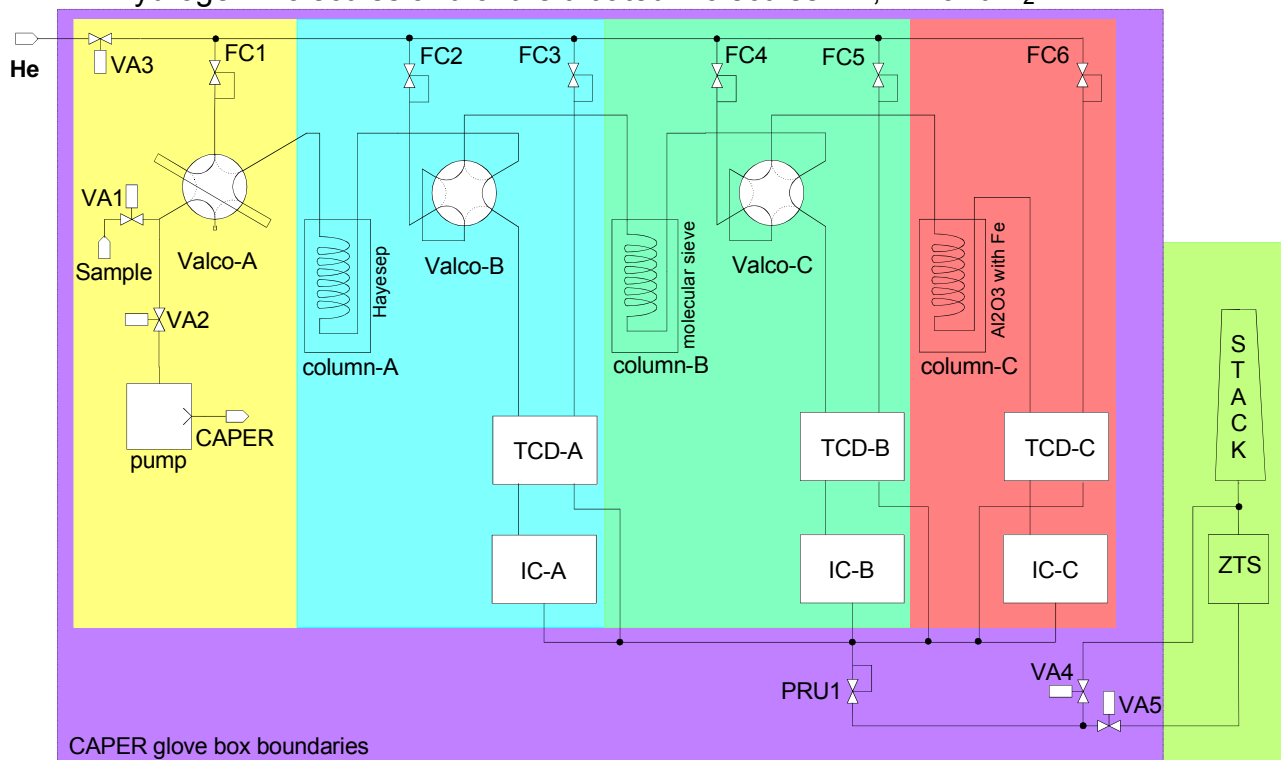


Fig. 3.3.1: Flow diagram of GC3.

In the following the various parts of GC3 mentioned briefly above will be discussed in more details.

3.3.2) Preparation of sample for GC3

The position of Valco-A during the preparation of a sample for analysis is given in the top of Fig. 3.3.2. No possibility for compression exists. Samples can only be injected for analysis with the gas pressure achieved after opening VA1 due to expansion.

The preparation of the sample for injection is performed in the following way: After evacuation of the capillary with a combination of Normetex- and metal bellows pumps (schematically presented in Fig. 3.3.1 by a single pump symbol) through valve VA-2, VA-1 is opened, the gas sample to be analysed expands into the evacuated capillary. Purging of the loop with helium is not possible.

3.3.3) Injection stage of GC3

The small injection volume shown in the top of Fig. 3.3.2 between two ports of Valco-A is part of the injection loop.

The carrier gas flows through the other ports of the Valvo-A when the gas chromatograph is in standby mode or a sample is prepared for analysis. At the start of an analysis the Valco-A is switched. The carrier gas passes now through the small injection volume and injects the sample into column-A. This position is shown in the second picture from the top of Fig. 3.3.2.

3.3.4) Operation of GC3

The sample to be analysed is injected from the sample loop of Valco-A into column-A by switching Valco-A.

Analysis of ^3He and of the six hydrogen molecules

^3He and hydrogen which first exit column-A are transferred by Valco-B to column-B, where they again exit first. They are then injected by Valco-C into column-C where ^3He and the hydrogen isotope separation occurs at 77 K. ^3He and the six hydrogen molecules are finally detected by TCD-C and IC-C. The carrier flow of interest during this time is shown in the second diagram from the top in Fig. 3.3.2.

Analysis of O_2 , N_2 and CO

When hydrogen has exited column-B and passed through Valco-C, Valco-C is switched into the other position as indicated in the third flow diagram from the top in Fig. 3.3.2. All further gases e.g. O_2 , N_2 , CO , etc., eluting from column-B are directly transferred to the detectors TCD-B and IC-B for analysis. The carrier gas flow through column-C is now controlled by FC4.

Analysis of methane, CO_2 , water and higher hydrocarbons

When CO has passed Valco-B, it is switched into the position shown in the flow diagram at the bottom of Fig. 3.3.2. All other gases, eluting later from column-A are transferred directly to the detectors TCD-A and IC-A for analysis. The carrier gas flow through column-B is now controlled by FC2.

General remarks

The switching of Valco-C is necessary to avoid the trapping of the other gas species in the 77 K cold packed column, because then these gas species would not be detected. In the same way the switching of Valco-B is required, because otherwise the gases CO_2 and higher hydrocarbons would be trapped in column-B which is filled with molecular sieve.

The switching of the Valco valves at the correct times is critical as well as the adjustment of the various flow controllers for the carrier gas to avoid jumps in the base lines of the TCDs due to pressure changes.

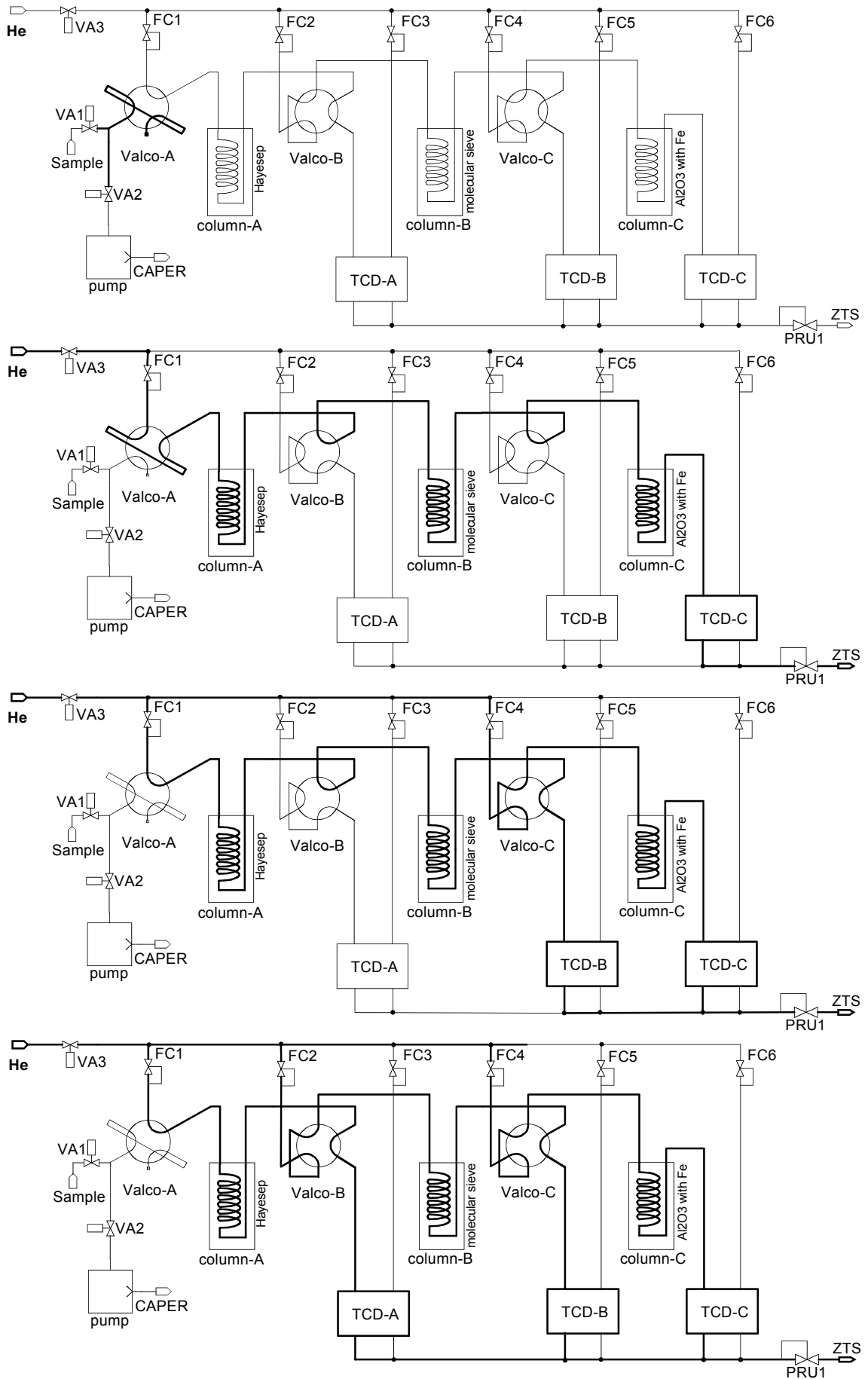


Fig. 3.3.2: Preparation of a sample for injection (top) and carrier flows highlighted during transfer of the sample to column-C and TCD-C (2. picture from top), to column-B and TCD-B (3. picture from top) and to column-A and TCD-A (bottom). ICs are not shown.

3.3.5) Treatment of the exhaust gases of GC3

The exhaust gases of the three ICs are collected in a common manifold and transferred either to ZTS or stored in a special reservoir not shown in Fig. 3.3.1 for later reprocessing and regaining the tritium. An up-stream pressure regulator is mounted into the connecting line inside the Capex glove box because part of ZTS is operated in the pressure range between 75 and 90 kPa (a). In the absence of these upstream pressure gauges the TCD baselines would be far noisier as the pressure changes within the ZTS can cause base line fluctuations.

3.3.6) The columns and detectors used in GC3

The columns and detectors of GC3 can be divided into three parts which fulfil different objects:

- column-A, TCD-A and IC-A for the detection of methane, CO₂, water, higher hydrocarbons,
- column-B, TCD-B and IC-B for the determination of O₂, N₂, CO, etc.,
- column-C, TCD-C and IC-C for the observation of ³He, the hydrogen molecules and their tritiated contents.

Details of the used columns, detectors, the gas species to be detected and the concentration ranges to be analysed are listed in Tables 3.1, 3.2, 3.3 and 3.4.

3.3.7) Photos of the gas chromatograph GC3

Fig. 3.3.3 shows the section of the CAPER glove box A which contains in the upper part the Siemens Sichromat GC3. Sample containers are connected to GC3 by using the gloves in the lower section of the glove box.



Fig. 3.3.3: View on the right end of the CAPER glove box A which contains GC3.

Fig. 3.3.4 presents an enlarged view of the GC3 behind the upper window already presented in Fig. 3.3.3. The actuator of a Valco valve and the upper parts of three needle valves to control the carrier gas flows are shown sticking out over the top surface. In addition, part of the instrumentation in the front side is easily recognised.



Fig. 3.3.4: Photo of GC3 inside the Caper glove box A.

Fig. 3.3.5 presents the electronic control unit of the Siemens GC3 in the lower left side, three Keithley units (upper left corner) to measure the currents of the three ionisation chambers used in GC3 and on the right side the screen for graphical display of the measured chromatograms after treatment with the commercial Chromeleon software.



Fig. 3.3.5: Part of the electronic units to control the gas chromatograph GC3.

3.4) The micro gas chromatograph μ GC1

3.4.1) Flow diagram of μ GC1

The schematic flow diagram of the micro gas chromatograph μ GC1 is presented in Fig. 3.4.1. The μ GC1, type M200, was purchased from the Company Agilent Technologies.

The main components of the μ GC1 are

- the pre-column (molecular sieve 10 m),
- the reference column,
- the oven for the pre-column and reference column,
- the external analytical column ($\text{Al}_2\text{O}_3+\text{MnCl}_2$, 4 m x 0.53 mm),
- liquid nitrogen dewar,
- the oven for the external column required for regeneration,
- pressure reducing flow restrictions,
- the micro thermal conductivity detector (μ TCD),
- various valves such as sample valve, stream switching valve, inject valve, foreflush valve, backflush valve, reference column valve,
- pump.

3.4.2) Operation of μ GC1

By opening the sample valve a part of the sample to be analysed is sucked via the external pump into the sample chamber and finally vented (see Fig. 3.4.1). This technique allows the injection of a mid-stream sample and minimises possible contamination. During all this time carrier gas is running through the μ GC1 and the micro Thermal Conductivity Detector (μ TCD). After a certain pumping or venting time, the sample valve is closed, the foreflush valve and the inject valve opened, the stream switching valve moved into the next position and the sample in the fixed volume compressed by the carrier gas into the pre-column and then forced through it. The flow rate depends now on the difference of the pressures between the inlet of the pre-column and the outlet after the μ TCD, on the flow resistance of the pre-column and analytical column and their temperatures. When the gases of interest have eluted from the pre-column and entered the analytical column, the foreflush mode can be considered as finished and the backflush mode can start. In the backflush mode the foreflush valve is closed and the backflush valve is opened and the stream switching valve is moved into the other position. Gas species already in the analytical column are moved further by carrier gas passing through the backflush valve and are further separated until they exit the analytical column and enter the micro TCD. On the other hand, the gas species which did not manage to exit the pre-column, are now forced by the carrier gas passing through the backflush valve, but running now in opposite direction through the pre-column, back into the sample chamber and are transferred by the external pump into the vent. In the backflush mode the flow rate through the analytical column depends on the difference of the pressures downstream of the carrier gas supply and at the outlet of the TCD and on the sum of the flow resistances generated by the flow restrictor and the analytical column. The flow rates through the analytical column in foreflush and backflush modes should be controlled such that the base line of the micro TCD will not drift significantly when the switching occurs. This is best achieved when the flow resistance of the flow restrictor is equal to the one of the pre-column.

Details of the used capillary columns are listed in Table 3.5.

Table 3.5: Information of the columns used in μ GC1 and μ GC2.

Tag of Column	Type	Inner Diameter, Length	Temperature used/K	Maximum Temperature/K
μGC1				
Pre-column	Molecular sieve 5A	0.32 mm, 10 m	383	453
Analytical column	Al ₂ O ₃ doped with MnCl ₂	0.53 mm, 4 m	77	473
Reference column	Capillary	--	383	453
μGC2				
Module a				
Analytical column	HayeSepA	0.5 mm, 25 cm	308 - 423	433
Reference column	Capillary	--	308 - 423	433
Module b				
Analytical column	Molecular sieve 5Å	0.32 mm, 4 m	313 - 353	433
Reference column	Capillary	--	313 - 353	433

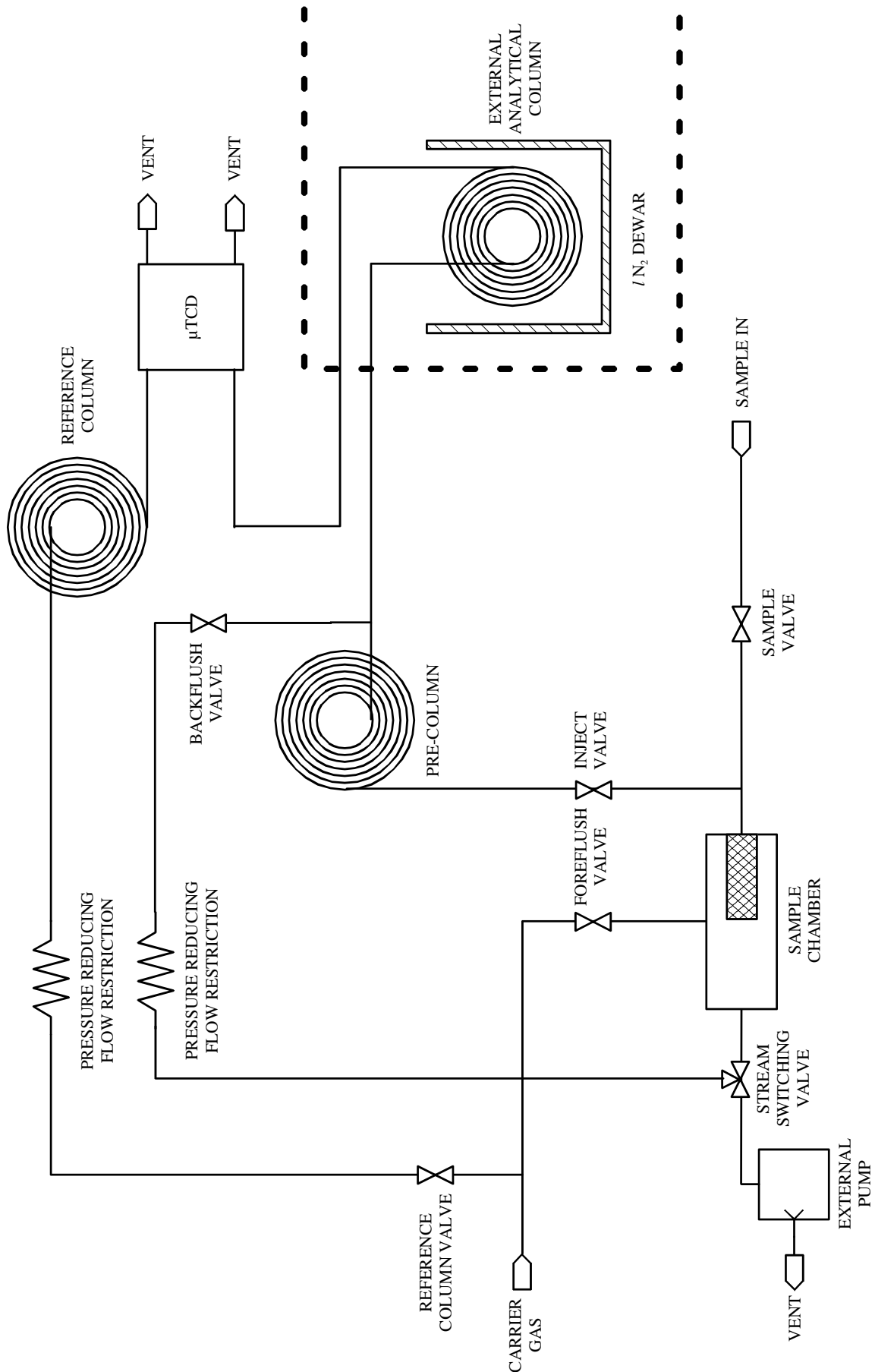


Fig. 3.4.1: Flow diagram of the μ GC1. The equipment between the dashed lines shows the external column in a special dewar.

3.5) The micro gas chromatograph μ GC2

3.5.1) Flow diagram of μ GC2

The schematic flow diagram of one of the two modules of the micro gas chromatograph μ GC2 is presented in Fig. 3.5.1. Two modules (Module a; Module b) are incorporated in μ GC2 of the type CP2002 which was purchased from the Company Chrompack GmbH (now Varian Deutschland GmbH).

The main components of the μ GC2 are

- pressure reducing flow restrictions,
- the analytical columns (HayeSepA 25 cm (module a) and molecular sieve 4 m (module b)),
- the reference columns,
- the ovens,
- the micro thermal conductivity detectors (μ TCDs),
- various valves such as sample in valve, switching valve, inject valve, reference column valve,
- the pump.

3.5.2) Operation of μ GC2

When a sample is to be injected into the sample loop, the sample is continuously purged by the vacuum pump with the switching valve in the position as indicated in Fig. 3.5.1. After the purging time, the switching valve is moved into the other position and the sample injected into the analytical side. In this way it is guaranteed that only the sample to be determined is injected into the analytical column. In the columns which can be heated the separation of the different gas species in the sample occurs and the gas species eluting at different retention times are measured quantitatively with the micro thermal conductivity detectors (TCDs).

3.5.3) Photos of the micro gas chromatographs μ GC1 and μ GC2

The experimental set-up of the two micro gas chromatographs μ GC1 and μ GC2 used at the Tritium Laboratory Karlsruhe (TLK) is shown in Figs. 3.5.2, 3.5.3 and 3.5.4.

Fig. 3.5.2 shows the two μ GCs next to each other. A flow meter to measure the exhaust flow rates is placed on top of the Agilent μ GC1. On the right side of μ GC1 the external analytical capillary column is easily recognisable. On its left side, one can see the Chrompack μ GC2 which is used to measure impurities in gas mixtures. The small electronic equipment on its left side is an electronic recorder.

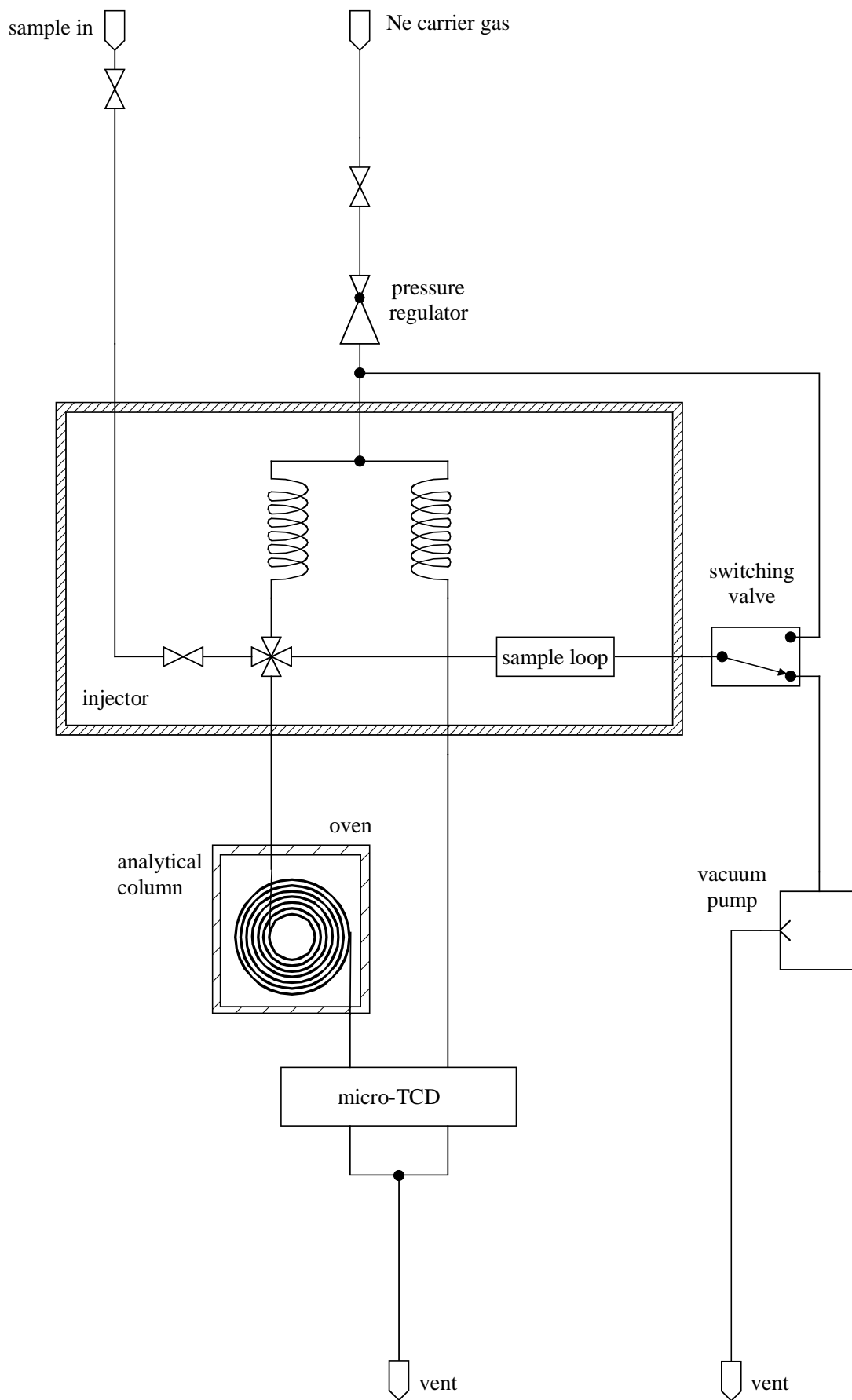


Fig. 3.5.1: Flow diagram of one of the two modules of the μ GC2: The equipment between the dashed lines shows the external column in a special dewar.

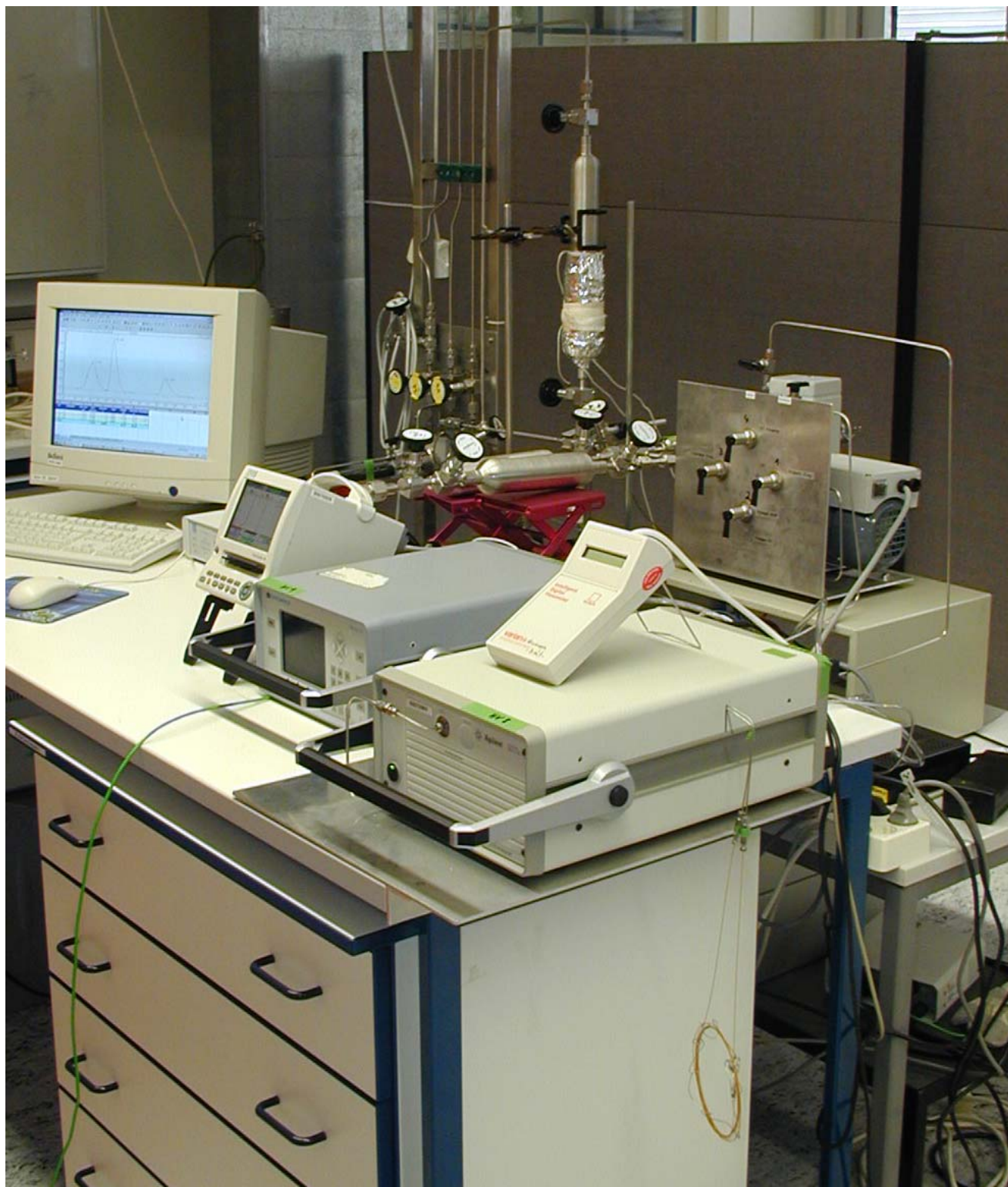


Fig. 3.5.2: View on μ GC1 (instrument on right side with flow meter), μ GC2 (on the left side of μ GC1), electronic recorder (on the left side of μ GC2) and gas inlet system with valves, pipe work and mechanical pump in the background.

Fig. 3.5.3 shows a bird view on the micro gas chromatography instrumentation. In the right upper corner the electronic transfer unit and the display unit for showing the chromatograms are visible.



Fig. 3.5.3: Bird view on the experimental set-up of the micro gas chromatographs μ GC1 and μ GC2 and on the pipe work used for preparation and injection of samples.

Fig. 3.5.4 shows the Agilent μ GC1 with the capillary column inserted (left side) and removed (right side) from the dewar. Easily recognisable are the 1/16" stainless steel connections, the zero dead volume connectors and a few of the connections at the back of the μ GC1.



Fig. 3.5.4: Agilent μ GC1 with external analytical column placed in liquid nitrogen and freely hanging. The oven for regeneration of the column is visible behind the dewar in the photo on the right side.

3.6) Major components of the gas chromatographs GC1, GC2 and GC3

3.6.1) Thermal Conductivity Detectors (TCDs)

Commercial thermal conductivity detectors of the type C79211-A3005-A4 from the Siemens AG are used in the three gas chromatographs GC1, GC2 and GC3. The TCD has three ranges, each different from the other ones by a factor of 16. The output voltage can be reversed to obtain always positive peaks in the TCD chromatograms. The temperature and the bridge current normally used as well as the maximum bridge current of the various TCDs are shown in Table 3.2.

3.6.2) Helium ionisation Detector (HeD)

A commercial helium ionisation detector of the type C79211-A3020-A1 from the Siemens AG is used in System 1 of GC1. Gases passing through the HeD are irradiated by the β^- -electrons produced by the decay of tritium dissolved in a thin titanium-tritide (TiT_x) layer and their secondary electrons. When helium is used as carrier gas, helium atoms are ionised by these electrons and metastable helium can be produced. The metastable helium can lose its energy by special interaction with other gases. In this process other gases present can become ionised and their charges can be measured in an ionisation chamber. The probability of gases in the helium carrier to get ionised by the metastable helium atom is far higher than by direct impact of β^- -electrons or their secondary electrons. This process guarantees that even very small concentrations (ppm) of gases are ionised and detected.

The activity of the TiT_x -layer was 16.1 GBq at the time of purchase. The surface conditions of the TiT_x -layer as well as the purity of the carrier gas are important factors for the functioning of a HeD. A very small amount of hydrogen is added to the carrier gas to produce a constant flow of "impurities" through the HeD-A and to achieve a constant "zero" signal.

The leak rate of the HeD-A does not fulfil the TLK specifications for leak tightness because gas chromatographs and their detectors normally work at pressures higher than the surrounding atmosphere and contamination of the samples to be analysed does normally not occur. In the case of the HeD-A a higher leak rate was tolerated because the outer parts of the HeD-A are purged with helium gas to remove any desorbed tritium before its release. Desorption of very small amounts of activity from the TiT_x -layer occurs even at room temperature despite the high affinity of hydrogen and tritium to titanium and the presence of oxygen layers on the surfaces. This non-avoidable desorption is the reason that the HeD-A is operated at relatively low temperature in comparison to the other detectors. See Table 3.2. HeDs have to be calibrated from time to time because the tritium concentration in the TiT_x layer decreases with time and therefore also the response.

3.6.3) Ionisation Chambers (ICs)

Ionisation chambers of small active volume of 3.5 cm^3 were designed by TLK and built by the company Münchner Apparatebau (MAB). Only tritium compatible materials are used and the leak rate of these ICs is smaller than $10^{-10} \text{ Pam}^3\text{s}^{-1}$. The IC has two ceramic feedthroughs for voltage application and current measurement and two 1/8" Cajon connectors that the gases can flow directly through the active volume. The applied voltage is 90 V. Background current changes between 0.1 and 3

pA depending on the contamination level. 1% tritium in these ICs causes a signal of 100 nA.

Three ICs of this type are used in GC1, two in GC2 and three in GC3.

3.6.4) Columns used in the various gas chromatographs

In the conventional gas chromatographs only packed columns are used. The wall material of the columns is stainless-steel with the exception of Cu for the low temperature column (column-B of GC1 and column-C of GC3). These columns contain Al_2O_3 doped with iron to promote the ortho-para interconversion. This simplifies the analysis of the chromatograms which would otherwise contain separate peaks for ortho- and para-hydrogen when no iron were present.

The column-A of GC2 contains in reality 2 columns in sequence, one PORAPAK QS and one CHROMOSORB 104.

Details of the columns with respect to the packing material, diameter, total length, temperature normally used and maximum temperature are given in Table 3.1.

3.6.5) Use of Valco valves

Commercial Valco valves of the type C79211-A3022-A4 from the Siemens AG are used.

Valco-A of GC1 contains ceramic parts as rotor and stator. Due to the smaller leak rate of the ceramic Valco valve no purge gas is used.

Samples are injected into the gas chromatographs and carrier gas flows are diverted by switching these Valco valves. They are designed to avoid any dead, unpurged volumes and for instantaneous switching of multiple gas flows. Due to the construction and the movement of the inner parts, the Valco valve does not fulfil the stringent leak tightness requirements of a tritium handling facility. With the exception of the ceramic valve only Valco valves with the possibility to purge the outer volume with carrier gas are used. In this way a reduction of tritium release into the glove box atmosphere is achieved. This is especially important during the compression and injection when the pressure of the gas sample is higher than the glove box atmosphere. The Valco valves are operated at 420K. Their maximum operating temperature is given as 493K.

The purge gas also helps to reduce the contamination of the gas sample by in-leakage of glove box atmosphere, e.g. during the evacuation at the start of a compression when the compression loop is filled with subatmospheric pressure because then mainly the gas used for purging will leak into the compression loop. The purge gas is very often of the same type as the carrier gas and will therefore not be detected in the GC-system. The main negative effect is that the presence of the purge gas will reduce the total amount of gas sample to be analysed during the compression.

3.6.6) Carrier gases and flows used in GC1 and GC2

The helium gas used as carrier is supplied from a multi gas cylinder supply. Its purity is better than 99.9996% and it is sent through a metal catalyst to reduce the impurity level even further before being supplied to the GCs.

The nitrogen stems from a liquid nitrogen source, where liquid nitrogen is evaporated and compressed to 0.8 MPa. The nitrogen gas passes through a SAES getter before being fed to the GC-system. Its purity is better than 99.9999%.

For GC1 and GC2 the flows of the carrier gas through analysis- and reference side of the TCDs and through the HeD-A as well as the purge flows through the Valco valves are given in Table 3.3 together with their supply pressures.

3.6.7) Pipe work and valves

Mainly stainless-steel tubes of 0.16 cm (1/16"), 0.32cm (1/8"), and 0.64cm (1/4") diameter are used. The connections are Cajon VCR or special gas chromatographic fittings. The valves (size 4, all metal with metal bellows) used were purchased from the company Nupro.

3.7) Injection of calibrated gas mixtures into GC1, GC2, GC3, μ GC1 and μ GC2

3.7.1) Injection of calibrated gas mixtures into GC1 and GC2

Any gas chromatograph used for quantitative analysis needs to be checked frequently with respect to the used calibration factors and for the occurrence of drifts. This is best done by the use of well known calibration gas mixtures which are permanently connected to the GCs and which therefore can easily be analysed.

Fig. 3.7.1 shows schematically the connection of various gas bottles containing inactive calibration gas mixtures with the GC1 and GC2. The gas bottles are located within a safe gas bottle cubicle through which a constant air stream passes which is monitored for the occurrence of leaked combustible gases.

Each gas bottle is equipped with a gas bottle valve, a two stage pressure regulator with a pressure indicator at the entrance and at the exit and a further manual valve. Gas bottles can be exchanged and the air between the gas bottle valve and the manual valve can be pumped off by using the pump KP902 to avoid contamination of gases with air.

The gas bottles are connected via a common manifold which is also used to transfer samples for calibration purposes to the TMT glove box. Samples are injected into GC1 or GC2 by means of the automatic valves AV023 and AV020, respectively. If a further calibrated gas mixture is required, then the interconnecting line will be evacuated using KP902 and if necessary even purged a few times and finally filled with the new calibrated gas mixture.

In addition, also the carrier gas supplies for Ne and He are shown. He is supplied from a special He ring manifold which serves also other equipment of the TLK, whereas Ne is supplied from a special gas bottle located also in the safe gas bottle cubicle.

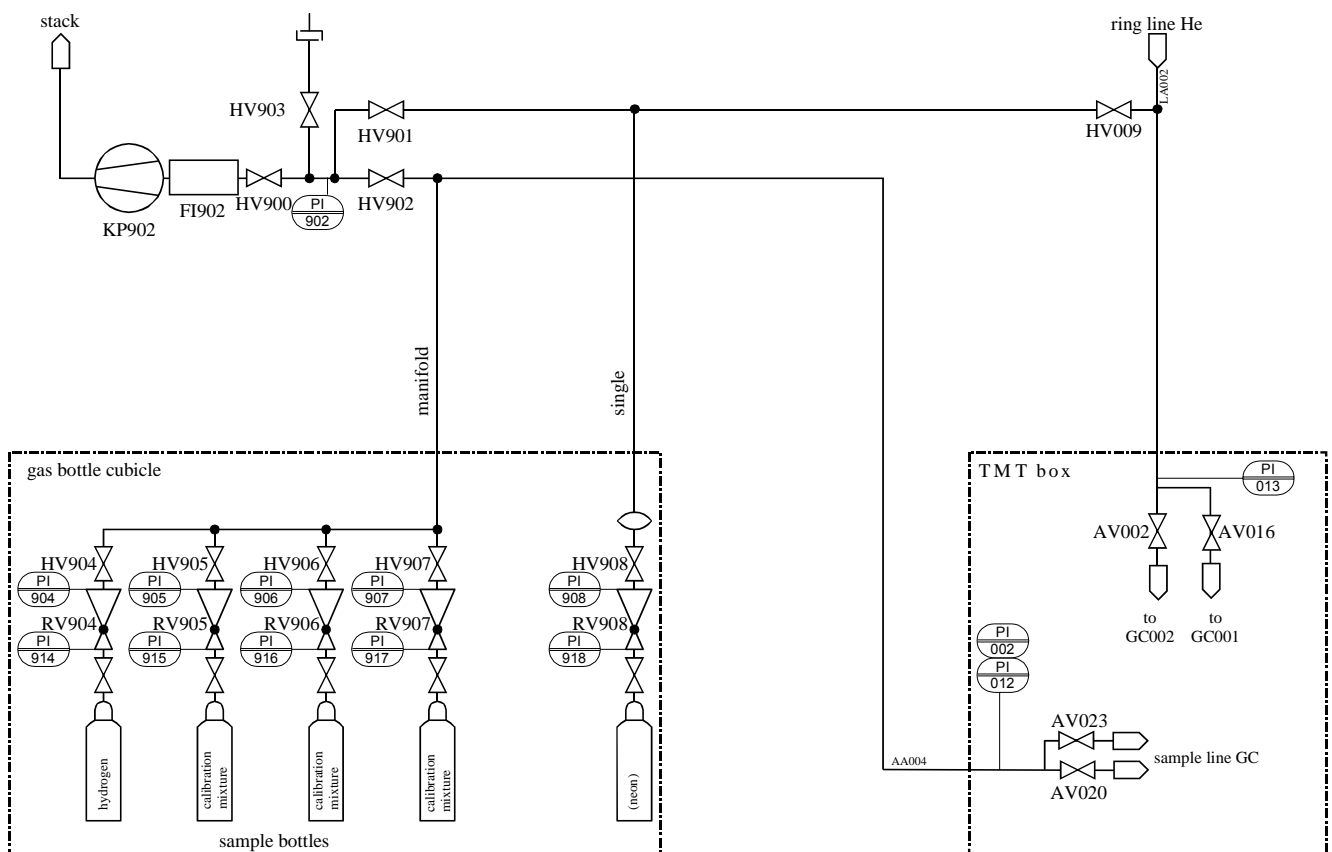


Fig. 3.7.1: Connections of calibrated gas mixtures to GC1 and GC2 of TMT.

3.7.2) Injection of calibrated gas mixtures into GC3

The permanent installation of gas bottles with calibrated gas mixtures for analytical gas chromatographs may be expensive, but is the preferred and clean solution. Another possibility is to connect special small sample containers with calibrated gas mixtures to the entrance of the GCs. This technique is used in case of GC3 in the CAPER facility. The main disadvantage of this solution is the possibility of the injection of other gas species because of leaking connections or not well evacuated and purged containers. Furthermore the continuous reconnection and disconnection within glove boxes is work intense and should be limited as far as possible because the newly made connections can often not be checked with the required standards, e.g. with a highly sensitive He-leak detector.

3.7.3) Injection of gas mixtures into μ GC1 and μ GC2

The injection of gas mixtures into μ GC1 and μ GC2 is shown schematically in Fig. 3.7.2. Certified gas mixtures and the carrier gases He and Ne are stored in the safe gas cylinder cubicle shown in the lower right corner. In addition samples from other experiments can be connected using sample cylinders of which two are presented in Fig 3.7.2. On the left side a further bottle containing either He or Ne is connected which is used to dilute gas mixtures to be analysed if required. The mixing is done in the closed gas loop with the manual valves HV010 and HV011. Into the evacuated loop a certain amount of the gas mixture to be diluted is added and then the loop is topped up either with Ne or He. The gases are circulated in the vertical loop by simply heating the reservoir between the valves HV010 and HV011. In this way mixtures of hydrogen isotopes with helium or neon were created to reduce the injected hydrogen gas amount, to achieve perfect separation of the different hydrogen molecules and to avoid overfilling of the capillary column. See Section 5.

The pipe work, the valves, the pump and the reservoir between the valves HV010 and HV011 partly covered with Al foil to distribute the heat generated by a simple electrical heater are easily visible in Figs. 3.5.2 and 3.5.3.

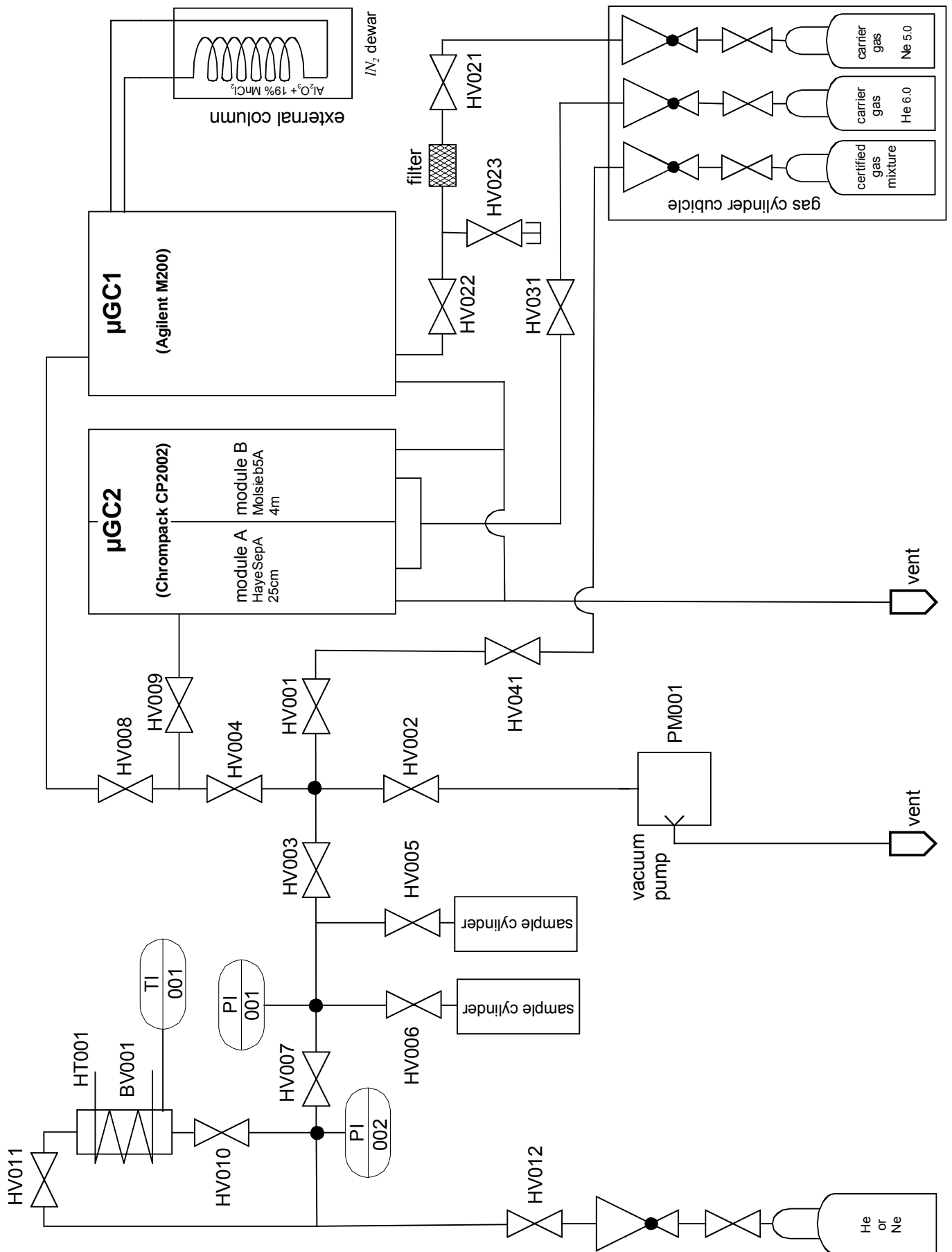


Fig. 3.7.2: Connections of calibrated gas mixtures for μGC1 and μGC2.

4) Analysis by means of conventional gas chromatography

In the following various results obtained with the three gas chromatographs GC1, GC2 and GC3 are reported. In Section 4.1 the compression pressures used for the injection of compressed gas samples into GC1 and GC2 are determined, whereas the minimum pressure for which still full compression can be achieved is presented in Section 4.2. The anomaly of the thermal conductivity of He-H₂ gas mixtures and its influence on the use of thermal conductivity detectors is discussed in Section 4.3. In the subsequent Sections 4.4 to 4.5 various chromatograms for inactive and tritium containing hydrogen gas mixtures, also with impurities, are presented and comparative studies are performed between the three different GCs. Many chromatograms are presented to demonstrate the usefulness of the gas chromatographs employed and the variety of measurements, which can be performed with conventional gas chromatography. The calibration factors of the various gas species are listed for the detectors of GC1 and GC2 in Section 4.6.

4.1) Determination of the compression pressures in the injection loops of GC1 and GC2

In the conventional gas chromatographs of TMT compressed and uncompressed samples can be injected into the GCs for analysis.

4.1.1) The compression pressures in the injection volumes of GC1

The peak areas observed by any detector should vary linearly with the pressure of the gas sample in the injection loop. This technique is often employed to check the linearity of the detectors in use. A very accurate pressure gauge is required to measure the pressure in the injection volume.

Here the already otherwise proven linearity of the TCD-detector is used to determine experimentally the compression pressure in the injection loop just before the injection.

The circles plotted in Fig. 4.1.1 are the results of the injections of pure deuterium of different pressures via Valco-A into the system 1 of GC1 and of the determinations of their peak areas. During this process the valve VA1 in Fig. 3.1.1 is open to allow the determination of the gas pressure by a pressure gauge connected to the left side of VA1 and VA2 is kept closed. Clearly the experimentally determined circles are well described by a linear relationship as indicated by the red straight line.

The two further experimental points characterised by squares were obtained after compression of the gas in the capillary in front of Valco-A. The pressure indicated on the x-axis is the pressure in the injection loop before the compression, when VA1 was open and VA2 closed. After closing VA1, VA2 was opened, the gas sample compressed with the carrier gas He and then the sample injected into GC1 via rotation of Valco-A. As expected the D₂ peak area of the compressed samples is independent of the pressure in the injection loop before the compression. Simple horizontal extrapolation up to the straight line gives the pressure in the injection volume after the compression which was determined to be 0.15 MPa for the injection volume of Valco-A. From the experimental set-up it is clear that the injection volume of Valco-C of GC1 sees the same compression pressure of 0.15 MPa.

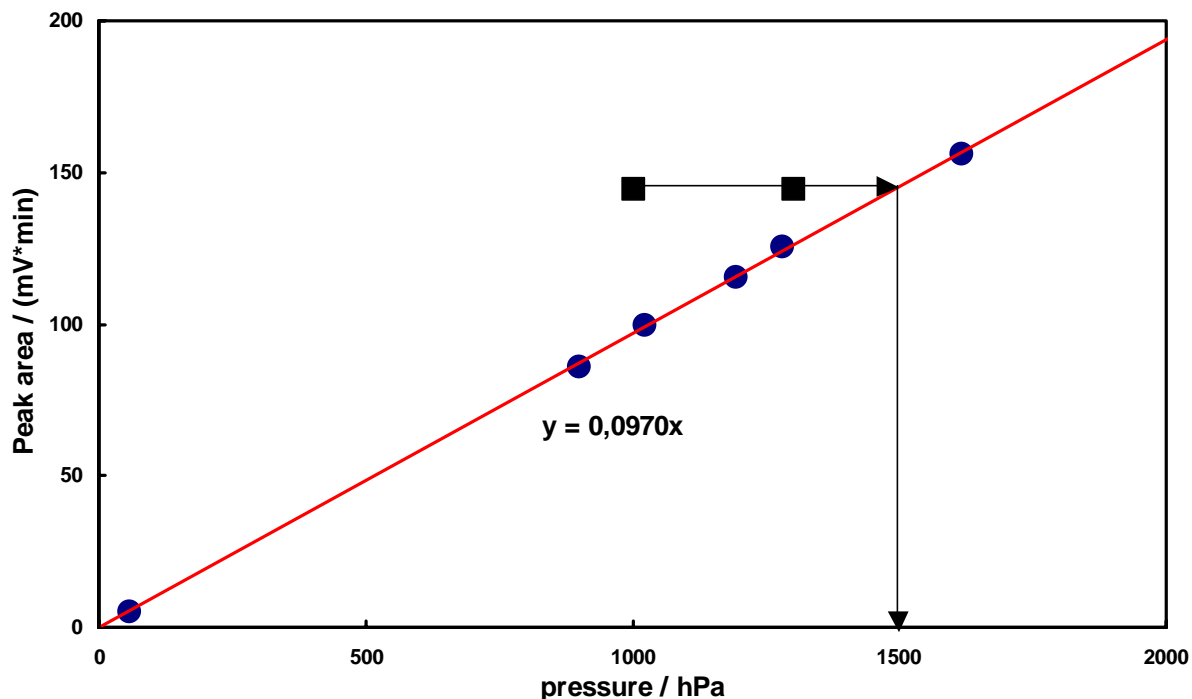


Fig. 4.1.1: Area of the D₂ peak as a function of the pressure in the injection loop of GC1.

4.1.2) The compression pressure in the injection volume of GC2

The compression pressure in the injection volume of Valco-A of GC2 (see Fig. 3.2.1) was determined in a similar way as for GC1. Dry air samples of various, but known pressure were injected and their peak area of the TCD-B of GC2 determined. Again a linear relationship is observed as shown in Fig. 4.1.2.

Horizontal extrapolation through the data points obtained for compressed samples as indicated by the horizontal arrow gives a compression pressure of 0.21 MPa for the injection volume of Valco-A of GC2.

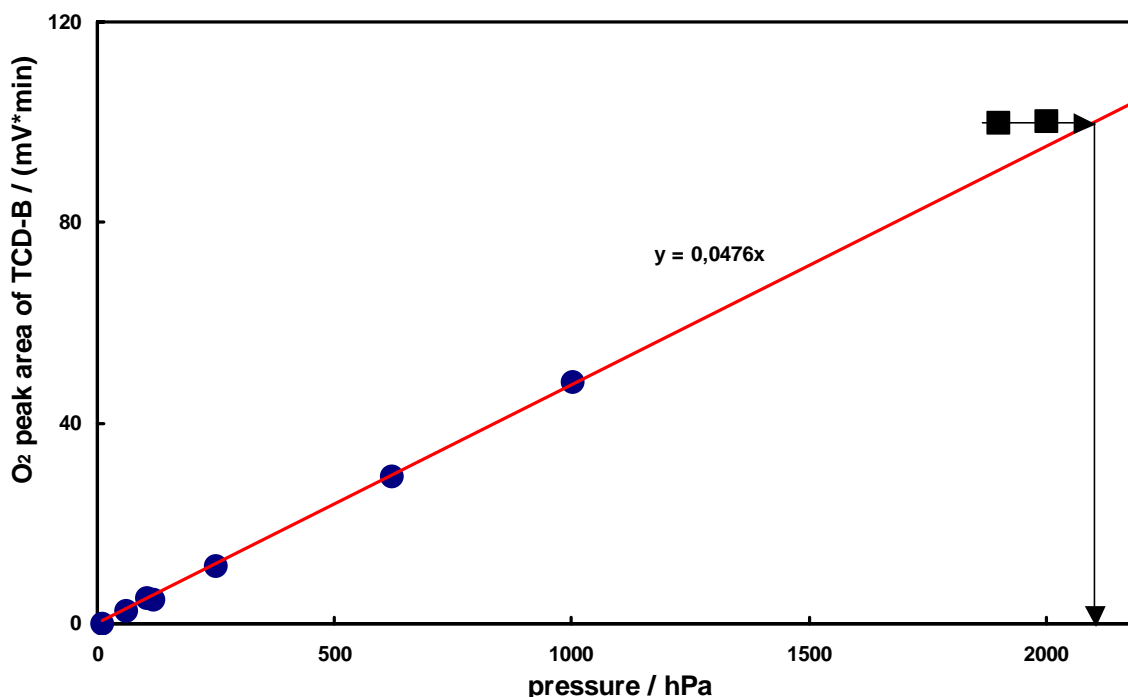


Fig. 4.1.2: Area of the O₂ peak as a function of the pressure in the injection loop of GC2.

4.2) Minimum pressures in the compression loops required for full compression in GC1 and GC2

In the previous section the maximum pressures achieved during the compression were determined for GC1 and GC2. These pressures depend on the down stream pressure regulators (FC1) installed in the compression lines for GC1 (see Fig. 3.1.1) and GC2 (see Fig. 3.2.1).

Another important information is the knowledge of the minimum pressures in the compression loops for which full compression in the injection volumes can be achieved. These pressures are determined experimentally by decreasing the pressure of the gas sample in the injection loop, compressing the sample via opening VA2 and analysis of the observed peak areas of the gas species in the compressed sample. Fig. 4.2.1 shows peak areas for pure H₂ as a function of the pressure in the injection loop of system 1 of GC1. Below 2.2 kPa the peak area decreases continuously because also the gas He used for compression is transferred into the injection volume and the sample gas is compressed primarily into the dead end of the compression loop next to the Valco valve. This reduces the amount of protium which can be injected into GC1 and therefore the peak area. The He transferred with the sample into the injection volume is not observed because helium is used as carrier gas. The peak areas are equal within the experimental error for pressures above 2.5 kPa.

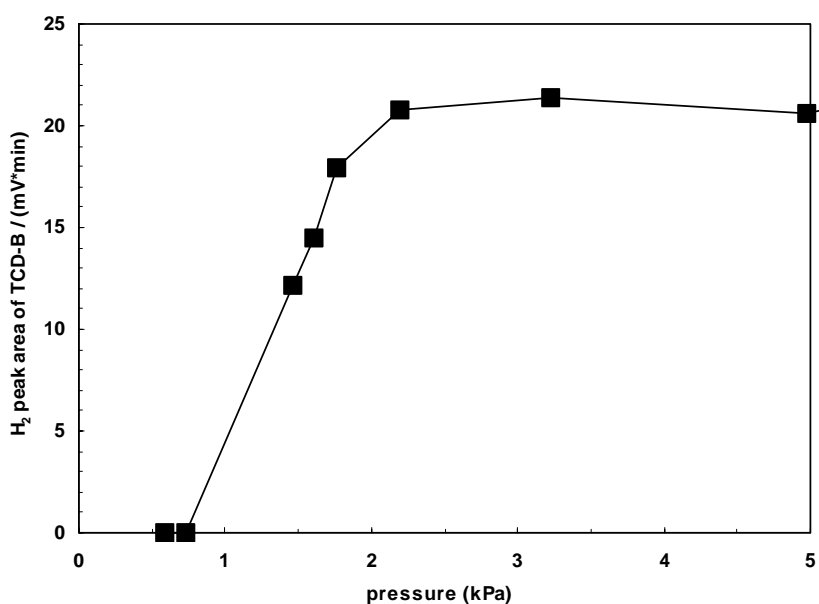


Fig. 4.2.1: H₂ peak areas obtained with TCD-B of GC1 after compression as a function of the pressure in the injection loop of system 1.

Fig. 4.2.2 presents similar experimental data obtained with the TCD-C of system 2 of GC1 for a hydrogen-helium mixture. Above 1.8 kPa the peak areas for helium and for hydrogen are constant. This means that sufficient gas to be analysed is available in the compression loop for the compression of pressures above 1.8 kPa and that the gas used for compression can not enter the injection volume of Valco-C. Below 1.8 kPa the peak area for hydrogen decreases because helium used as compression gas enters the injection volume. A further clear evidence is that the peak area for helium increases below the 1.8 kPa as additional He is injected. This time helium is detected because system 2 of GC1 uses nitrogen as carrier gas.

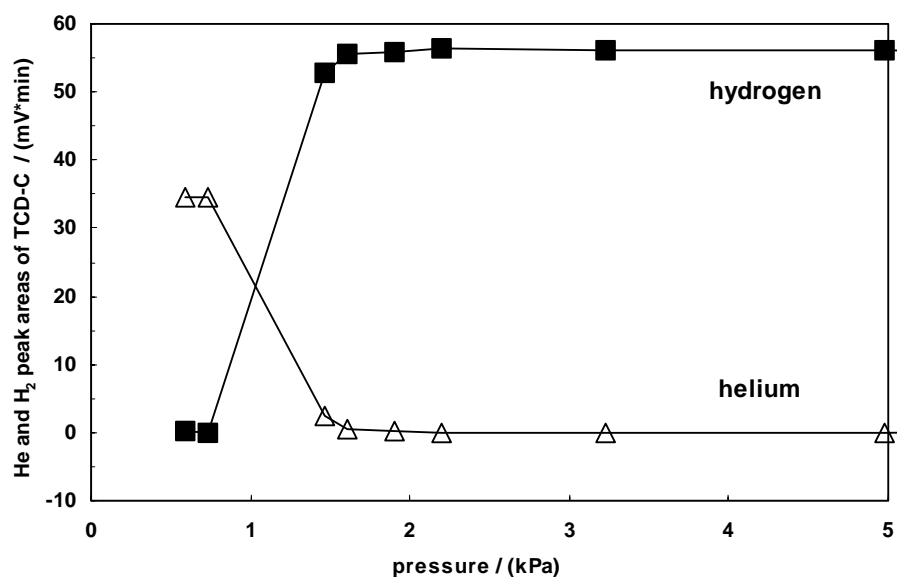


Fig. 4.2.2: Helium and hydrogen peak areas obtained with TCD-C of GC1 after compression as a function of the pressure in the injection loop of system-2.

Similar experiments were also performed for GC2 and the same observations were made. All pressures higher than the pressure which leads to the first reduction in peak area can be used to achieve a compressed sample of the same composition as the original sample at lower pressure.

The lowest pressures for which full compression can be achieved, are 2.5 kPa, 1.8 kPa and 3.0 kPa for system 1 and system 2 of GC1 and for GC2, respectively.

4.3) Analysis of protium by thermal conductivity detectors with He as carrier gas

Helium (He)-protium (H_2) gas mixtures show a minimum in the common thermal conductivity behaviour [1.32]. As a consequence thermal conductivity detectors (TCD) are of limited use when the concentration of protium (H_2) is to be determined and helium is employed as carrier gas. This was already briefly mentioned in Chapter 3 during the presentation of the flow diagrams for GC1 and GC2. In GC1 protium of a flow rate of approximately 2 cm^3 per minute is added in front of TCD-B to achieve a certain mixture of He- H_2 . In this way the protium concentration in the He- H_2 mixture can only increase by the addition of further protium originating from the sample during an analysis. As a consequence the total thermal conductivity of the He- H_2 changes mainly linearly in contrast to the behaviour when no or not enough protium is added in front of a TCD. The latter behaviour is observed with the TCD-B of GC2 when large amounts of protium are injected with the sample because no H_2 is added in front of TCD-B of GC2 and He is used as carrier gas.

The experimental conditions of GC2 during the analysis reported below were

- Carrier gas: He, purity 99.9996%,
- Columns: as specified in Table 3.1 for GC2,
- Sample: see text,
- Uncompressed samples.

Fig. 4.3.1 shows TCD-B chromatograms of the 2 vol% gas mixture specified in Table 4.1 and measured with GC2 up to retention times of 3.6 minutes. The amount of sample injected into GC2 was changed by simple modification of the pressure in the injection loop. The area under the peak of O_2 at the retention time of 3.25 minutes changes linearly with the pressure given in hPa as expected, but the peaks at just below 2.8 minutes which are attributed to protium, show various shapes which will be explained in the following in more detail.

Table 4.1: Composition of the 2 vol% gas mixture in H_2 :
0.98% O_2 , 2.14% N_2 , 1.97% CH_4 , 2.00% CO , 2.04% CO_2 , 90.87% H_2 .

As long as the resulting H_2 concentration in the carrier gas stays far below the H_2 concentration belonging to the thermal conductivity minimum, the peak area changes almost linearly with concentration as is observed in Fig. 4.3.1 maybe up to a pressure of 527 hPa. When the H_2 concentration in the carrier gas helium causes the corresponding minimum in the thermal conductivity, the shape of the TCD-B signal shows a broad maximum. When the H_2 concentration goes beyond this minimum, then the height of the TCD-signal decreases and reaches the base line when the thermal conductivity of the He- H_2 mixture is again equal to the pure He gas. Up to this protium concentration the same value of the thermal conductivity of the He- H_2 mixture can be achieved by two different protium concentrations. Therefore the relationship between the thermal conductivity and the concentration of protium is not any more unique. If even more H_2 is present in the He gas, then the thermal conductivity of the gas mixture becomes larger than the one of pure He and the TCD-B signal gets negative with respect to the base line. The size of the minimum in the TCD-signal depends only on the maximum protium concentration in the helium carrier gas. When the H_2 concentration in the carrier gas starts to decrease again, the TCD-signal follows again the same behaviour. The TCD-B shape of the H_2 peaks in most of the chromatograms shown in Fig. 4.3.1 is

asymmetrical because the concentrations profiles of H₂ eluting from the separation column are asymmetrical.

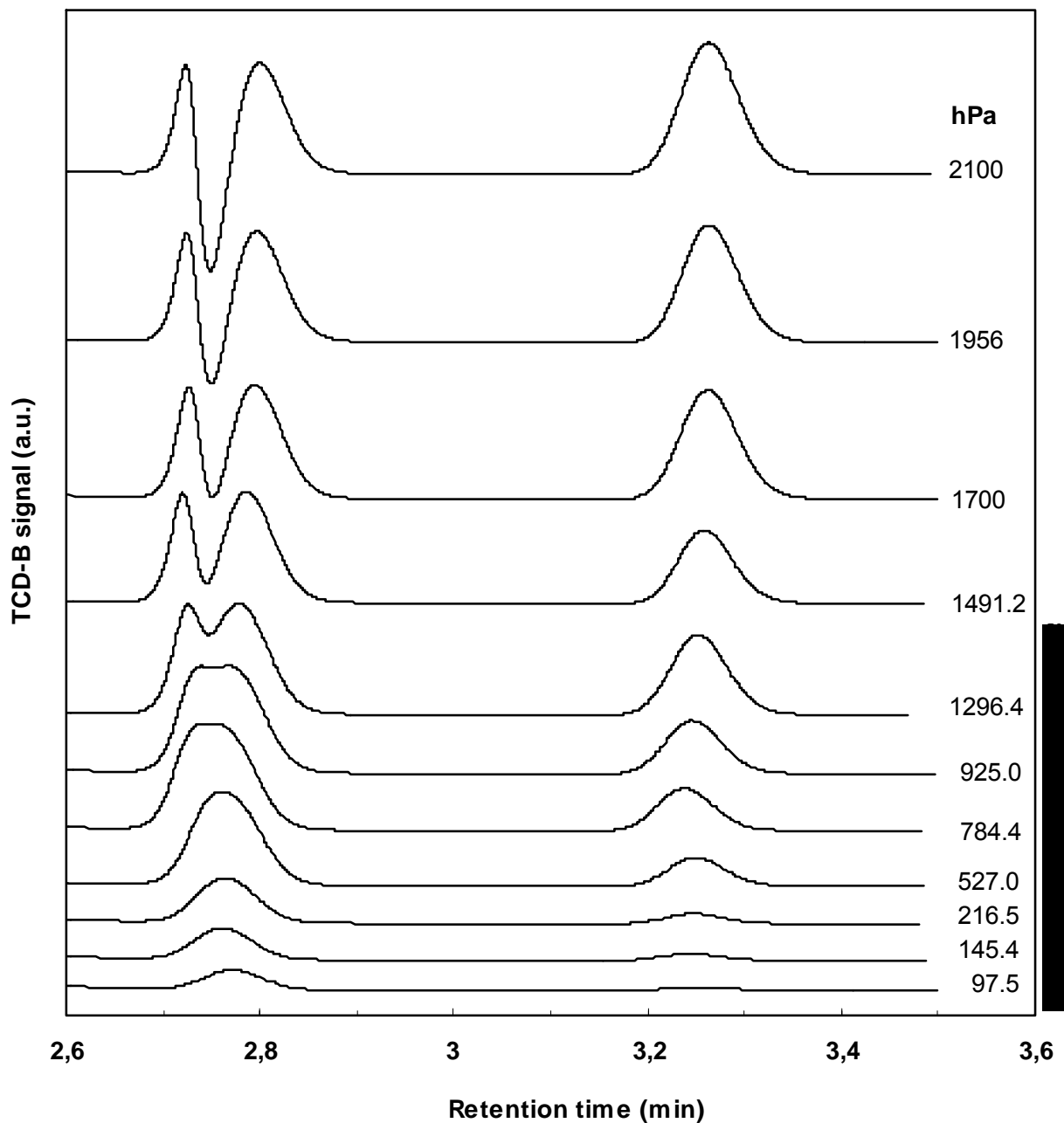


Fig. 4.3.1: TCD-B chromatograms obtained with GC2 as a function of the injection pressure in the compression loop for the 2 vol% gas mixture given in Table 4.1. The peaks at 2.8 and 3.25 minutes are due to H₂ and O₂, respectively.

No protium shapes with a minimum in the H₂-peak (similar to the ones in Fig. 4.3.1) have been observed with the TCD-B of GC1 for gases containing even pure protium because enough protium is added in front of the TCD-B of GC1.

4.4) Analysis of ^3He , hydrogen gas and hydrocarbon mixtures

4.4.1) Observation of hydrogen gas mixtures with GC1

In this section only chromatograms obtained with the TCD-B or IC-B of GC1 are presented.

The experimental conditions of GC1 during the analysis reported below were:

- Carrier gas: He, purity 99.9996%
- Columns:
 - Column-A: Porapak (6 m),
 - Column-B: Al_2O_3 (2 m),
- Samples: see text below,
- Detectors:
 - TCD-B
 - IC-B
- Compressed sample: yes/no.

Inactive hydrogen gas mixtures observed with TCD-B of GC1

a) The chromatogram of the inactive hydrogen mixture containing 49.0% H_2 , 2.3% HD and 48.7% D_2 is shown in Fig. 4.4.1. The chromatogram is obtained with TCD-B of GC1 for a compressed sample. The H_2 and the D_2 peaks are highly asymmetrical, a sign that the gas amount injected is too high to be handled adequately by the column-B of GC1, whereas the HD peak form is nicely symmetrical. The reason is that all the HD molecules find enough free active sites during their passage through column-B resulting into a symmetrical peak, whereas in the case of D_2 due to the large number of D_2 molecules not enough active sites are available resulting in too many molecules exiting the column at a too short retention times leading to the asymmetry in the peak form. As a consequence the HD and D_2 peaks are very near together and in the case, when HT at low concentrations were present in the gas mixture, part or even most of the HT would be covered by the D_2 peak and possibly not detected by the TCD-B.

It is interesting to note that the peak area of H_2 is far lower than the D_2 peak although the H_2 concentration is comparable to the D_2 one. This is a consequence of the addition of H_2 to the helium carrier gas in front of the TCD-B. If no protium were added to the carrier gas and no anomaly in the thermal conductivity of He- H_2 existed, the TCD-B signals for H_2 and D_2 should have opposite signs. As this is not the case, the mixture created by the addition of protium to the carrier gas must have a total thermal conductivity slightly smaller than the one of pure He, but still higher than the one of deuterium. This explains why the same amount of protium produces a smaller peak than deuterium as seen in Fig. 4.4.1.

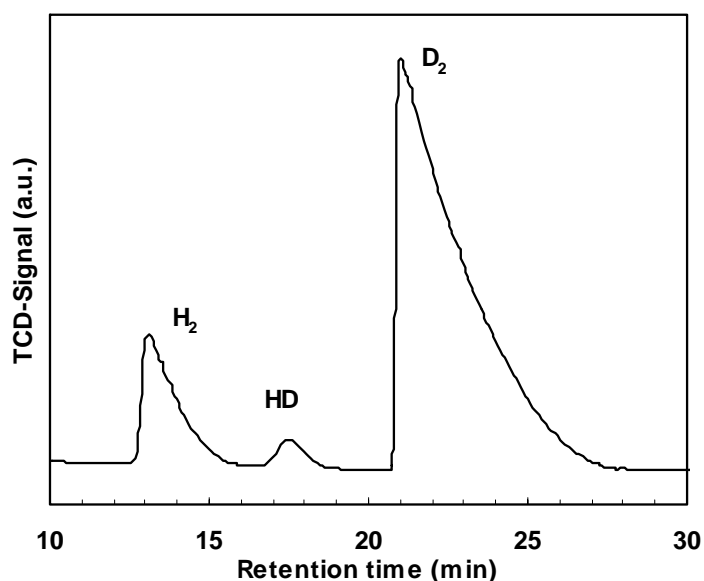


Fig. 4.4.1: TCD-B chromatogram of a hydrogen isotope mixture with 49.0% H₂, 2.3% HD and 48.7% D₂ measured with GC1.

b) Further examples of inactive hydrogen gas mixtures are given in Fig. 4.4.2. At the top, in the middle and at the bottom the chromatograms of pure protium (purity 99.9999%), of a hydrogen gas mixture of 25.4% H₂, 48.0% HD and 26.6% D₂ and of “pure” deuterium (0.3% HD, 99.7% D₂) are shown, respectively. Compressed hydrogen samples were injected into GC1, the separation occurred in column-B of system 1 at 77 K and the gas species were detected with the TCD-B. The peak shape is highly asymmetrical for all major gas species due to the large injected sample amount. Only the enlarged HD peak of the “pure” deuterium gas is symmetrical due to the comparatively small number of HD molecules injected.

A further important observation is that the retention times for the hydrogen gas species changes with their content in the injected sample. The retention time decreases for the gas species with larger concentrations. This is clearly observed for the three molecules H₂, HD and D₂. The pure H₂ and D₂ peaks appear at shorter retention times than the corresponding peaks of the gas mixture presented in the middle of Fig. 4.4.2. A qualitative explanation for this behaviour was already given above.

This observation of retention times changing as a function of the amount of injected hydrogen gas species is a nuisance as it makes the clear identification of the hydrogen molecules slightly more difficult. Therefore, in the case of tritiated hydrogen gas mixtures, when sometimes not all six hydrogen molecules are observed, the use of a further detector, e.g. of an ionisation chamber, can be very helpful in identifying correctly the observed peaks.

The three TCD-B chromatograms of GC1 show clearly that the sensitivity for protium is lower than for deuterium if He is used as the carrier gas and protium is added in front of the TCD-B of GC1 on the measurement side. In other words the sensitivity of the TCD-B increases with increasing mass of the hydrogen molecules or tritium (T₂) shows the highest sensitivity of all hydrogen molecules.

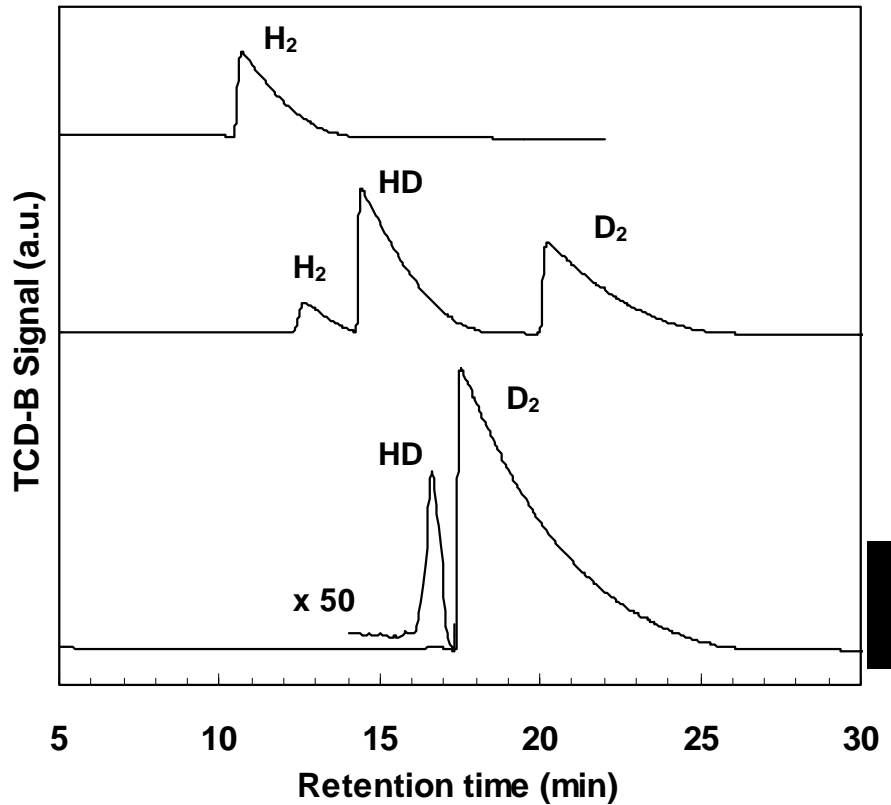


Fig. 4.4.2: TCD-B chromatograms of 99.9999% protium (top), of a 25.4% H₂, 48.0% HD and 26.6% D₂ hydrogen gas mixture (middle) and of 0.3% HD, 99.7% D₂ gas mixture (bottom) measured with GC1.

c) Fig. 4.4.3 shows further TCD-B chromatograms of protium-deuterium gas mixtures. Again the same facts as already discussed in the text above are observed. Large hydrogen peaks elute with shorter retention times than small ones. The TCD-B response in the case of deuterium is larger than for protium. See also the calibration factors for TCD-B given in Table 4.7.

Further changes of the retention times can also be caused by variations of the liquid nitrogen level in the dewar.

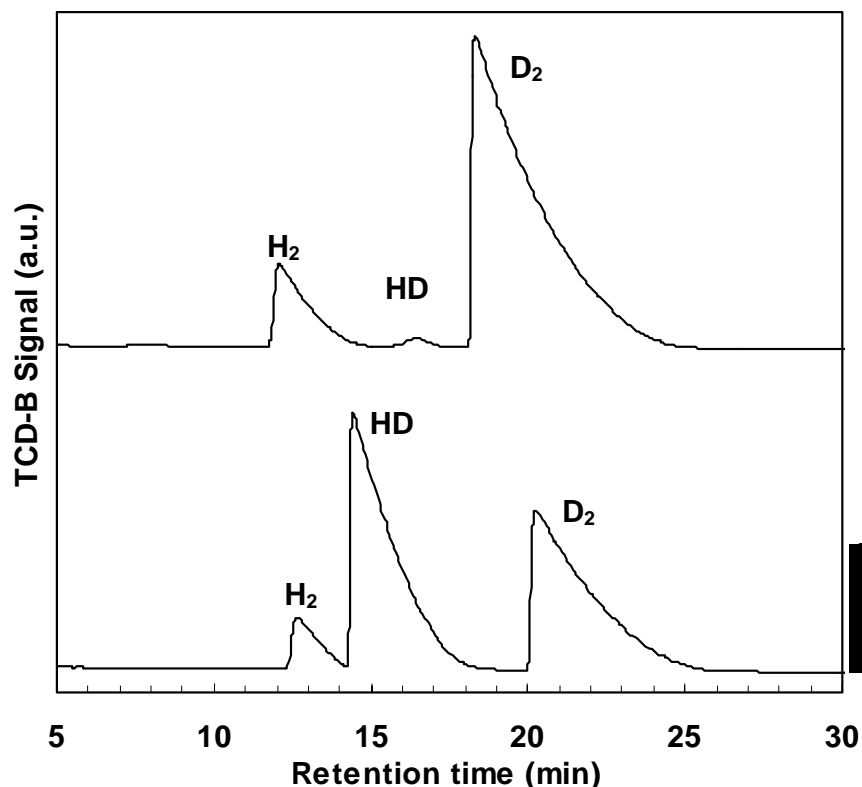


Fig. 4.4.3: TCD-B chromatograms of a 48.1% H₂, 1.1% HD and 50.8% D₂ hydrogen gas mixture (top) and a 25.4% H₂, 48.0% HD and 26.6% D₂ hydrogen gas mixture (bottom) measured with GC1.

Hydrogen gas mixtures with tritium observed with TCD-B of GC1

a) Fig. 4.4.4 presents the TCD-B and IC-B chromatograms of the hydrogen-tritium gas mixture listed in Table 4.2. A straight line is introduced below the peaks of the six hydrogen species to simulate the baseline. Clearly recognisable are six and three peaks measured by the TCD-B and IC-B detectors, respectively. An uncompressed sample with the approximate pressure of 20.4 kPa was injected into System 1 of GC1. The separation was performed with the low temperature column-B. The observed T₂ peak area of the TCD-B signal corresponds to a concentration of 200 ppm in a compressed sample. This shows that tritium concentrations of just about 100 ppm can still be detected with the TCD-B in a compressed sample, whereas they are easily detected with ionisation chambers.

Table 4.2: Hydrogen-tritium gas mixture:
1.7% H₂, 20.2% HD, 0.86% HT, 76.6 D₂, 0.49% DT, 0.15% T₂.

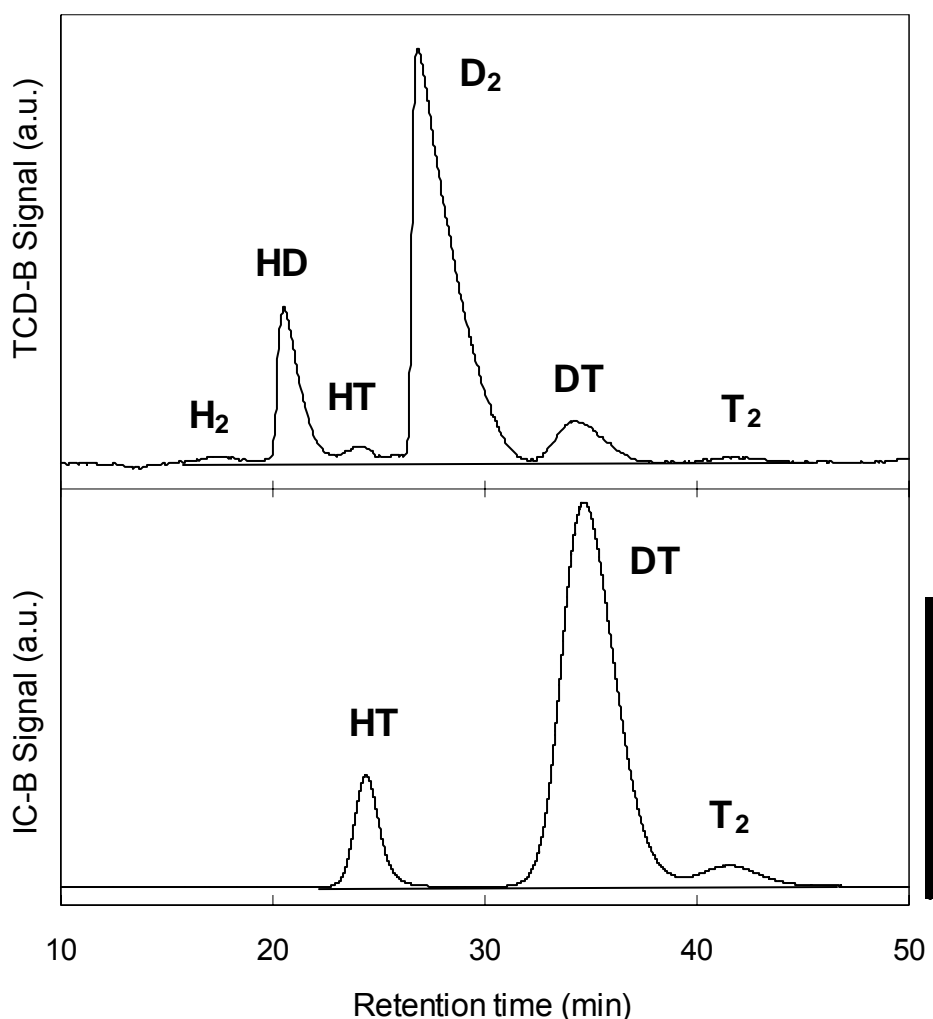


Fig. 4.4.4: TCD-B and IC-B chromatograms of the hydrogen-tritium gas mixture given in Table 4.2 and measured with GC1.

b) The TCD-B chromatograms of 99.9999% protium (top), of 0.3% HD, 99.7% D₂ (middle) and of 0.23% HT, 0.11% DT and 99.66% T₂ (bottom) measured with GC1 are shown in Fig. 4.4.5. Compressed gas amounts of the three mixtures were injected. Again it is easily recognised that the peak area for tritium is the largest, whereas the area for protium is the smallest, a clear sign that He with a small addition of protium is used as carrier gas in front of the TCD. Furthermore, it is interesting to note that the DT peak is not observed in the case of the tritium chromatogram at the bottom. The reason for this is that the main T₂ peak elutes fast, the DT peak slowly and that the two peaks T₂ and DT can overlap when compressed samples are injected. The concentration of the DT peak can only be determined by the analysis of uncompressed samples where all three peaks are detected separately.

c) The TCB-B chromatogram of a tritium mixture containing 0.23% HT, 0.11% DT and 99.66% T₂ is presented in the top of Fig. 4.4.6, whereas the other chromatograms were obtained with IC-B. The HT and T₂ peaks are well separated, but the DT peak is only visible in the two chromatograms at the bottom. The three chromatograms at the top were measured for compressed samples, whereas the two lower ones were obtained

for uncompressed samples of a pressure of 5.1 kPa and 600 Pa. Due to the use of amplification factors of 5000 and 50000 to show the small peaks of HT and DT in the two lower chromatograms the large T_2 peak is cut off and not shown. In the case of the compressed samples the DT peak is not seen because of overlap with the strong T_2 peak. The second chromatogram from the top, the ionisation chamber signal, shows the data as measured. Large peaks seen by the ionisation chamber are reduced by the used Keithley instrument by a factor of 1000 to achieve high accuracy of the recorded data over many orders of magnitude. The curve which is multiplied by the factor of 10^{-3} is clearly indicated. The HT peak of the ionisation chamber shows a far better signal to noise ratio than the TCD-B signal (compare the two chromatograms at the top). This is a clear indication of the far higher sensitivity of ionisation chambers for tritiated gases in comparison to thermal conductivity detectors.

The experimentally observed curve (second from top) for T_2 shown is converted by a simple program to obtain the continuous curve shown in the third spectrum which is used for analysis of the IC results.

The concentration of the DT peak was determined using chromatograms of uncompressed samples where the DT peak is separated from the T_2 peak, see the two spectra at the bottom of Fig. 4.4.6. By means of the IC signal the concentration of tritiated peaks can be determined with higher accuracy than with TCDs.

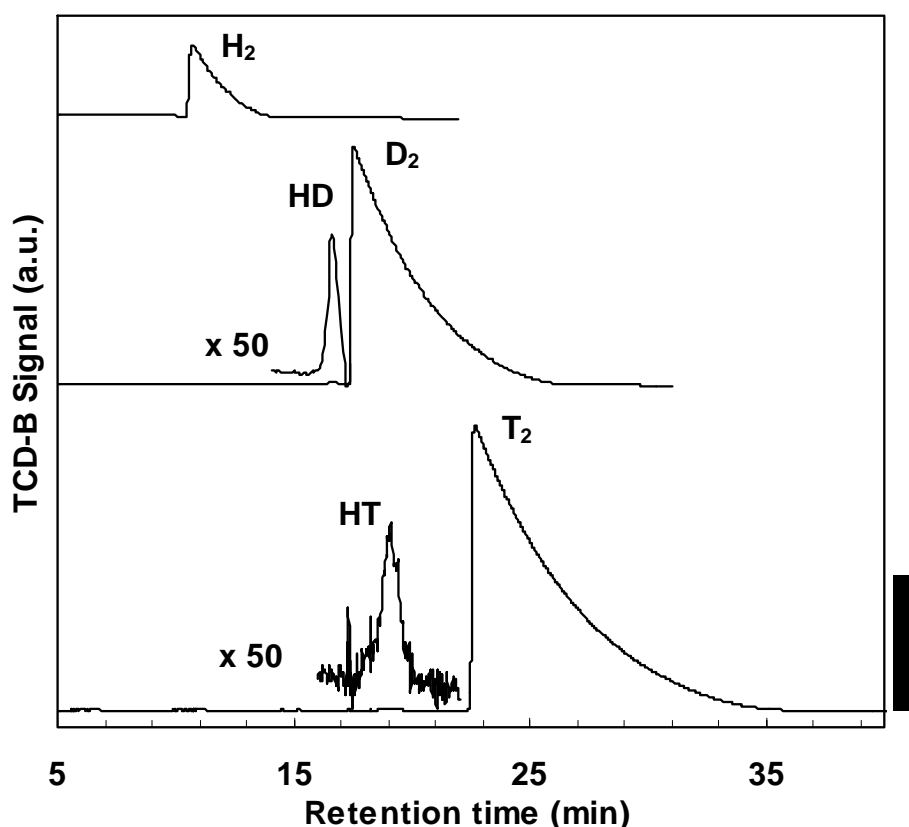


Fig. 4.4.5: TCD-B chromatograms of 99.9999% protium (top), of 0.3% HD, 99.7% D_2 (middle) and of 0.23% HT, 0.11% DT and 99.66% T_2 (bottom) measured with GC1.

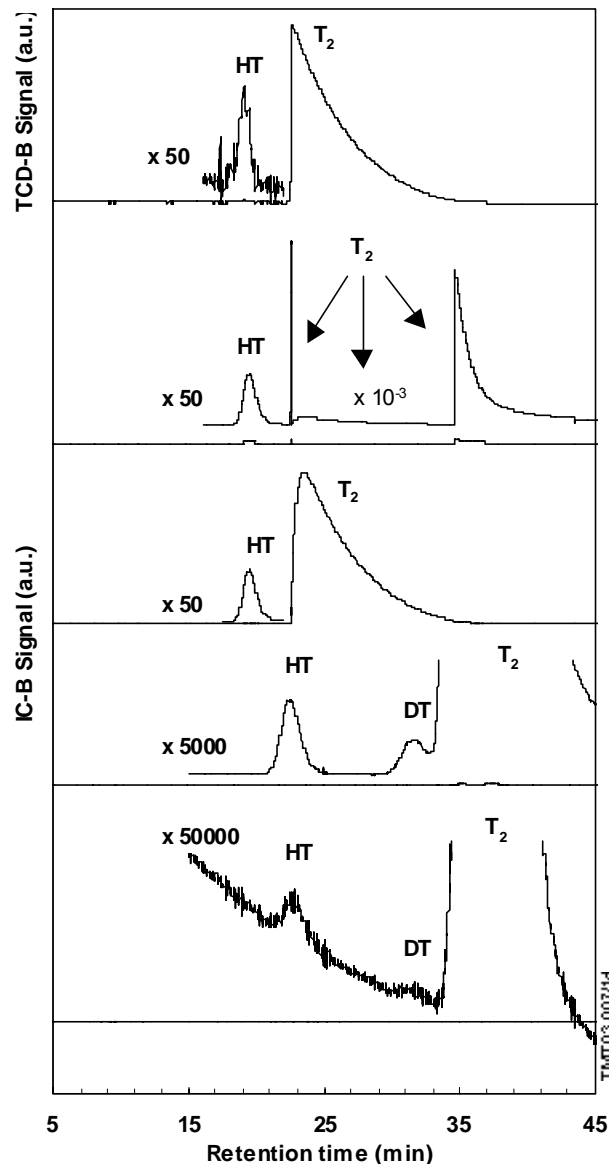


Fig. 4.4.6: One TCB-B (top) and four IC-B chromatograms of a tritium mixture containing 0.23% HT, 0.11% DT and 99.66% T_2 measured with GC1. Top three chromatograms are obtained with compressed samples, second lowest and lowest chromatograms with 5.1 kPa and 600 Pa, respectively.

4.4.2) Observation of hydrocarbon mixtures with GC1, GC2 and GC3

The gas mixture of hydrocarbons in He specified in Table 4.2 was measured with GC1, GC2 and GC3.

Table 4.3: Composition of the calibrated 1% hydrocarbon gas mixture in He:
 1.01% CH_4 , 0.99% C_2H_4 , 0.98% C_3H_6 , 1.99% C_2H_2 , 1.96% 1- C_3H_4 , 1.00% N- C_4H_{10} ,
 92.07% He.

HeD chromatogram of GC1

The HeD chromatogram of the hydrocarbon mixture listed in Table 4.3 and measured with GC1 is shown in Fig. 4.4.7. The observed separation is achieved with the Porapak Q column-A of system 1 of GC1 and the species are detected with the helium-ionisation detector. A separation of the peaks for C_2H_4 and C_2H_2 is not obtained. Even lower temperatures of column-A than $40^\circ C$ are required. The relatively short retention times for the higher hydrocarbons are obtained with a temperature controlled oven, starting at $40^\circ C$ for 20 minutes and then increasing the temperature up to $100^\circ C$ with a rate of $10^\circ C$ per minute. The increase of the baseline after 20 minutes is due to the temperature increase of column-A because usually column-A is only used at $40^\circ C$, but was heated during this analysis releasing trapped impurities and showing an increased background. In Fig. 4.4.7 the hydrocarbon peaks are labelled by their chemical abbreviations. Their concentrations are given in Table 4.3. Normally these concentrations cause high overshooting of the various peaks in the case of the He ionisation detector if compressed samples were injected. Here in fact a very small gas sample of a pressure of approximately 160 Pa was injected to obtain the observed peaks. The observed peak areas would be caused in the case of a compressed sample by hydrocarbon concentrations in the 10 to 20 ppm range. Therefore, concentrations down to 0.1 ppm can be analysed with the He ionisation detector.

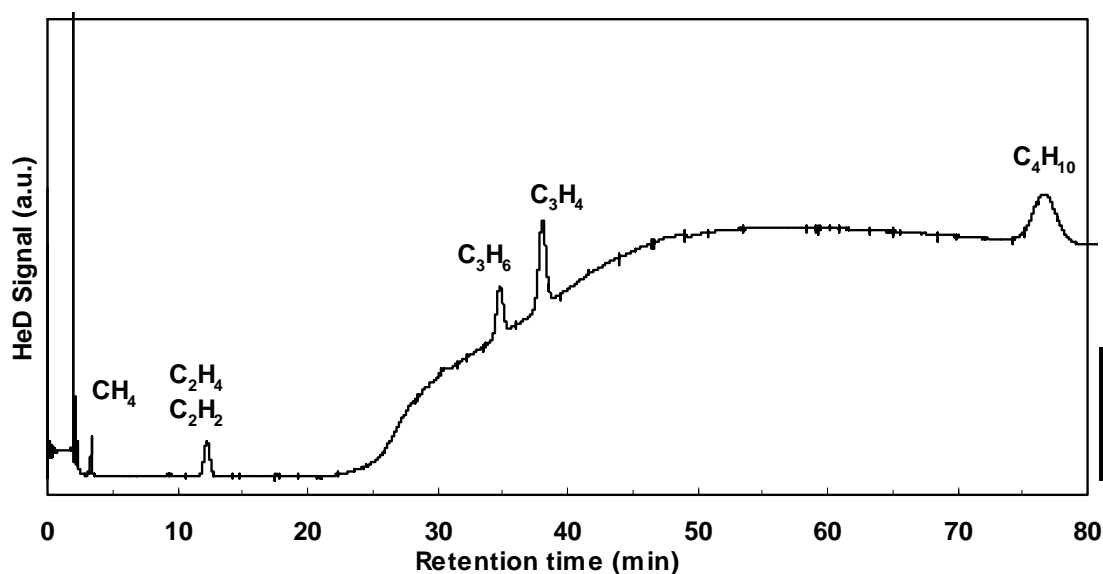


Fig. 4.4.7: HeD-A chromatogram of the gas mixture given in Table 4.3 and measured with System 1 of GC1.

TCD-A chromatogram of GC2

The TCD-A and TCD-B chromatogram obtained with GC2 for the gas mixture listed in Table 4.3 are presented in Fig. 4.4.8. Compressed samples are used. Valco B (see Fig. 3.2.1) is switched after methane passed through. All later eluting hydrocarbons are transferred to TCD-A because otherwise they would be trapped in column-B. The peaks of C_2H_4 and C_2H_2 are clearly separated. All hydrocarbons present in the gas mixture are easily detected. Only He is not seen because He is used as the carrier gas.

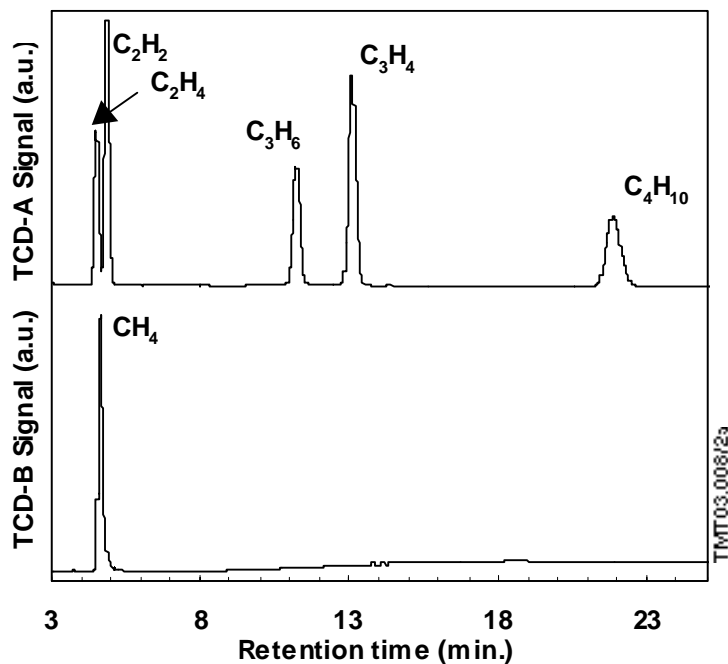


Fig. 4.4.8: TCD-A and TCD-B chromatograms of the gas mixture given in Table 4.3 and measured with GC2.

TCD-A chromatogram of GC3

The chromatogram of the hydrocarbon mixture listed in Table 4.3 and measured with GC3 is shown in Fig. 4.4.9. The separation presented in Fig. 4.4.9 is achieved with the HayeSep R column-A of GC3. More than 100 minutes are required for the elution of the C_4H_{10} gas species with the column-A at 343K. Again all six peaks are observed. The peak width increases with longer retention times. The peak areas are again proportional to the given compositions in the gas mixture. By heating the column-A to higher temperatures shorter retention times than 120 minutes could be achieved.

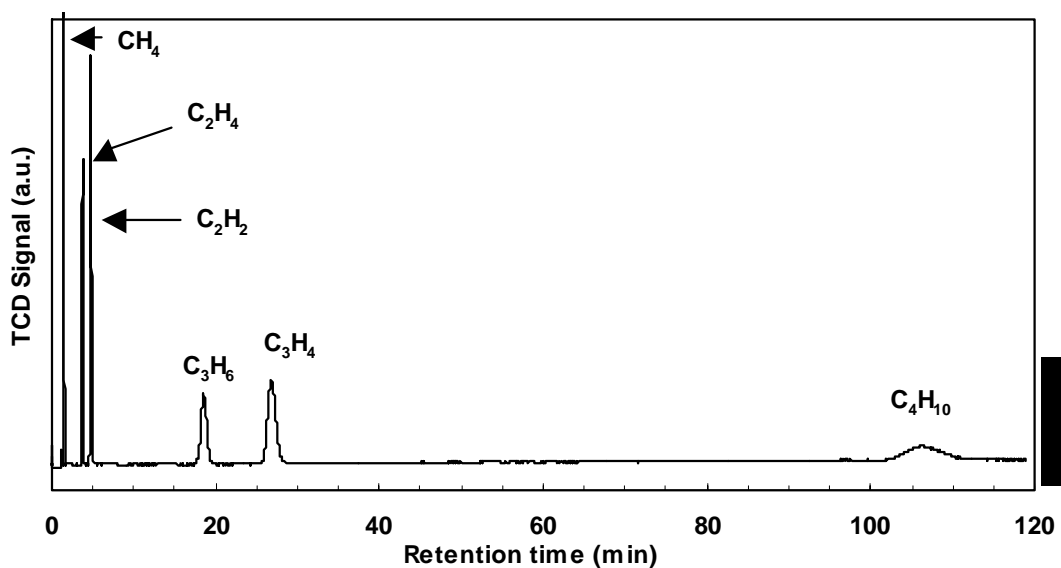


Fig. 4.4.9: TCD-A chromatogram of the gas mixture given in Table 4.3 and measured with GC3.

Comparison of the HeD chromatogram of GC1 with the TCD chromatograms of GC2

Fig. 4.4.10 shows the HeD-chromatogram of a gas mixture listed in Table 4.4. A compressed sample was injected. All gas species in the mixture are clearly observed with the exception of He which is used as carrier gas. To show this the HeD chromatogram is presented in two pieces: at the bottom for the retention times from 2 to 7 minutes and at the top from 10 to 86 minutes. The chromatograms show the sensitivity of the helium-ionisation detector (HeD) and indicate that far lower concentrations than the ones in the mixture can be detected.

Table 4.4: Composition of the calibrated 100 vpm gas mixture in He:
106 vpm CH₄, 106 vpm C₂H₆, 104 vpm C₃H₈, 103 vpm N-C₄H₁₀, 62.6 vpm CO, 53.6 vpm CO₂, 19.3 vpm N₂, balance He.

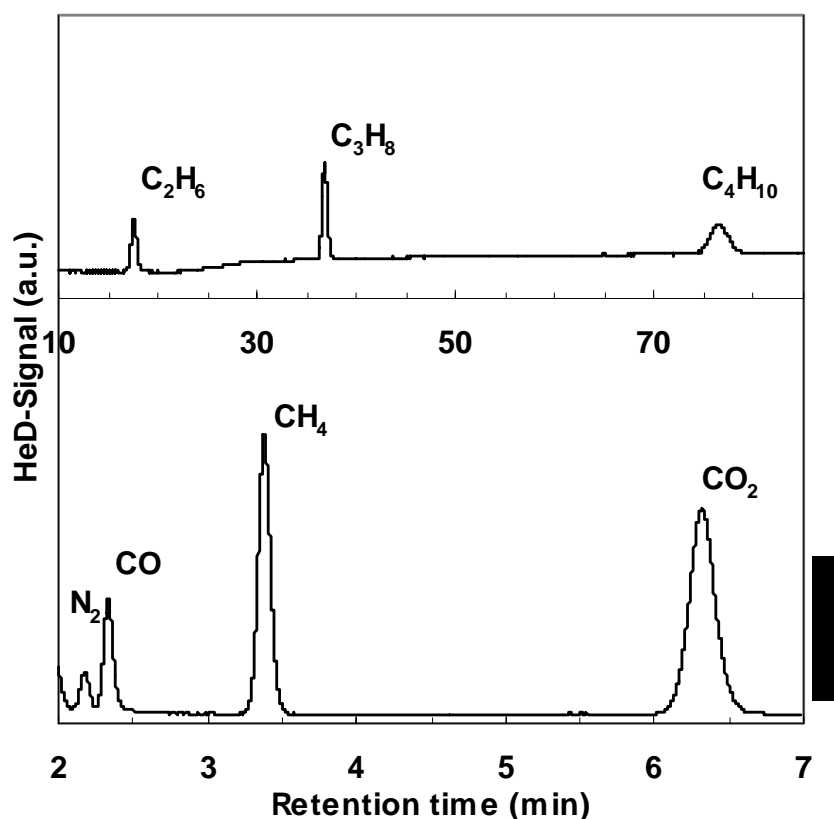


Fig. 4.4.10: HeD signal of the 100 vpm gas mixture listed in Table 4.4 and measured with GC1.

Additional TCD-A chromatogram of GC2

The chromatogram of the hydrocarbon mixture listed in Table 4.3 and measured with GC2 is shown in Fig. 4.4.11. Instead of the five peaks in Fig. 4.4.7 all six hydrocarbons are well separated in Fig. 4.4.11. Again the temperature of the oven for the Porapak QS/Chromosorb 104 columns and for the molecular sieve column was temperature controlled (starting for 8 minutes at 373 K and then ramping the temperature by 10 K per minute to 423 K). In this way relatively short retention times are achieved even for the heaviest hydrocarbons of this study. The peak areas demonstrate the concentrations of the various gas species in the gas mixture. It is worthwhile to note that the method usually employed for GC2 was modified for this measurement. Valco-B in Fig. 3.2.1 was from the start of the injection positioned such that all gas species were directly diverted to TCD-A. In this way all hydrocarbons are detected by TCD-A alone and can be compared easier. In the usually used method CH_4 would be detected by TCD-B and all other ones by TCD-A.

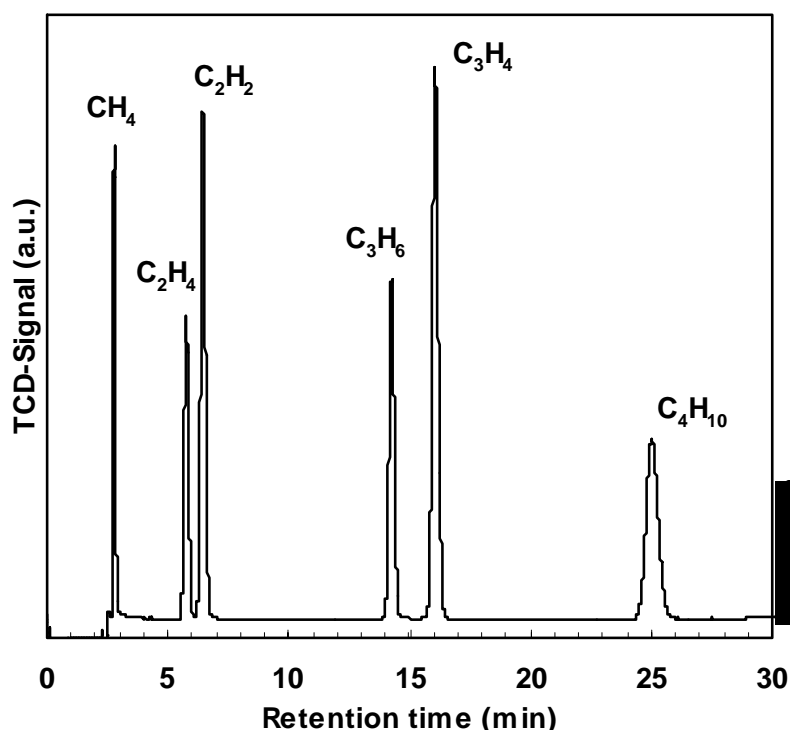


Fig. 4.4.11: TCD-A chromatogram of the gas mixture given in Table 4.3 and measured with GC2 with a slightly modified method (for details see text).

4.4.3) Observation of ^3He and low concentrations of hydrocarbons in tritiated gas mixtures by means of GC1

The storage of tritium in metals is generally considered as the safest tritium storage technique. After absorption of tritium in a metal tritide storage bed various residual gases stay in the gas phase which are not absorbed by the metal at room temperature. These gases can be noble gases, because their solubility in metals is negligible, or other gases which do not react with the storage materials at room temperature. If the tritium is stored for longer times in the getter, then during the desorption of the tritium also a certain fraction of the tritium decay product helium-3 is released. Whereas the

tritium can be absorbed again by the cold getter material, He-3 and other impurities stay in the gas phase.

The gases above a storage bed, which were not absorbed at room temperature, were collected, compressed into a small sample cylinder and their composition studied with the gas chromatographic system GC1 of TMT. The chromatograms measured are presented in the Figs. 4.4.12, 4.4.13 and 4.4.14. The experimentally determined gas composition is given in Table 4.5.

The IC-B signal (see bottom chromatogram of Fig. 4.4.12) shows clearly the tritiated hydrogen molecules HT, DT and T₂. As expected the T₂ peak is most prominent. No other peaks are observed with IC-B.

The background signal near the retention time of the ³He peak is amplified by a factor of 50 to demonstrate that He, in this case ³He, does not cause the appearance of tritium contamination peaks as observed for nontritiated gases such as H₂, HD, D₂, N₂, O₂, etc. Due to the large concentration of more than 99.99% of ³He in the studied gas mixture the appearance of such a contamination peak in an IC chromatogram should be very likely for any other non-tritiated gas except He. Helium due to its electronic structure is mainly transferred into a metastable state by decay electrons and secondary electrons. Metastable helium is capable of ionising all other gases with the exception of He itself. Therefore, contamination peaks due to He passing through an ionisation chamber are not expected, but contamination signals are observed for almost all other gases if their concentrations in the ionisation chamber is large enough.

The TCD-B signal shows only one peak, in fact a negative peak. This peak is caused by ³He which is one of the decay products of tritium. The peak had been identified as being due to ³He by the use of special available ³He gas mixtures. By means of these gas mixtures the calibration factors for ³He in the carrier gases ⁴He and N₂ of GC1 were determined. See Section 4.6. As a side result the negative peak tells that the thermal conductivity of ³He is greater than the common thermal conductivity of the ⁴He/H₂ gas mixture passing continuously through the TCD-B because the other peaks in connection with deuterium and tritium are all positive. Even a magnification of the TCD-B signal by a factor of 50 (not shown in Fig. 4.4.12) did not reveal any indication of the presence of peaks for HT, DT and T₂ in the TCD-B chromatogram. This is a clear indication of the far higher sensitivity and of the far lower detection limits achievable with ionisation chambers in comparison to thermal conductivity detectors.

Fig. 4.4.13 presents the HeD-A and IC-A chromatograms of GC1 for the gas listed in Table 4.5. Only impurities with retention times longer than 3 minutes are shown. Clearly methane and CO₂ are the major impurities. With a higher amplification also higher hydrocarbons such as C₂Q₄ and C₂Q₆ are easily detectable by the HeD-A and by the IC-A. A comparison of the concentrations calculated by means of the HeD-A and the IC-A shows clearly that tritium is occupying approximately 90% of the possible hydrogen sites of the hydrocarbons.

The chromatograms of System 2 of GC1 are given in Fig. 4.4.14. Again by far the most dominant peak is due to ³He. The sum peak for hydrogen is only recognisable by means of the high amplification factor of 500. The strong ³He peak can be used to check the calibration factor for helium-3. The main IC signal is caused by the contribution of HT, DT and T₂. The peak due to tritiated methane is not shown as it elutes at a retention time of approximately 21.5 minutes.

The GC1 analysis revealed clearly that the main fraction of the gas not absorbed by the cold getter material was ³He. The other gases of very small concentrations were HT, DT and T₂ and methane, higher hydrocarbons and CO₂.

Table 4.5: Residual gas mixture after absorption of the hydrogen in a cold getter bed:
19 ppm HT, 12 ppm DT, 121 ppm T₂, 16.3 ppm CQ₄, 3.0 ppm CO₂, 0.52 ppm C₂Q₄,
1.36 ppm C₂Q₆, balance: ³He. Approximately 90% of Q in the hydrocarbons are tritiated.

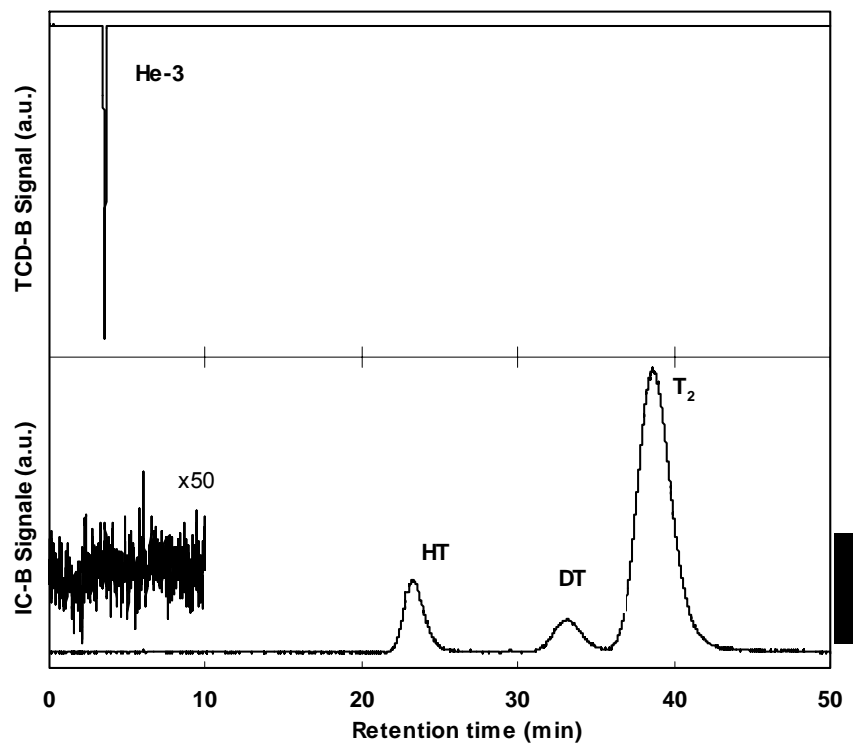


Fig. 4.4.12: TCD-B and IC-B chromatograms of the gas mixture specified in Table 4.5. and measured with GC1

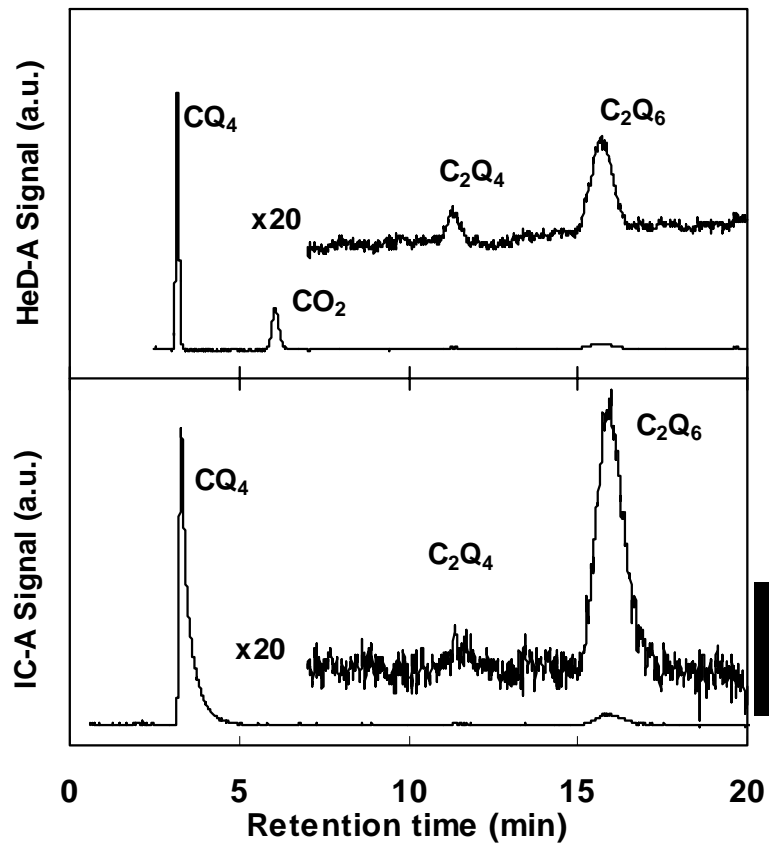


Fig. 4.4.13: HeD-A and IC-A chromatograms of the gas mixture specified in Table 4.5 and measured with GC1.

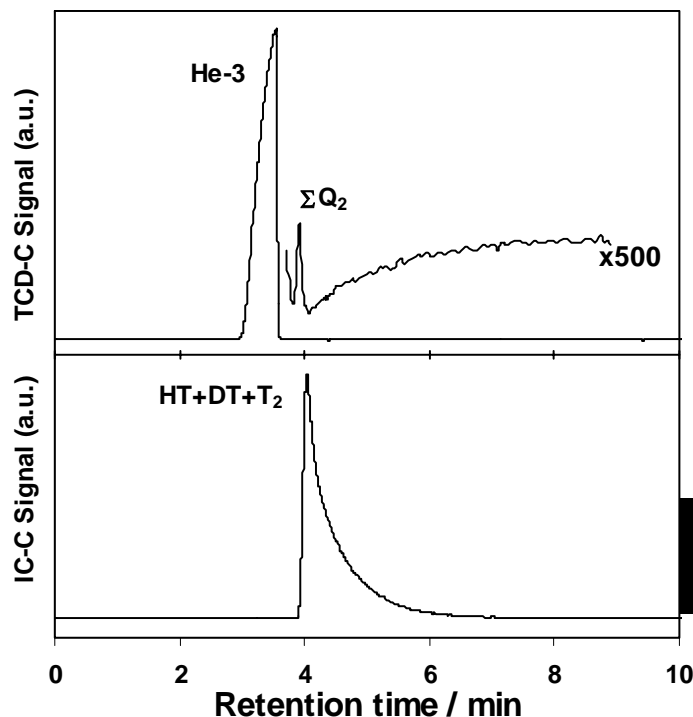


Fig. 4.4.14: TCD-C and IC-C chromatograms of the gas mixture specified in Table 4.5 and measured with GC1.

4.4.4) Observation of ^3He and highly tritiated hydrogen mixtures by means of GC1

The TCD-B and IC-B chromatograms of a ^3He -hydrogen mixture are presented in the Figs. 4.4.15 and 4.4.16, respectively, for the following concentrations: 53.1% ^3He , 1.3% HT, 0.6% DT and 45.0% T_2 .

The TCD-B chromatogram obtained with GC1 shows the three tritiated peaks HT, DT and T_2 . Not visible in these TCD-B chromatograms is the ^3He peak because the data obtained for retention times below 15 minutes are not shown to present the tritium relevant peaks more clearly. The top chromatogram is obtained for a compressed sample. In Fig. 4.4.6 the chromatogram of a compressed sample of almost pure tritium did not reveal the DT peak due to overlap of the DT and T_2 peak. In Fig. 4.4.15 the DT and T_2 peak overlap only partially. The change in overlap is mainly due to the fact that the injected amount of hydrogen in Fig. 4.4.15 is approximately half of the amount injected in Fig. 4.4.6. At the bottom of Fig. 4.4.15 the measured chromatogram and the one amplified by a factor of 5 are shown for an uncompressed sample injected with a pressure 0.031 MPa. Now the three tritiated hydrogen peaks are very nicely separated. This shows also that the explanations given in previous sections are correct, that for correct interpretation of measured chromatograms measurements under various conditions should be performed and that gas chromatography also requires a certain amount of experience for the correct interpretation and analysis of the experimental data. Furthermore, again a very large shift of the retention time as a function of the injected gas amount is observed.

Figs. 4.4.16 and 4.4.17 show the IC-B chromatograms of the compressed and uncompressed tritium gas mixture specified above. These IC-signals were obtained during the same runs as the TCD-B chromatograms. The IC current of the Keithley

instruments is recorded by the connected electronic in such a way that after increases of the current by a factor of 1000, the output signal of the Keithley instrument which is recorded by a connected PC, is automatically reduced by a factor of 1000. This explains the sharp structures observed in the IC-signals presented in top of Figs. 4.4.16 and 4.4.17. The top IC-B chromatogram of Fig. 4.4.16 shows a symmetrical peak of HT and a sharp structure caused by the strong increase of the DT signal. A very sharp drop follows as the signal sent to the PC is reduced by the Keithley instrument by a factor of 1000. The chromatogram shows a flat structure as long as the factor 1000 is reducing the outlet signal. A very sharp increase occurs when the IC-B current goes again below the critical number where the reduction of the signal is not any more required.

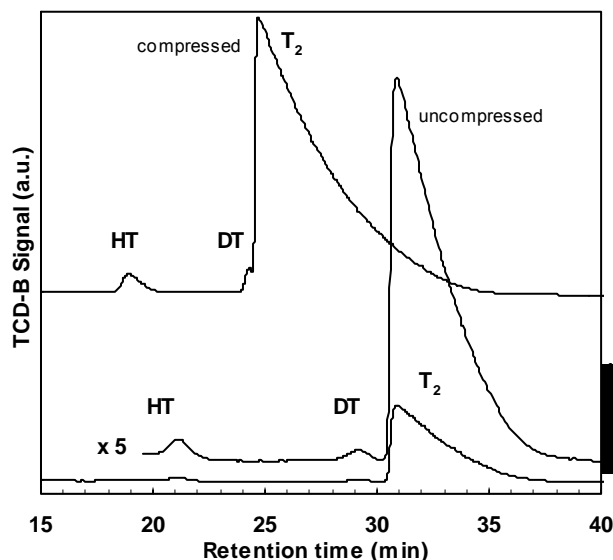


Fig. 4.4.15: TCD-B chromatograms of a gas mixture containing 53.1% ^3He , 1.3% HT, 0.6% DT and 45.0% T_2 and measured with GC1.

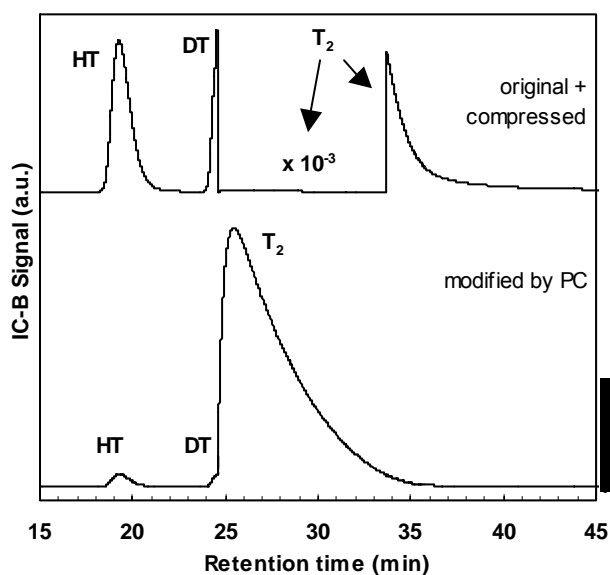


Fig. 4.4.16: IC-B chromatograms of a gas mixture containing 53.1% ^3He , 1.3% HT, 0.6% DT and 45.0% T_2 and measured with GC1.

Very similar behaviour is observed for the top IC-B chromatogram shown in Fig. 4.4.17. Now, due to the injection of the smaller gas amount, also the DT signal is seen as a symmetrical peak and the switching occurs only just in front of the strong tritium signal. The bottom IC-chromatograms shown in Figs. 4.4.16 and 4.4.17 present the continuous shape as expected from the TCD-B chromatograms in Fig. 4.4.15 because the reductions introduced by the Keithley electronic were corrected by a simple program multiplying the reduced values by a factor of 1000.

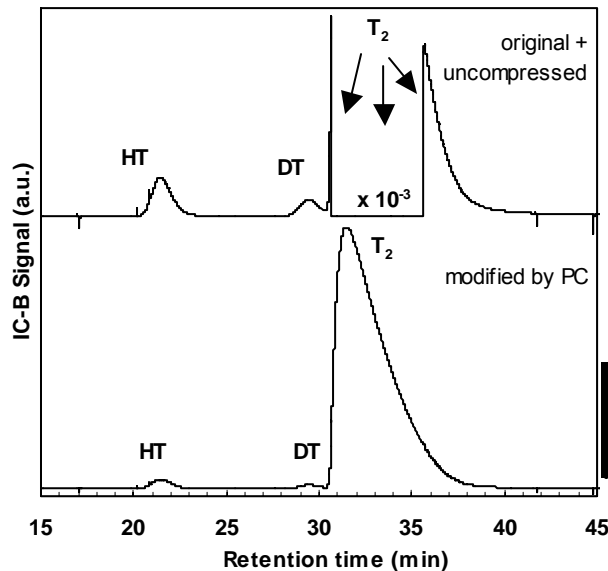


Fig. 4.4.17: IC-B chromatograms of a gas mixture containing 53.1% ^3He , 1.3% HT, 0.6% DT and 45.0% T_2 , measured with GC1 and processed with PC.

Fig. 4.4.18 presents the TCD-B chromatograms already shown in Fig. 4.4.15, but now for all retention times up to 40 minutes. Please note that the upper x-axis presents the retention time only for the compressed sample, whereas the lower retention time belongs to the uncompressed sample.

The ^3He peaks are clearly visible in both chromatograms. The ^3He peaks are negative with respect to the other peaks observed. As these peaks (HT, DT and T_2) have smaller thermal conductivity than the He carrier gas with the small addition of protium in front of TCD-B, the thermal conductivity of ^3He must be higher than the one of the He/protium mixture.

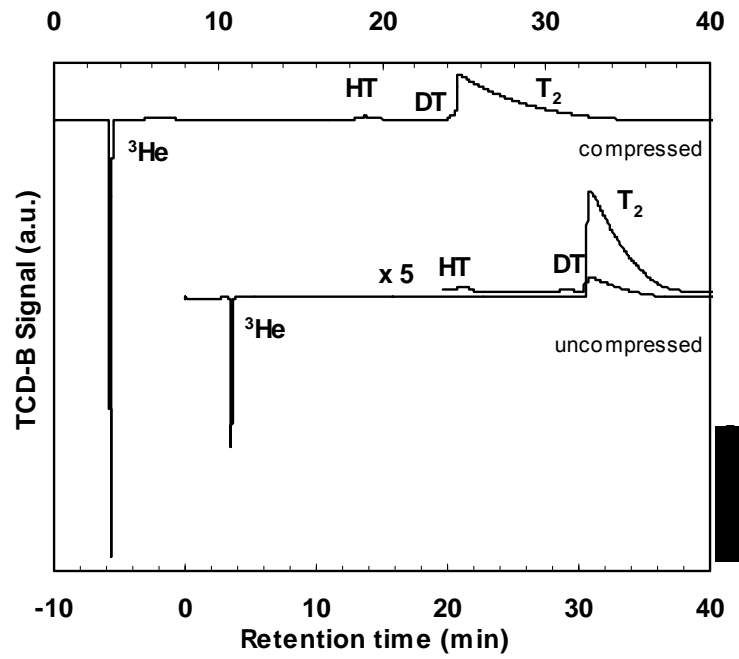


Fig. 4.4.18: TCD-B chromatograms of a gas mixture containing 53.1% ^3He , 1.3% HT, 0.6% DT and 45.0% T_2 and measured with GC1.

4.5) Comparative study of GC1, GC2 and GC3 by means of a special gas mixture

A comparison of the different chromatograms obtained with GC1, GC2 and GC3 shall be made for a gas mixture received from PETRA, another subsystem of the TLK dedicated e.g. to the studies of radiochemistry in tritium containing mixtures /1.33/. The composition of this gas mixture determined by the three conventional GCs of the TLK is listed in Table 4.6.

The experimental conditions of the three GCs during the analysis reported below were:

- Carrier gas:
 - GC1:
 - System 1: He,
 - System 2: N₂,
 - GC2: He,
 - GC3: He,
- Columns: the columns used in GC1, GC2 and GC3 are specified in Table 3.1,
- Sample: specified in Table 4.6
- Compressed sample:
 - yes for GC1 and GC2,
 - no for GC3.

Table 4.6: Composition of the gas mixture measured by means of GC1, GC2 and GC3: ⁴He (91.11%), ³He (3.58%), HD (0.75%), HT (0.41%), D₂ (1.47%), DT (1.71%), T₂ (0.53%), N₂ (0.027%), O₂ (0.002%), CO (0.051%), CO₂ (0.084%), CQ₄ (0.26%), C₂Q₆ (0.013%), C₃Q₈ (0.002%).

4.5.1) Use of gas chromatograph GC1

System 1 of GC1

The gas mixture produced in PETRA was compressed into a special gas sample container, transferred to TMT and analysed with GC1.

After expansion of the sample from the gas sample container into the evacuated injection volumes of Valco-A and Valco-C (see Fig. 3.1.1) and the injection of the compressed samples into system 1 and system 2 the gas species ³He, HD, HT, D₂, DT and T₂ elute from column-B as shown in Fig. 4.5.1 by the TCD-B and IC-B with fairly long retention times of up to 40 minutes. On their way through the gas chromatographic system the just mentioned gas species passed not only through column-B, but also through column-A. It is important to note i) that the top of the ³He peak is cut off in the top spectrum of Fig. 4.5.1, ii) that the contribution of ³He is in reality observed as a negative peak, but is shown here after inversion as a positive peak and iii) that the signal of the observed hydrogen molecules was amplified by a factor 6. The values determined for ³He and the hydrogen molecules are listed in Table 4.6.

The IC-B signal shows the three peaks of HT, DT and T₂ well separated. It is clear that the T₂ area needs to be divided by the factor two for a simple comparison of the different observed IC areas to account for the two tritium atoms in T₂ in contrast to only one in HT or DT. It is worthwhile to note again that the IC-B signal does not show any signs of a ³He contamination peak.

Valco-B is switched at 2.0 minutes into the other position (shown in the bottom picture of Fig. 3.1.2). At this time ³He and the sum peak of hydrogen which are the fastest eluting gases have just exited column-A and passed through Valco-B. All other gas

species which require more time to pass through column-A than helium and hydrogen are transferred by the switched Valco-B to the HeD-A and IC-A and observed by these detectors. Their chromatograms are presented in Fig. 4.5.2. The bypassing of column-B is of fundamental importance because most of the later eluting gas species would be at least partly trapped in the liquid nitrogen cooled column-B packed with Al_2O_3 (see Table 3.2). Due to the high sensitivity of the helium ionisation detector the HeD-A signal goes into saturation for the peaks $\text{N}_2+\text{O}_2+\text{CO}$, C_2Q_4 and CO_2 because their concentrations are higher than 200 ppm. C_2Q_6 becomes visible after large magnification and shows a symmetrical peak. Its concentration was determined to be 130 ppm.

System 2 of GC1

After the injection by Valco-C the gases are transferred into column-C and measured with TCD-C and IC-C. Fig. 4.5.3 presents their chromatograms. Helium and hydrogen elute again with short retention times because their interaction with the packing material used in the column is small.

The main peak is due to helium. As ^3He and ^4He exit column-A at approximately the same time, they are observed as one sum peak. To calculate the correct ^4He contribution, the ^3He contribution calculated with the ^3He concentration obtained from the TCD-B chromatogram has to be subtracted from the area measured for $^3\text{He}+^4\text{He}$. The resulting peak area for ^4He is finally to be divided by the known calibration factor (peak area per 1% ^4He) to obtain the ^4He concentration in percent. Two further, rather small peaks are observed which are caused by hydrogen and methane.

The TCD-C signal for hydrogen is caused by all hydrogen molecules, but due to their different thermal conductivities they all contribute in a slightly different, but not linear way to the sum peak. Therefore, the ΣQ_2 peak of a TCD does not allow the determination of the total hydrogen concentration when more than two different hydrogen molecules contribute to the peak. The analysis of the TCD-C peak for hydrogen is straightforward when only one type of hydrogen molecule is present.

The IC signal shows only two peaks due to the tritiated contributions in hydrogen and methane. The IC-C signal observed at the same retention time as the hydrogen in the TCD-C spectrum is caused by the integral contribution of HT, DT and T_2 . A general numerical determination of the concentrations of HT, DT and T_2 by means of the IC-C area is not possible, only under special assumptions such as thermodynamic equilibrium, etc. Possible contributions due to induced effects from the other hydrogen molecules H_2 , HD and D_2 are neglected here, as their concentrations are very small (see Table 4.6 or Fig. 4.5.1).

Higher hydrocarbons elute at far higher retention times (>30 minutes), but are not presented here. They can be forced to appear at lower retention times by choosing a temperature program for column-C and heating column-C to even higher temperatures.

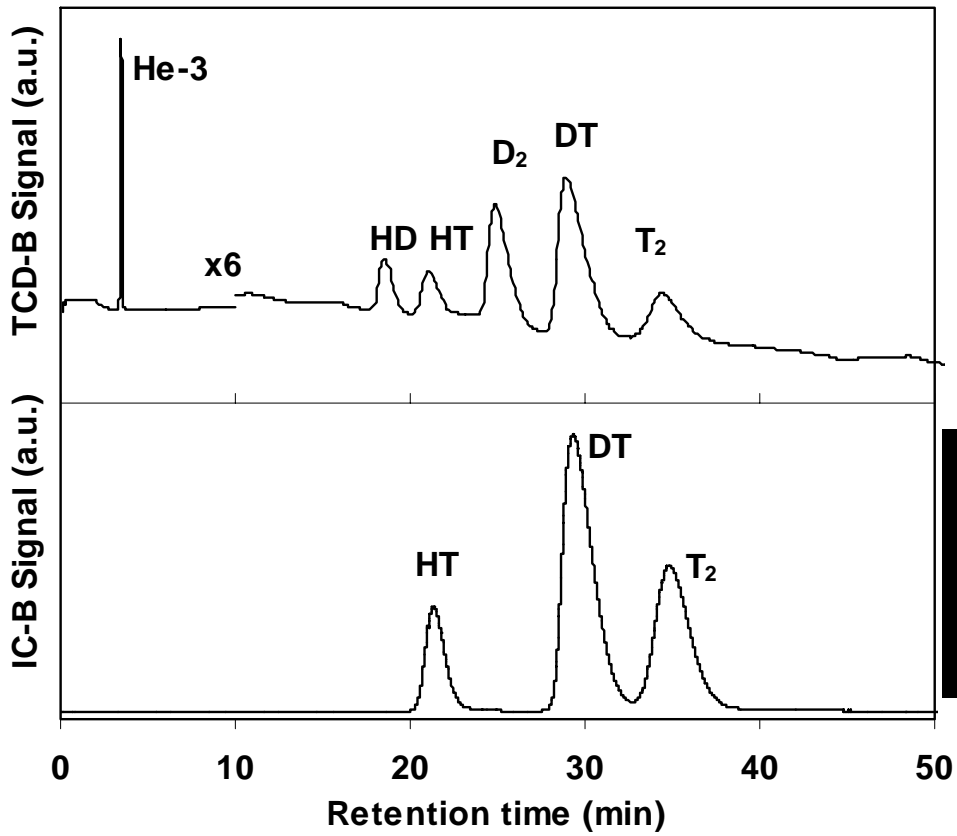


Fig. 4.5.1 TCD-B and IC-B chromatograms for the gas mixture listed in Table 4.6 and measured with GC1.

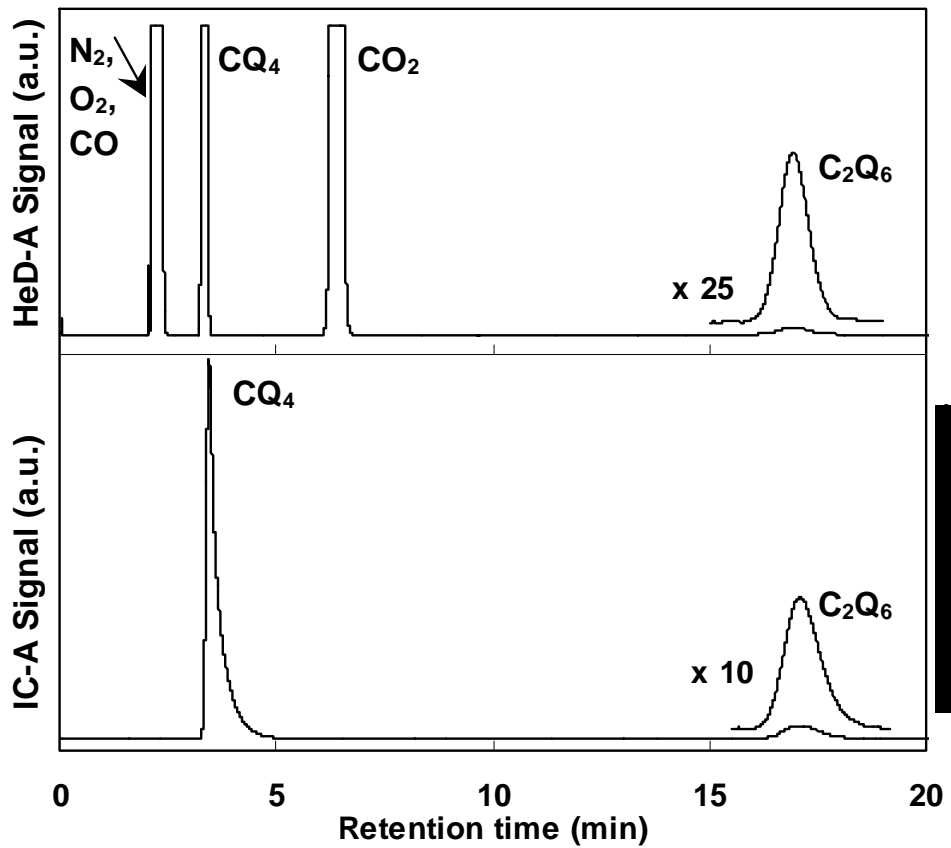


Fig. 4.5.2: HeD-A and IC-A chromatograms for the gas mixture listed in Table 4.6 and measured with GC1.

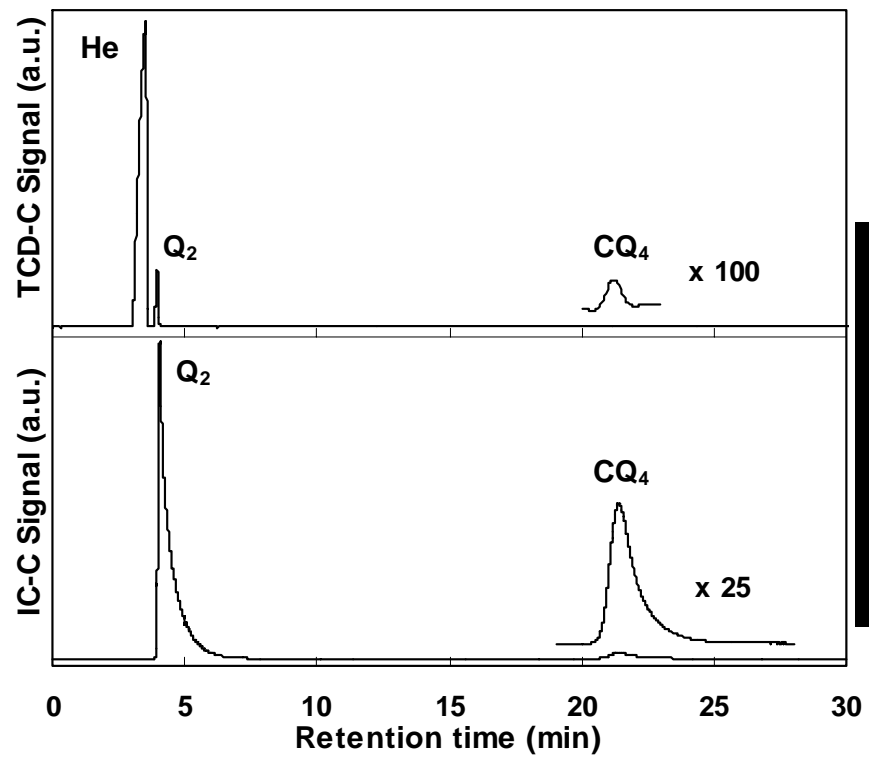


Fig. 4.5.3: TCD-C and IC-C chromatograms for the gas mixture listed in Table 4.6 and measured with GC1.

4.5.2) Use of gas chromatograph GC2

The gas mixture listed in Table 4.6 was injected into GC2 by switching the Valco-A after compression of the gas in the injection volume up to 0.21 MPa. The compressed sample enters first Col-A which consists of two columns. The gas species ^3He , Q_2 , O_2 , N_2 , CO , CQ_4 exit these two columns first, but the six gas species overlap partly and an accurate determination of their respective concentrations is not possible. For this reason, they are injected by Valco-B into a further column-B, where good baseline separation is achieved. They are analysed by the detectors TCD-B and IC-B.

When the gas species mentioned above have passed through Valco-B, it is switched to transfer the later eluting gases, i.e. CO_2 , NQ_3 , Q_2O , higher hydrocarbons, etc. to TCD-A and IC-A. Valco-B is switched after 2.5 minutes. At this point in time the base line of the TCD-A shows a large variation caused by changes in the carrier flow rates. It is obvious that those jumps of the base line should be avoided as the analysis of peak areas riding on a changing background line can become difficult. On the other hand, sometimes it is very difficult to get rid of these base line drift and it can better to reduce the number of Valco valves required for analysis if possible.

Figs. 4.5.4 and 4.5.5 present the chromatograms obtained by GC2 for the gas mixture listed in Table 4.6. TCD-A detects clearly CO_2 and C_2Q_6 . At higher retention times very small, but broad structures are visible which could be attributed to higher hydrocarbons. This interpretation is also confirmed by the IC-A signal, but no qualitative or quantitative assessment is possible based on the TCD-A spectrum.

Due to the higher sensitivity of ionisation chambers IC-A sees the tritiated fractions of C_2Q_6 and of even higher hydrocarbons such as C_3Q_8 and C_3Q_4 .

In the TCD-B spectrum ^3He appears as a negative peak, because He is used as carrier gas. The other peaks Q_2 , O_2 , N_2 , CQ_4 and CO are well separated by column-B. The non-separated sum peak Q_2 appears as a positive and almost symmetrical because the contribution of protium in the hydrogen peak is too small to lead to an anomaly in the thermal conductivity.

IC-B measures again the $\text{HT}+\text{DT}+\text{T}_2$ contribution of the hydrogen and the tritiated fraction of methane.

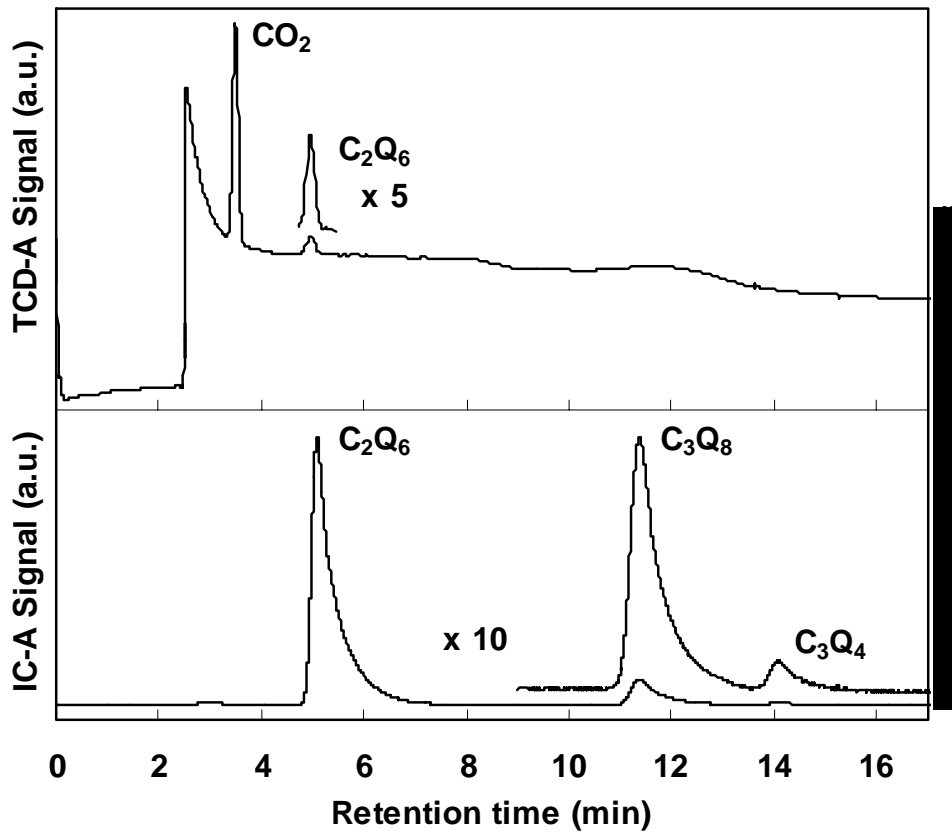


Fig. 4.5.4: TCD-A and IC-A chromatograms for the gas mixture listed in Table 4.6 and measured with GC2.

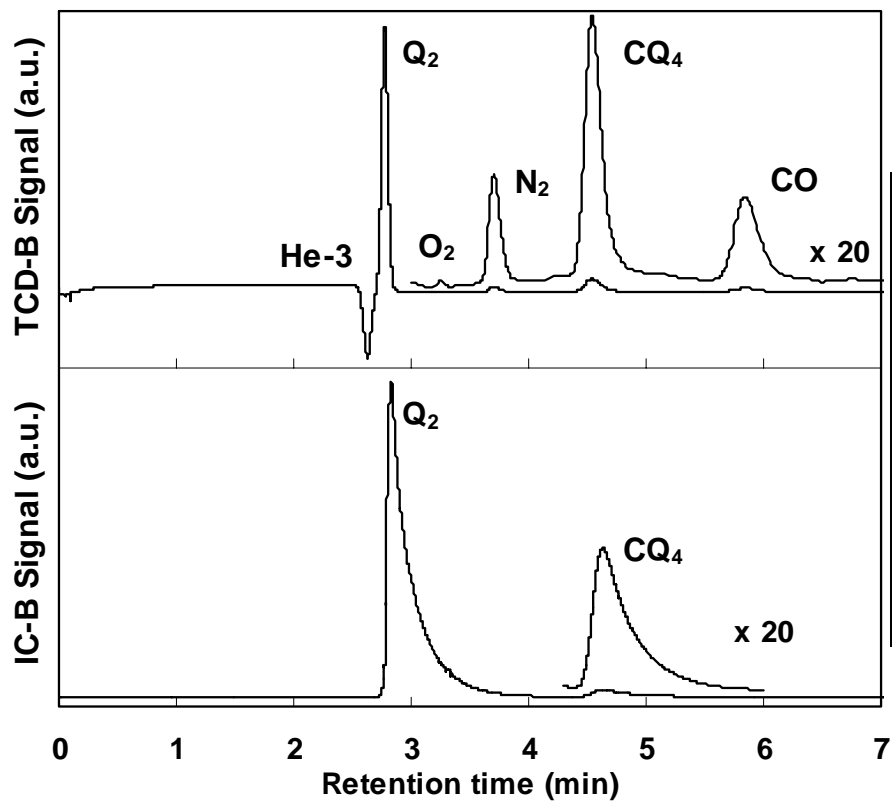


Fig. 4.5.5: TCD-B and IC-B chromatograms for the gas mixture listed in Table 4.6 and measured with GC2.

4.5.3) Use of gas chromatograph GC3

A sample of the gas mixture listed in Table 4.6 is injected for analysis from the sample loop into column-A by switching Valco-A. No compression loop exists.

At the start of an analysis the three Valco valves are in the position as shown in the second picture from the top of Fig. 3.3.2. ^3He and hydrogen exit column-A first, are moved by Valco-B into column-B, exit column-B first and are transferred via Valco-C into column-C where the separation of the hydrogen molecules occurs which yields the TCD-C and IC-C chromatograms presented in Fig. 4.5.6. ^3He and the five heavier hydrogen molecules are observed by the TCD. Due to the injection of a sample with a pressure of only 23 kPa the signal to noise ratio is not as good as for GC1 (see Section 4.5.1 and Fig. 4.5.1). This clearly shows that a compression stage is of great advantage for samples with low pressure. IC-C detects again HT, DT and T_2 which are well separated.

When hydrogen has passed Valco-C, it is switched. This occurs after 1.21 minutes of the start and is necessary because otherwise the other gases eluting from column-B would be trapped in column-C at 77 K. Therefore, all further gas species exiting column-B are transferred directly to TCD-B and IC-B. The TCD-B chromatogram is presented in Fig. 4.5.7. The two detected peaks are attributed to N_2 and CO.

When CO has passed Valco-B, it is also switched to avoid injection of later eluting gas species into column-B. Instead after 1.69 minutes of the commencement of analysis all gas species, especially all hydrocarbons, exiting column-A are transferred to TCD-A and IC-A for analysis. This is clearly seen in the chromatograms of Fig. 4.5.8 which presents the peaks of C_4Q_4 , CO_2 , C_2Q_6 and C_3Q_8 . The switching of Valco-B is required because otherwise CO_2 and the higher hydrocarbons would be trapped in the molecular sieve filled column-B.

IC-A measures the tritiated fraction of the hydrocarbons. C_3Q_8 is not detected by the TCD, but still by the IC. A comparison between the concentrations obtained with TCD-A and IC-A shows clearly that approximately 40% of the hydrogen in the hydrocarbons is replaced by tritium atoms.

Again the switching of the gas streams by the Valco-B and Valco-C from the subsequent column to the detectors at the correct times is essential because otherwise later eluting gases will be trapped in these columns downstream of the Valco valve and not observed which will lead to a wrong analysis of the chemical composition of the gas mixture.

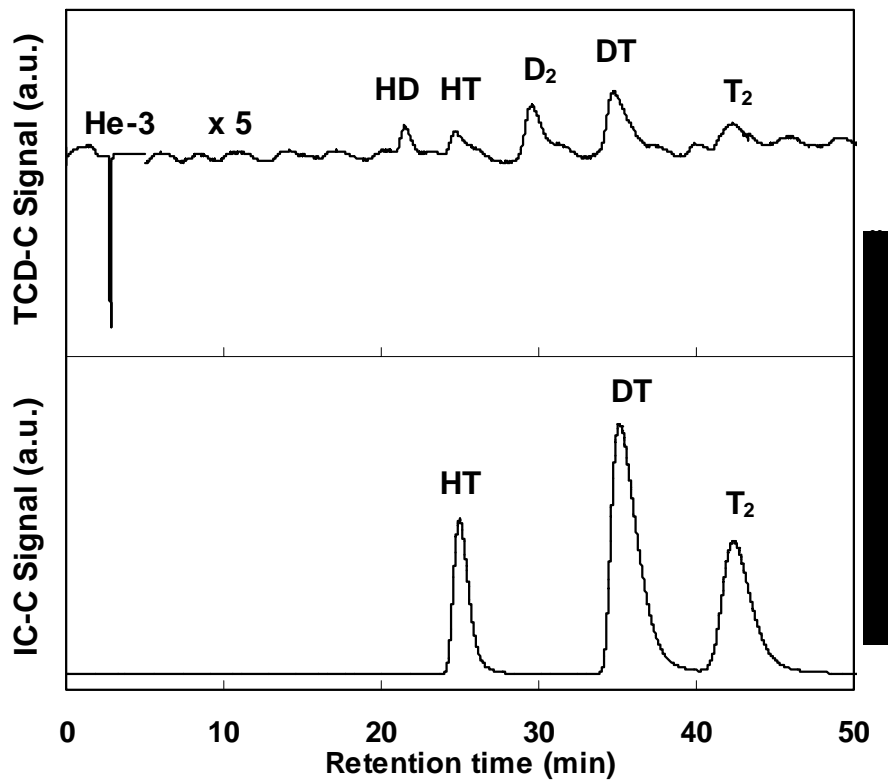


Fig. 4.5.6: TCD-C and IC-C chromatograms of the gas mixture listed in Table 4.6 and measured with GC3.

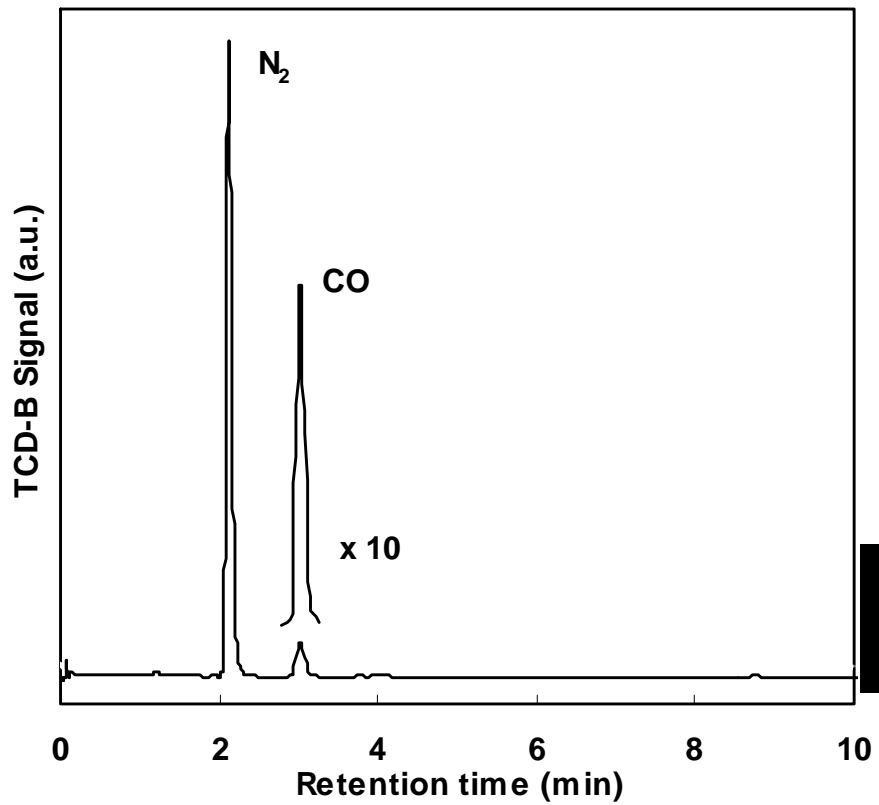


Fig. 4.5.7: TCD-B chromatogram for the gas mixture listed in Table 4.6 and measured with GC3.

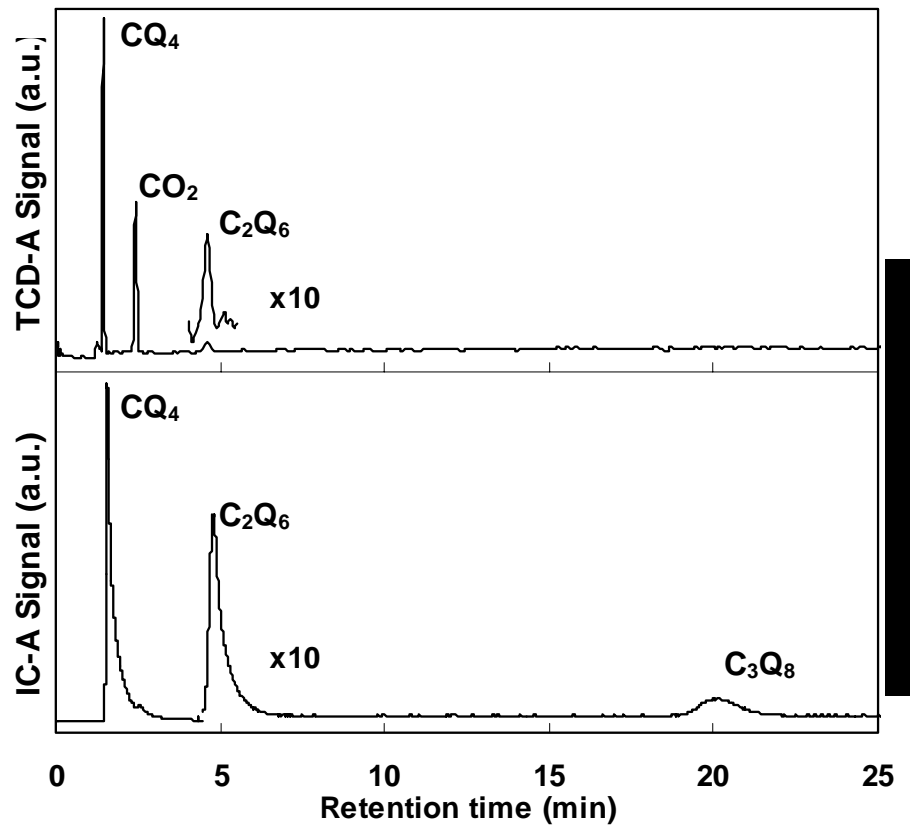


Fig. 4.5.8: TCD-A and IC-A chromatograms for the gas mixture listed in Table 4.6 and measured with GC3.

4.6) Calibration factors for the gas chromatographs GC1 and GC2

Gas chromatography can be used for qualitative or quantitative analysis of gas mixtures. In the case of qualitative analysis the interest is mainly in the knowledge of the gas species and not so much in the determination of their relative content, whereas the determination of the gas species as well as their concentrations in the gas mixture are important for quantitative knowledge.

Retention times and calibration factors of many different gas species are listed for the detectors HeD-A, IC-A, TCD-B, IC-B, TCD-C and IC-C of GC1 in the Table 4.7 and for the detectors TCD-A, IC-A, TCD-B and IC-B of GC2 in the Table 4.8.

The calibration factors were determined using either pure gases or calibrated gas mixtures purchased from industry. Only in the case of the calibration factors for ionisation chambers various different analytical runs were necessary to determine the calibration factors. In the case of tritium gas the purest tritium available at the TLK was used.

In the case of the TCDs the used carrier gas is important for the determination of the calibration factors. The type of carrier gases used in GC1 and GC2 are listed in Table 3.3.

Table 4.7: Calibration factors for various compressed gas species and detectors in GC1

HeD-A of system 1 (method 13: Col-A 40°C for 20min 10°C/min up to 100°C)		
gas species	retention time	calibration factors HeD-A
	minutes	Peak area (mV*min)/1ppm
N ₂	2.14	0.0757
CO	2.43	0.0718
CQ ₄	3.38	0.1443
CO ₂	6.33	0.4497
C ₂ Q ₄ +C ₂ Q ₂	12.26	Qualitative
C ₂ Q ₆	17.68	0.1857
C ₃ Q ₆	34.84	Qualitative
C ₃ Q ₈	36.85	0.3222
C ₃ Q ₄	38.10	Qualitative
C ₄ Q ₁₀	76.78	0.3446
IC-A of system 1 (method 13: Col-A 40°C for 20min 10°C/min up to 100°C)		
gas species	retention time	calibration factors IC-A
	minutes	Peak area (mV*min)/Ci/m ³
CQ ₄	3.38	0.4369
C ₂ Q ₄ +C ₂ Q ₂	12.26	0.4369
C ₂ Q ₆	17.68	0.4369
C ₃ Q ₆	34.84	0.4369
C ₃ Q ₈	36.85	0.4369
C ₃ Q ₄	38.10	0.4369
C ₄ Q ₁₀	76.78	0.3446

TCD-B of system 1 (method 13: Col-B at 77K)			
gas species	retention time	calibration factors TCD-B	
	minutes	Peak area (mV*min)/1%	
He-3	3.59	0.6950	
H ₂	15.3	0.1936	
HD	18.6	0.8839	
HT	20.9	1.5010	
D ₂	26.1	1.4097	
DT	29.5	2.0160	
T ₂	34.0	2.5190	
IC-B of system 1 (method 13: Col-B at 77K)			
gas species	retention time	calibration factors IC-B	calibration factors IC-B
	minutes	Peak area (mV*min)/1%	Peak area (mV*min)/Ci/m ³
HT	21.27	9074.7	T:0.7358
DT	30.10	9074.7	0.7358
T ₂	34.51	18149.4	0.7358
TCD-C of system 2 (method 13: Col-C at 60°C)			
gas species	retention time	calibration factor TCD-C	
	minutes	Peak area (mV*min)/1%	
He-3	3.58	0.3941	
He-4	3.24	0.3448	
Q ₂	4.27	100% H ₂ : 0.5473; 100% D ₂ : 0.3816; 50% H ₂ /D ₂ : 0.4590	
O ₂	7.87	0.01336	
CQ ₄	22.1	0.1848	
IK-C of system 2 (method 13: Col-C at 60°C)			
gas species	retention time	calibration factors IC-C	calibration factors IC-C
	minutes	Peak area (mV*min)/1%	Peak area (mV*min)/Ci/m ³
HT+DT+T ₂	4.31	T ₂ : 19512	T: 0.8056
CQ ₄	22.3	CT ₂ Q ₂ :19512	

Note1: Assumption: 2 T atoms in any molecule, same IC response as for T₂

Table 4.8: Calibration factors for various compressed gas species and detectors in GC2

TCD-A of GC2 (method 8: Col-A at 120°C for 8 min 10°C/min up to 150°C)			
gas species	retention time	calibration factors TCD-A	
	minutes	Peak area (mV*min)/1%	
CO₂	3.53	12.058	
C₂Q₄	4.52	12.166	
C₂Q₂	4.87	10.769	
C₂Q₆	5.18	13.330	
C₃Q₆	11.23	15.931	
C₃Q₈	11.72	15.863	
C₃Q₄	13.10	13.985	
C₄Q₁₀	21.87	18.343	
IC-A of GC2 (method 8: Col-A at 120°C for 8 min 10°C/min up to 150°C)			
gas species	retention time	calibration factors IC-A	calibration factors IC-A
	minutes	Peak area (mV*min)/1%	Peak area (mV*min)/Ci/m ³
C₂Q₄	4.52	24119.48	0.99582
C₂Q₂	4.87	24119.48	0.99582
C₂Q₆	5.18	24119.48	0.99582
C₃Q₆	11.23	24119.48	0.99582
C₃Q₈	11.72	24119.48	0.99582
C₃Q₄	13.10	24119.48	0.99582
C₄Q₁₀	21.87	24119.48	0.99582
TCD-B of GC2 (method 8: Col-B at 100°C for 8 min 10°C/min up to 150°C)			
gas species	retention time	calibration factors TCD-A	
	minutes	Peak area (mV*min)/1%	
He-3	2.57	0.3819	
Q₂	2.75	qualitative	
O₂	3.17	4.2216	
N₂	3.60	5.038	
CQ₄	4.52	4.302	
CO	6.30	5.285	
IC-B of GC2 (method 8: Col-B at 100°C for 8 min 10°C/min up to 150°C)			
gas species	Retention time	calibration factor IC-B	calibration factor IC-B
	minutes	Peak area (mV*min)/1%	Peak area (mV*min)/Ci/m ³
HT+DT+T₂	2.79	T ₂ : 14278.94	T: 0.58953
CQ₄	4.58	CT ₂ Q ₂ : 14278.94	0.58953

Note1: Assumption: 2 T atoms in any molecule, same IC response as for T₂

5) Analysis by means of micro gas chromatography

The purpose of this chapter is to introduce micro gas chromatography as a further tool for analysis of hydrogen gas mixtures and of impurities.

Two μ GCs are in use at the TLK. One (μ GC1 with an external analytical column) is employed to study the application of micro gas chromatography for hydrogen isotope analysis, the other one (μ GC2 with two modules and different columns) was already in use at the TLK for few applications.

In the following first the experience and the results obtained with μ GC1 in the analysis of helium-hydrogen mixtures will be presented. Afterwards chromatograms of various gas mixtures measured with μ GC2 are discussed which are expected to be similar to tokamak exhaust gases.

5.1) Analysis of helium and hydrogen isotope mixtures by means of μ GC1

Various gas mixtures were produced for the studies of helium–hydrogen mixtures with micro gas chromatography:

- 88% He and 12% hydrogen of an equilibrated 50% H/50% D mixture,
- 92% He and 8% hydrogen of an equilibrated 50% H/50% D mixture,
- 99% He and 1 % hydrogen of an equilibrated 50% H/50% D mixture,
- 89% He and 11% hydrogen of the mixture of 51.7% H₂, 1.6 % HD and 46.6% D₂.

The helium-hydrogen gas mixtures are produced in the following way: first the hydrogen gas mixtures are prepared by adding the correct amounts of gases to a cold metal getter bed. By simple heating the getter and by desorption an equilibrated hydrogen mixture is produced. Then the helium is added to the hydrogen mixture in a special, closed, vertical loop. The mixing is achieved by heating the reservoir in one of the two vertical pipes (see Figs. 3.5.2 and 3.7.2). The heated gas expands and causes a circulation of the gas in the closed loop.

Chromatograms obtained with the modified commercial μ GC1 for the gas mixtures mentioned above are presented in Fig. 5.1.1 to 5.1.4.

The experimental conditions of μ GC1 during the analysis reported below were

- Carrier gas: Ne, purity 99.999%,
- Pre-column: 10 m x 0.32 ID, molecular sieve 5A, 383 K, capillary column,
- Analytical column: Al₂O₃ + 19 w% MnCl₂, 4 m x 0.53 mm ID (4 metres cut from capillary column purchased from SUPELCO with 30 m x 0.53 ID), 77 K,
- Detector: μ TCD,
- Sample: He-H₂-HD-D₂ mixtures,
- Sampling time: 10 s,
- Injection time: 0.0 ms.

The flow diagram of μ GC1 was already discussed in Chapter 3.4.

Neon is chosen as carrier gas to avoid the anomaly in the thermal conductivity of He/H₂ mixtures observed when thermal conductivity detectors and He as carrier gas are used for the analysis of protium. With Ne a lower detection limit is achieved as the hydrogen

isotope signals are larger when Ne is used instead of He due to the greater differences in the thermal conductivity of the hydrogen gas species and of the carrier gas used. In future fusion machines He will be used for many different purposes, but Ne very rarely. Therefore the capability to measure He is far more important than Ne. As a consequence Ne should be used as carrier gas in future gas chromatographs for ITER because He is then detectable and can be determined quantitatively.

The μ GC1 used for hydrogen analysis is equipped with a backflush possibility. Other gases which could be trapped in the liquid nitrogen cooled analytical column are backflushed through the pre-column. The time when the backflush mode is to be started has to be specified by the operator and is determined in experimental trial runs.

The injection time chosen was always 0.0 seconds to inject the smallest possible gas amounts.

In all four TCD-chromatograms a dominant helium peak at a retention time of 100 seconds and the three hydrogen peaks of H_2 , HD and D_2 of the inactive hydrogen isotope mixtures are observed. A good separation between the various peaks is achieved. The three hydrogen peaks shown were amplified by the factors given next to the base line.

The μ GC chromatograms shown in the Figs. 5.1.1 to 5.1.5 are to be compared with the chromatograms obtained with conventional gas chromatography and shown in Chapter 4. The most obvious differences are the far shorter retention times for the hydrogen in case of micro gas chromatography. The retention times are reduced by more than an order of magnitude. With such short retention times even control of slowly changing composition in various processes is possible. The helium concentration in the gas mixtures shown in Figs. 5.1.1 to 5.1.3 increases from 88% over 92% to 99%. As a consequence the hydrogen amount decreases and larger amplification factors are required to show the hydrogen peaks with approximately equal height. A very clear base line separation between the HD and D_2 peaks is achieved. This gives great confidence for a base line separation and a clear analysis of tritiated gas mixtures because the DT peak which will appear between the HD and D_2 peaks finds enough space to fit between these peaks without any overlap.

A comparison of the H_2 and D_2 peaks shows that the D_2 is less well observed than H_2 when neon is used as carrier gas. This is a clear consequence of a thermal conductivity detector as its signal is proportional to the difference of the thermal conductivity of the gases to be detected and the carrier gas Ne. In the case of hydrogen and neon this difference decreases in the sequence H_2 , HD, HT, D_2 , DT and T_2 .

The calibration factors for H_2 , HD and D_2 measured with Ne and He and with μ GC1 are given in Table 5.1.

Table 5.1: Calibration factors for Micro GC1 for injection pressures of 0.1MPa

Micro TCD (77K, column head pressure 45psi, BF 15 sec, carrier gas neon)			
gas species	retention time	Injection pressure	calibration factor (CF) μ TCD
	minutes	mbar	CF = Peak area (mV*min)/1%
He	1.66	1000	0.1174
H ₂	2.38	1000	0.2671
HD	2.49	1000	0.2242
D ₂	2.84	1000	0.1365
Micro TCD (77K, column head pressure 45psi, BF 10 sec, carrier gas helium)			
gas species	retention time	Injection pressure	calibration factor (CF) μ TCD
	minutes	mbar	CF = Peak area (mV*min)/1%
H ₂	1.67	1000	0.00387
HD	1.76	1000	0.03476
D ₂	2.13	1000	0.06728
Micro TCD (room temperature, column head pressure 45 psi, BF 25.5 sec, carrier gas neon)			
gas species	retention time	Injection pressure	calibration factor (CF) μ TCD
	minutes	mbar	CF = Peak area (mV*min)/1%
O ₂	0.71	1000	0.0789
N ₂	0.84	1000	0.0745

As a further example Fig. 5.1.4 shows the chromatogram of a He and a non-equilibrated hydrogen mixture.

Fig. 5.1.5 shows in the top a chromatogram of a non diluted equilibrated 50% H/50% D hydrogen mixture. In the middle and bottom spectra the protium–deuterium mixture is diluted with helium resulting in 92% He/8% Q₂ and in 99% He/ 1% Q₂ gas mixtures. The injection volume of the used μ GC1 is specified as 1 micro-litre by the purchaser, but even this small volume is too large to achieve full separation when pure hydrogen isotope mixtures are injected. This is clearly seen by the top chromatogram in Fig. 5.1.5 where no He was present in the injected sample. Only hydrogen is injected. The peaks of H₂ and HD overlap and the peak shape of all three peaks is very asymmetrical. This is a clear indication that the capillary column is not capable of handling the large gas amount injected. Therefore, He is added to the gas mixtures to demonstrate that full separation can be achieved if the total hydrogen gas amount is reduced significantly. In the pre-column already a small separation between He and the sum peak of hydrogen occurs. Therefore, the presence of He in the sample does not influence the movement of hydrogen through the analytical column, because He and the sum peak Q₂ are eluting from the pre-column at different time and are therefore passing through the analytical column independently of each other because He elutes far faster through the analytical column than Q₂.

A further comparison between the top and the other chromatograms in Fig. 5.1.5 shows that the retention times for the hydrogen peaks and their shapes are quite different. The same behaviour was also observed for packed columns. If a too large hydrogen sample (top) is injected, part of the gas species elute earlier because a certain fraction of the active surface sites in a capillary column is already occupied. Under these conditions hydrogen atoms can move over longer distances before they are again trapped. The trapping behaviour is the main cause for the different retention times. If not enough trapping sites are available, part of the gas moves faster through the column which

means that the peak increases relatively sharply. For the remaining part, especially for the last fractions, again enough trapping sites are available and as a consequence the peak decreases very slowly to the base line and the same retention times are observed for these fractions as for very small injected gas amounts. In summary as a consequence the peaks are highly asymmetrical with a sharp rise at short retention times and a very slowly decreasing shape at long retention times.

An other advantage are the small amounts of gas sample required for analysis and passing through the columns. This could mean that it might not be necessary in special systems to recover the tritium passed through the columns of GC due to the small amount. This can be of a great advantage when active commissioning of the analytical instrumentation commences.

A disadvantage of the small amount of injected samples is the smaller dynamic range of the whole instrument. Thermal conductivity detectors have a large dynamic range of at least four orders of magnitude which is a precondition of achieving a low detection limit. If the sample amount of injection is already reduced to achieve full separation then the dynamic range decreases, although the lower limit of detection may not be influenced.

Fig. 5.1.6 presents the results of two very similar helium-hydrogen mixtures with 88% (top) and 90% (bottom) He. The balance is made by an equilibrated 50% H/50% D mixture. The main parameter changed between the two chromatograms is the length of the analytical column. The upper chromatogram is obtained with a column length of 4 m between the connecting stainless steel fittings (see Figs. 3.5.2 and 3.5.4), whereas only a 3 m long column is used for the bottom spectrum. As expected the retention times for the helium and the hydrogen species are far shorter for the 3 m long column. As the H₂ and HD peaks overlap in the lower chromatogram, all future studies were performed with the 4 m long column.

In summary: the measurements presented above have shown that modified micro gas chromatography is well capable of analysing helium-hydrogen gas mixtures, in even far shorter times than with conventional gas chromatography. This means that micro gas chromatography is well suited for use in fusion devices and tritium handling facilities where the analysis of all six hydrogen molecules is important.

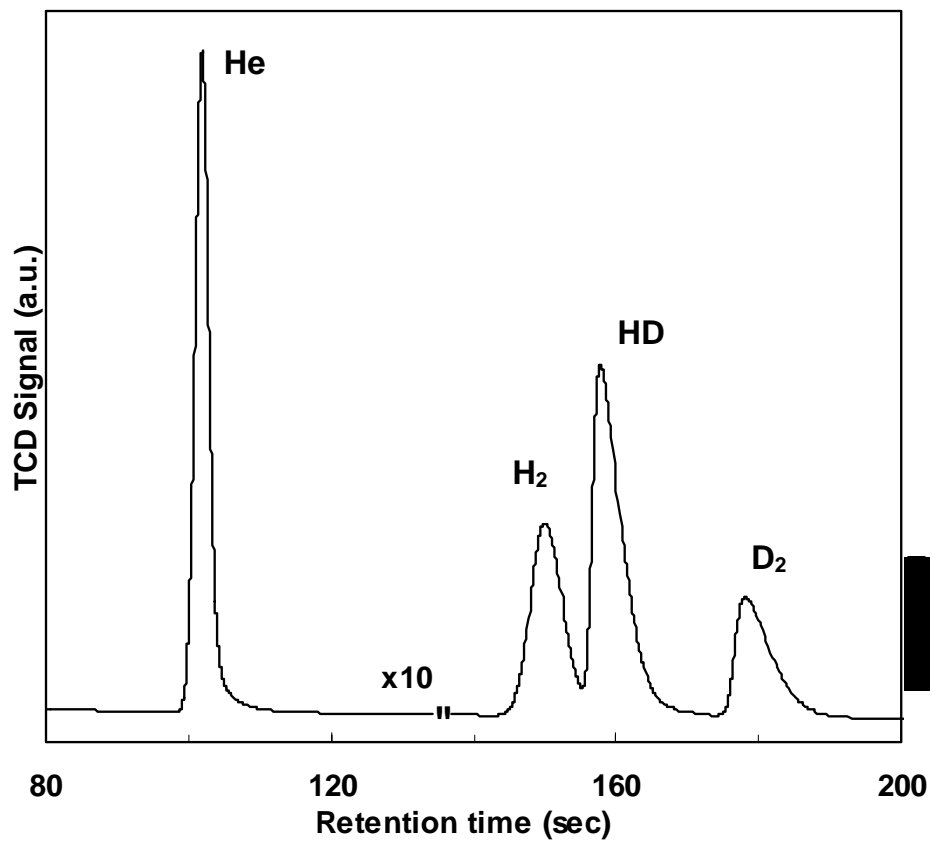


Fig. 5.1.1: μ TCD-chromatogram of μ GC1 for a gas mixture of 88% He and 12% hydrogen of equilibrated 50% H/50% D.

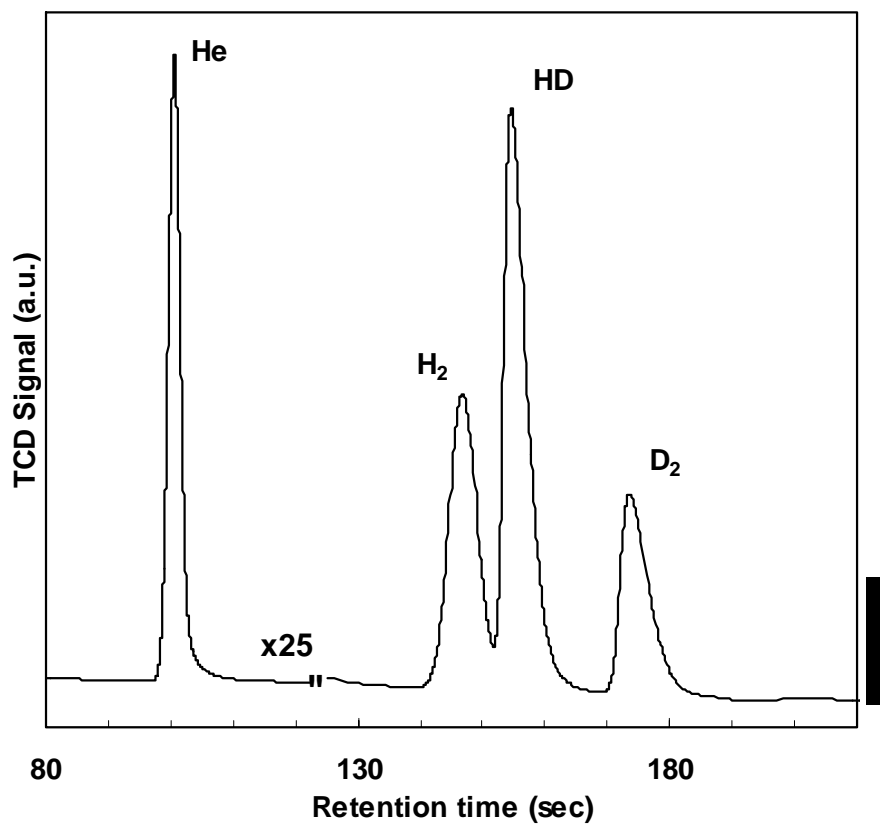


Fig. 5.1.2: μ TCD-chromatogram of μ GC1 for a gas mixture of 92% He and 8% hydrogen of equilibrated 50% H/50% D.

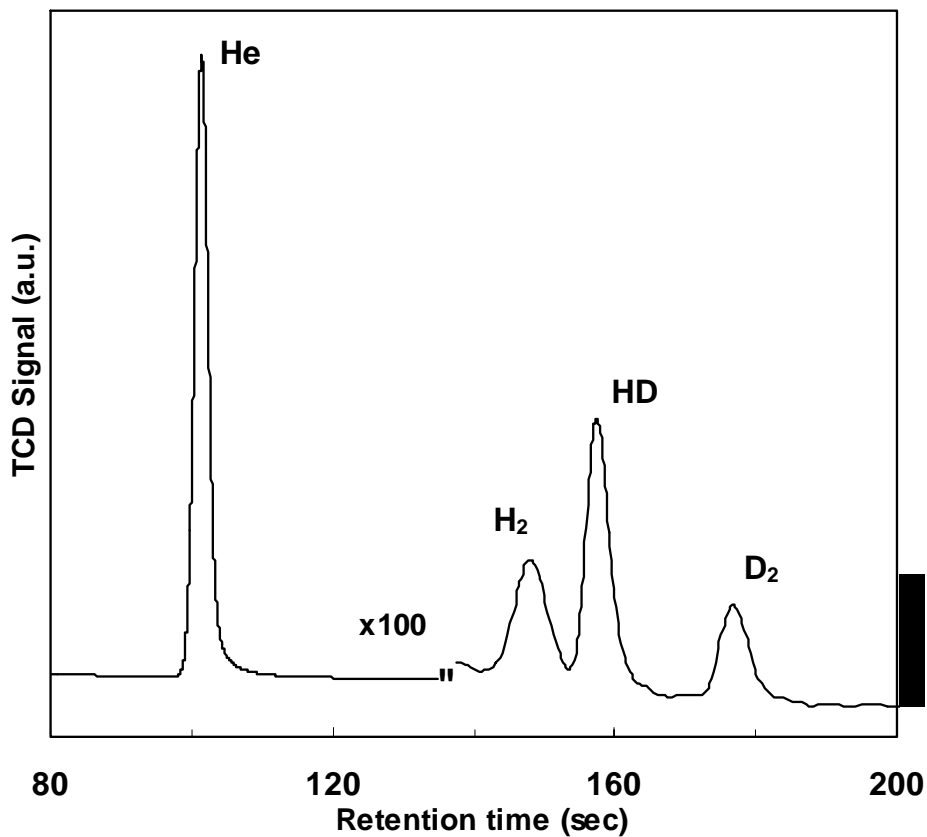


Fig. 5.1.3: μ TCD-chromatogram of μ GC1 for a gas mixture of 99% He and 1% hydrogen of an equilibrated 50% H/50% D.

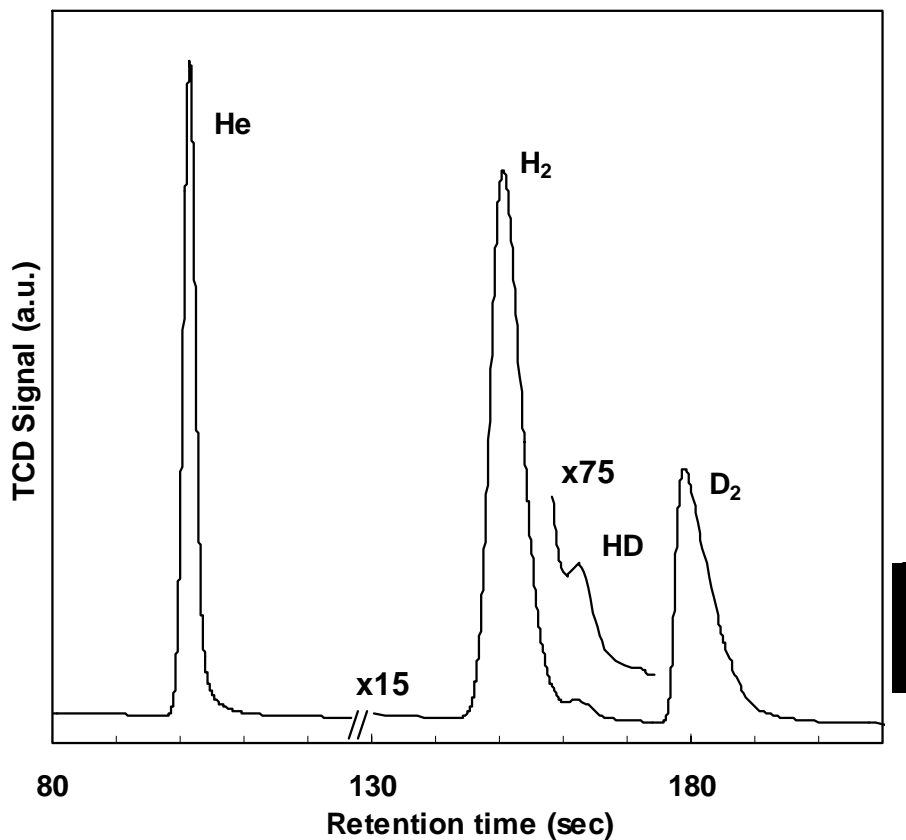


Fig. 5.1.4: μ TCD-chromatogram of μ GC1 for a gas mixture of 89% He and 11% hydrogen of the mixture of 51.7% H₂, 1.6% HD and 46.6% D₂.

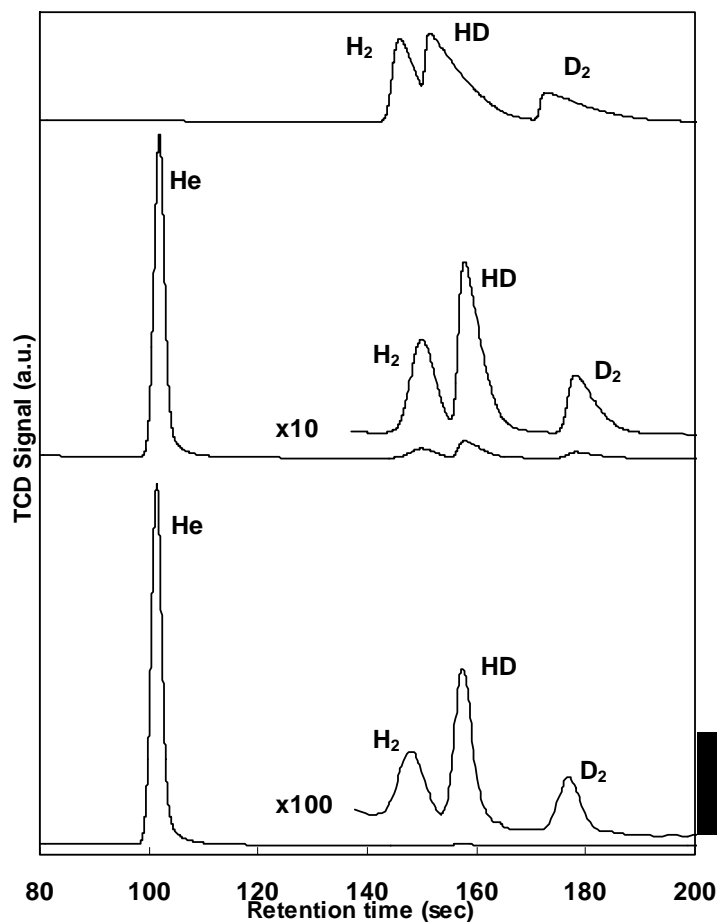


Fig. 5.1.5: μ TCD chromatograms of a non diluted equilibrated 50% H/50% D hydrogen mixture (top) and of an equilibrated 50% H/50% D mixture in 92% He (middle) and in 99% He (bottom).

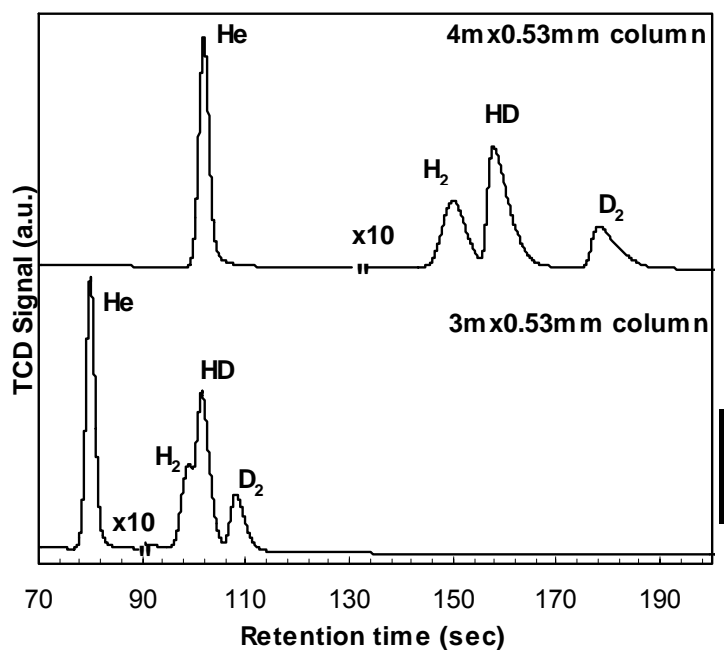


Fig. 5.1.6: μ TCD chromatograms for a gas mixture with 88% He (top) and 90% He (bottom), balance: equilibrated 50% H/50% D gas mixture.

5.2) Analysis of gas mixtures in fusion fuel cycle by means of μ GC2

In the previous section the usefulness of micro gas chromatography was shown for helium-hydrogen gas mixtures. In this section the usefulness of micro gas chromatography for the analysis of further gas species is demonstrated. This shall be done by employing a simple commercial micro gas chromatograph equipped with two modules, but not requiring any special modification.

Various gas mixtures simulating exhaust gases of fusion devices or gases to be processed in the tritium fuel cycle are analysed with the micro gas chromatograph μ GC2 to demonstrate its capability in quantitative measurements. A list of these gases is given in the Tables 5.2 to 5.5.

Table 5.2: Composition of the calibrated 80 ppm gas mixture in He:
76.9 ppm H₂, 79.0 ppm O₂, 81.1 ppm N₂, 81.5 ppm CH₄,
82.4 ppm CO, 80.6 ppm CO₂, balance He.

Table 5.3: Composition of the calibrated 100 ppm gas mixture in H₂:
19.3 ppm N₂, 106 ppm CH₄, 106 ppm C₂H₆, 104 ppm C₃H₈,
103 ppm C₄H₁₀, 62.6 ppm CO, 53.6 ppm CO₂, balance H₂.

Table 5.4: Composition of the calibrated 100 ppm gas mixture in He:
510 ppm H₂, 90 ppm N₂, 100 ppm CH₄, 100 ppm CO, balance He.

Table 5.5: Composition of the calibrated 2 vol% gas mixture in H₂:
0.98% O₂, 2.14% N₂, 1.97% CH₄, 2.00% CO, 2.04% CO₂, 90.87% H₂.

The chromatograms measured with the TCD-A of module a and TCD-B of module b of μ GC2 are presented in the Figs. 5.2.1 to 5.2.4 for the gas mixtures specified in Table 5.2 to 5.5, respectively.

The experimental conditions of μ GC2 during the analysis reported below were

- Carrier gas: He, purity 99.9999%,
- Module a:
 - Analytical column: HayeSepA, 25 cm x 0.5 mm,
 - Detector: μ TCD-A,
- Module b:
 - Analytical column: Molecular sieve 5A, 4 m x 0.32 mm,
 - Detector: μ TCD-B,
- Samples: see text below and Tables 5.2 to 5.5,
- Sampling time: 10 s,
- Injection time: 255 ms.

The chromatograms of Figs. 5.2.1 to 5.2.3 show clearly that concentrations down to 80 ppm can be easily detected. Due to the large peaks obtained for the 80 ppm gas species, far lower concentrations can be detected with the micro gas chromatographs and the micro thermal conductivity detector.

The bottom chromatogram in Fig. 5.2.1 shows the separation achieved with the HayeSepA column and measured with the TCD-A for the gas mixture listed in Table 5.2,

whereas the top chromatogram is obtained after injection of the gas mixture in the molecular sieve column. The peaks shown in the TCD-B spectrum are all well separated, whereas the first peak of the TCD-A signal is attributed to the species H_2 , O_2 , N_2 and CO which are not separated by the HayeSep column at $35^\circ C$. CO_2 is only detected by the TCD-A because it is trapped in the molecular sieve column of module b. Fig. 5.2.2 presents the chromatograms for the gas mixture listed in Table 5.3. Gas species with concentrations of less than 20 ppm are easily detected. Again CO_2 and the higher hydrocarbons are only detected by TCD-A because the molecular sieve of Module b traps these gas species. In Fig. 5.2.2 the gas species H_2 , N_2 , CO and CH_4 contribute to the sum peak because the HayeSep column is kept at $100^\circ C$. At this high temperature also the higher hydrocarbons up to C_4H_{10} are forced to elute within the measurement time of the micro GC. In contrast, in Fig. 5.2.1 only the species H_2 , O_2 , N_2 and CO are part of the sum peak and CH_4 is well separated from the sum peak due to the lower column temperature of only $35^\circ C$.

The H_2 peak area in Figs. 5.2.1 and 5.2.3 is far smaller than the areas of the other impurities present in the gas mixture. The reason is that the thermal conductivity of H_2 is very similar to the one of He in contrast to the other impurities. The H_2 peak in Fig. 5.2.2 and 5.2.4 shows the anomaly already discussed in detail in Section 4.3 because H_2 is the main gas component.

All chromatograms have in common that with increasing retention times the peak width gets broader.

In summary: micro gas chromatography is well suited to analyse different gas mixtures with high sensitivity and in short times. As the gas species used in the gas mixtures above were typical for the exhaust gases of a fusion machine, this analytical technique is well capable of analysing these gas mixtures.

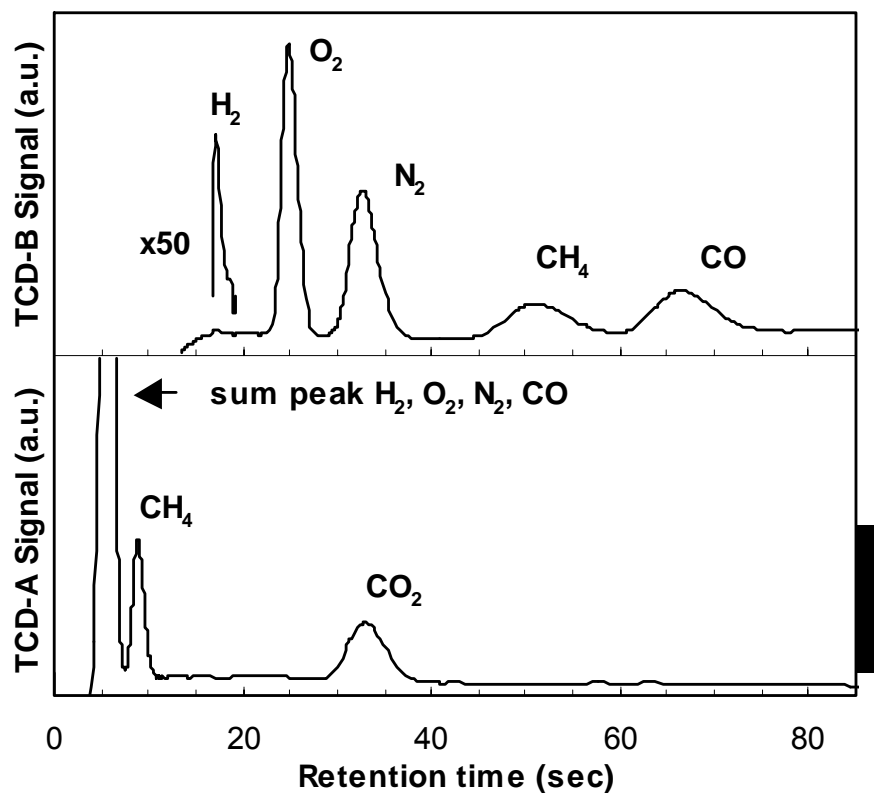


Fig. 5.2.1: μ TCD-A and μ TCD-B chromatograms of the 80 ppm gas mixture in He (listed in Table 5.2) measured with the HayeSepA column of module a at 35°C (bottom) and the molecular sieve column of module b (top) at 80°C using μ GC2.

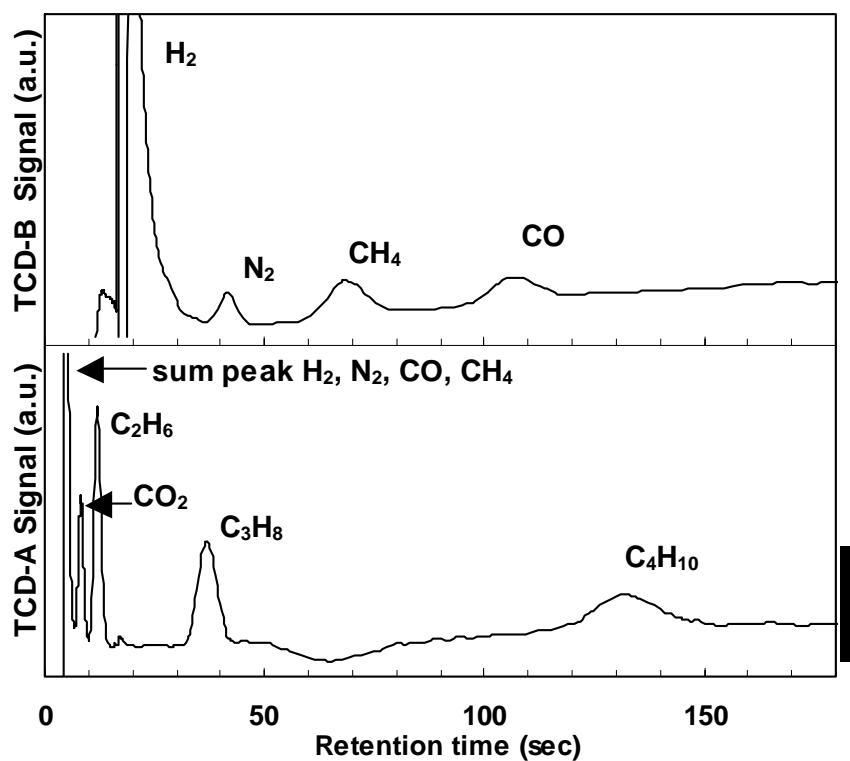


Fig. 5.2.2: μ TCD-A and μ TCD-B chromatograms of the 100 ppm gas mixture in H₂ (listed in Table 5.3) measured with the HayeSepA column of module a (bottom) at 100°C and the molecular sieve column of module b (top) at 60°C using μ GC2.

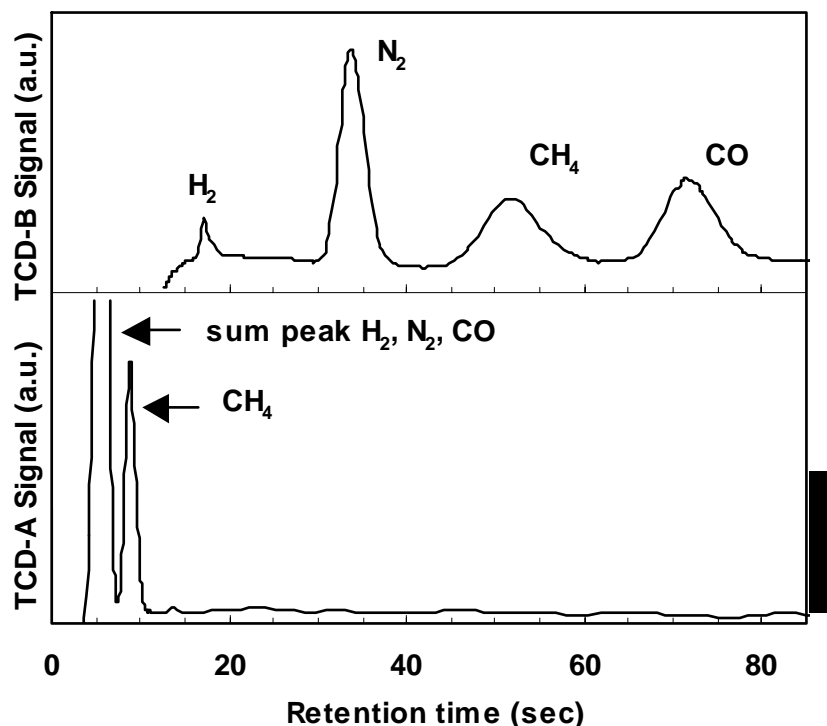


Fig. 5.2.3: μ TCD-A and μ TCD-B chromatograms of the 100 ppm gas mixture in He (listed in Table 5.4) measured with the HayeSepA column of module a (bottom) at 35°C and the molecular sieve column of module b (top) at 80°C using μ GC2.

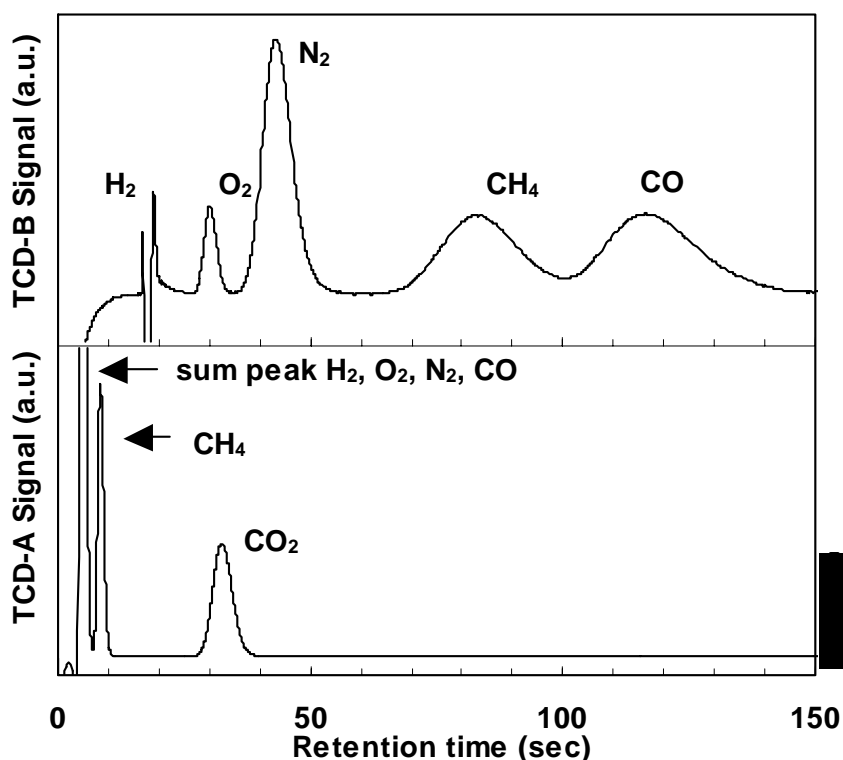


Fig. 5.2.4: μ TCD-A and μ TCD-B chromatograms of the 2 vol% gas mixture in H₂ (listed in Table 5.5) measured with the HayeSepA column of module a (bottom) at 35°C and the molecular sieve column of module b (top) at 35°C using μ GC2.

5.3) Comparison of chromatograms measured with GC2 and μ GC2

The chromatograms presented below were determined by means of the conventional gas chromatograph GC2 and the micro gas chromatograph μ GC2.

The experimental conditions of μ GC2 during the analytical runs reported below were:

- Carrier gas: He, purity 99.9999%,
- Module a:
 - Analytical column: HayeSepA, 25 cm x 0.5 mm,
 - Detector: μ TCD-A,
- Module b:
 - Analytical column: Molecular sieve 5A, 4 m x 0.32 mm,
 - Detector: μ TCD-B,
- Samples: see text below: Table 5.5 and 5.6,
- Sample time: 10 s,
- Injection time: 255 ms.

The experimental conditions of GC2 during the analytical runs reported below were:

- Carrier gas: He, purity 99.9996%
- Columns: Column-A: PORAPAK QS (3 m x 0.3 cm) + CHROMOSORB 104 (2 m x 0.3 cm), Column-B: Molecular sieve 5A (3 m x 0.3 cm),
- Samples: see text below: Table 5.5 and 5.6,
- Compressed sample: yes.

5.3.1) Chromatograms of a 1 vol% gas mixture in H_2

Chromatograms obtained for the same gas mixture listed in Table 5.6 by means of the conventional gas chromatograph GC2 (see Section 3.2) and the micro gas chromatograph μ GC2 with the two modules a and b (see Section 3.5) are presented in Figs. 5.3.1 and 5.3.2, respectively. In case of GC2 only one sample is injected and analysed by the various columns and detectors, whereas in the case of the micro gas chromatograph each module is fed by a single gas sample and analysed by the corresponding column and micro TCD.

Table 5.6: Composition of the calibrated 1 vol% gas mixture in H_2 :
5.09% He, 1.01% N_2 , 0.990% CH_4 , 0.987% CO, 1.00% CO_2 ,
0.964% C_2H_6 , 1.04% C_3H_8 , 88.919% H_2 .

The TCD-A spectrum (Fig. 5.3.1) of GC2 contains only three peaks CO_2 , C_2H_6 and C_3H_8 , because the fast eluting gases He, H_2 , N_2 , CH_4 and CO were injected further into column-B packed with molecular sieve. After CO passed the Valco-B valve it is switched and the gases CO_2 , C_2H_6 and C_3H_8 eluting later from column-A, which comprises two columns (Porapak and Chromosorb) in series, are transferred to the TCD-A for detection (for more details see the flow diagram of GC2 in Fig. 3.2.1). After 8 minutes the temperatures of the 3 columns, which are kept at the temperatures specified in Table 3.3, are ramped up to 150°C with a speed of 10°C/minute. The splitting and injection of the gas mixture into the different columns

(Porapak/Chromosorb and molecular sieve) is necessary because otherwise CO_2 and the higher hydrocarbons would be trapped in the column packed with molecular sieve and would not be observed. The retention times for CO and C_3H_8 are 5.9 minutes or 354 seconds after passage through the Porapak/Chromosorb and molecular sieve columns and 12.4 minutes or 744 seconds after exiting the Porapak/Chromosorb column, respectively. The first peak of the TCD-B shows a very sharp and deep minimum. This shape of the H_2 peak is caused by the already discussed anomaly in the thermal conductivity of He-H_2 mixtures (see Section 4.3). The signal to noise ratio of the TCD-signals are very good, because a compressed sample ($210 \text{ kPa times } 0.2 \text{ cm}^3$) was injected.

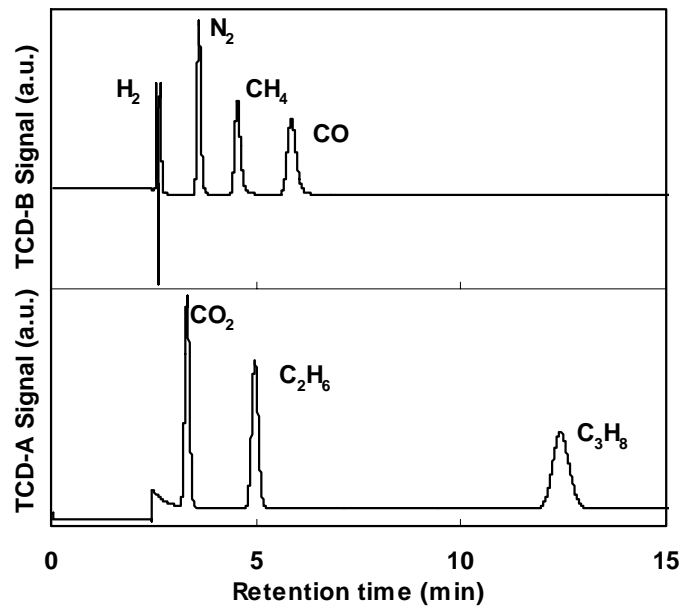


Fig. 5.3.1: TCD-A and TCD-B chromatograms of the 1 vol% gas mixture in H_2 (specified in Table 5.6) obtained with the conventional GC2 of the TMT.

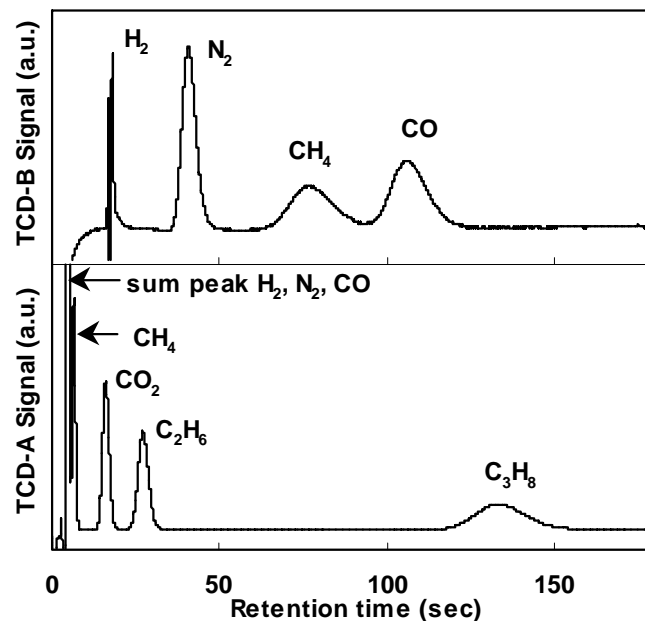


Fig. 5.3.2: $\mu\text{TCD-A}$ and $\mu\text{TCD-B}$ chromatograms of the 1 vol% gas mixture in H_2 (specified in Table 5.6) measured with the HayeSepA column of module a (bottom) and the molecular sieve column of module b (top) using μGC2 .

The μ TCD-A and μ TCD-B chromatograms obtained with the capillary HayeSep column at 60°C and the capillary molecular sieve column at 40°C, respectively, are presented in Fig. 5.3.2. The μ TCD-B chromatogram of Fig. 5.3.2 is very similar to the corresponding one of Fig. 5.3.1 with respect to the number and shape of the peaks. The main differences between Figs. 5.3.1 and 5.3.2 are the far shorter retention times obtained with the micro GC although its column temperatures were lower than the ones used for analysis with the GC2. The μ TCD-A signal shows the unresolved sum peak of H₂, N₂, CO and the well separated peaks of CO₂ and of the hydrocarbons CH₄, C₂H₆ and C₃H₈. The retention time of the last eluting gas specie C₃H₈ is 130 seconds, approximately 6 times shorter than for GC2.

5.3.2) Chromatograms of a 2 vol% gas mixture in H₂

Chromatograms obtained for the same gas mixture listed in Table 5.5 by means of the conventional gas chromatograph GC2 (see Section 3.2) and the micro gas chromatograph μ GC2 with the two modules a and b (see Section 3.5) are presented in Figs. 5.3.3 and 5.3.4, respectively. In the case of GC2 only one sample is injected and analysed by the various columns and detectors, whereas in the case of the micro gas chromatograph each module is fed by a single gas sample and analysed by the corresponding column and micro TCD.

Fig. 5.3.3 presents the TCD-A and TCD-B chromatograms of the conventional GC2 for the 2 vol% gas mixture in H₂ (see Table 5.5) in the lower and upper sections, respectively. Due to the high protium content and the He/protium anomaly the H₂ peak shows its characteristic shape. All other peaks show the usual peak form. When CO has passed through the Valco-B valve, it is switched and CO₂ is moved to the TCD-A for analysis (see the flow diagram of GC2 in Fig. 3.2.1).

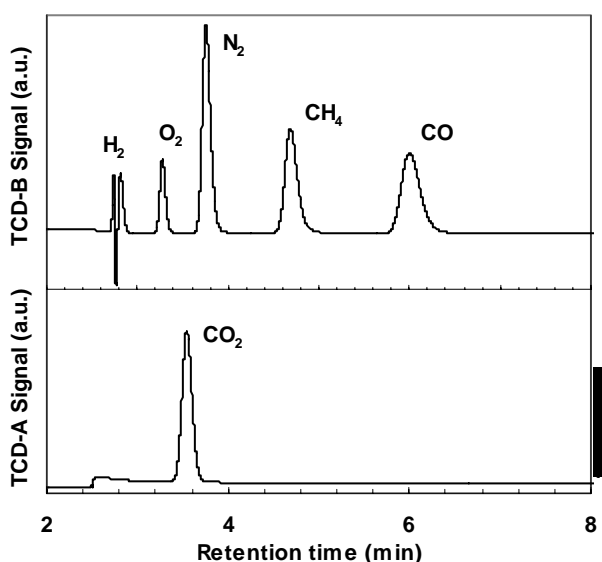


Fig. 5.3.3: TCD-A and TCD-B chromatograms of the 2 vol% gas mixture in H₂ (specified in Table 5.5) measured with the conventional GC2.

The μ TCD-A and μ TCD-B chromatograms of the 2 vol% gas mixture in H₂ (see Table 5.5) measured with the μ GC2 are shown in the lower and upper part of Fig. 5.3.4. The μ TCD-A and μ TCD-B chromatograms (Fig. 5.3.4) were obtained with the

HayeSepA column of module a and the molecular sieve column of module b, respectively. During the analysis both columns were kept at 35°C.

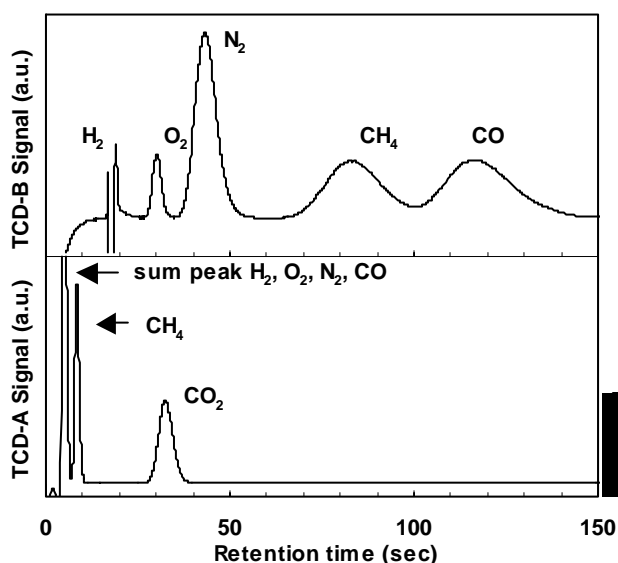


Fig. 5.3.4: μ TCD-A and μ TCD-B chromatograms of the 2 vol% gas mixture in hydrogen (specified in Table 5.5) measured with the HayeSepA column of module a (bottom) and the molecular sieve column of module b (top) using μ GC2.

All gas species listed in Table 5.5 are clearly visible in the chromatograms obtained with micro and conventional gas chromatography. No sum peak is seen in the TCD-A chromatogram of GC2 because both chromatograms are obtained with one injected sample and the gas streams are switched with the Valco-B valve available in the conventional GC2. In the case of the micro gas chromatograph independent samples were injected into the two modules of the μ GC2 and no Valco valves are in use, therefore the TCD-A shows an unresolved sum peak for H₂, O₂, N₂ and CO, but CH₄ and CO₂ are well separated.

Very different are the retention times obtained with the conventional and micro gas chromatographs. The retention times obtained by micro gas chromatography are far shorter than with conventional gas chromatography.

5.4) Use of further capillary columns for micro gas chromatography

The capillary column used for analysis of helium-hydrogen mixtures in Section 5.1 was purchased from Supelco, but this company has stopped the production of this type of column. Therefore, it was necessary to find other suppliers and to test their products.

A new supplier found was Vici Gig Harbor Group Inc. Two 30 m long capillaries were purchased:

- $\text{Al}_2\text{O}_3 + 2 \text{ w\% MnCl}_2$,
- $\text{Al}_2\text{O}_3 + 19 \text{ w\% MnCl}_2$,

4 m long pieces were cut from the purchased columns of a length of 30 m and connected as external, analytical column to the micro gas chromatograph μGC1 .

Four gas mixtures (pure H_2 ; pure D_2 ; 51.7% H_2 , 1.6 % HD and 46.6% D_2 ; and 29% H_2 , 47% HD and 24% D_2) were tested with these two 4 m long columns. The results are presented in the Figs. 5.4.1 and 5.4.2.

The experimental conditions of μGC1 during the analysis reported below were

- Carrier gas: Ne, purity 99.999%,
- Pre-column: 10 m x 0.32 ID, molecular sieve 5A, 383 K, capillary column,
- Analytical columns:
 - $\text{Al}_2\text{O}_3 + 2 \text{ w\% MnCl}_2$, 4 m x 0.53 mm ID (4 metres cut from capillary column purchased from Vici Gig Harbor Group Inc. with 30 m x 0.53 ID), 77 K, **or**
 - $\text{Al}_2\text{O}_3 + 19 \text{ w\% MnCl}_2$, 4 m x 0.53 mm ID (4 metres cut from capillary column purchased from Vici Gig Harbor Group Inc. with 30 m x 0.53 ID), 77 K,
- Sample: as given in the text,
- Sample time: 10 s,
- Injection time: 0.0 ms.

In the case of the column treated with 2% MnCl_2 the chromatograms (Fig. 5.4.1) for pure protium show clearly the contributions of para- and orthohydrogen at the low temperatures of 77K. This means that the amount of MnCl_2 on the Al_2O_3 is not enough to convert them back to normal hydrogen. The deuterium gas does not show this separation. The two lower spectra show an overlap of the H_2 and HD peaks.

Fig 5.4.2 presents the chromatograms obtained with the column treated with 19% MnCl_2 . No splitting into ortho- or parahydrogen is observed. The peak forms for H_2 , HD and D_2 have their normal simple shape required for correct and easy analysis. Therefore the 4 m long column with $\text{Al}_2\text{O}_3 + 19\% \text{ MnCl}_2$ is best suited for analysis of hydrogen gas mixtures. All peaks are very asymmetrical and no baseline separation is observed between the H_2 and HD peaks. This is attributed to the fact that pure hydrogen gas mixtures are injected and that the capillary column can not cope with the too large sample.

Fig. 5.4.3 shows the chromatogram of the same hydrogen gas mixture (29% H_2 , 47% HD and 24% D_2), but now diluted with 93% neon. An excellent separation of the three hydrogen molecules is achieved. In the case of a tritiated gas mixture there is enough space between the HD and D_2 peaks to accept the HT peak. Neon is not observed because it is used as carrier gas.

In summary: a new supplier (Vici) was found for the production of the external column required for the analysis of the helium-hydrogen mixtures. 4 m long capillary columns with $\text{Al}_2\text{O}_3 + 19\% \text{MnCl}_2$ are best suited for the separation of the hydrogen isotopes.

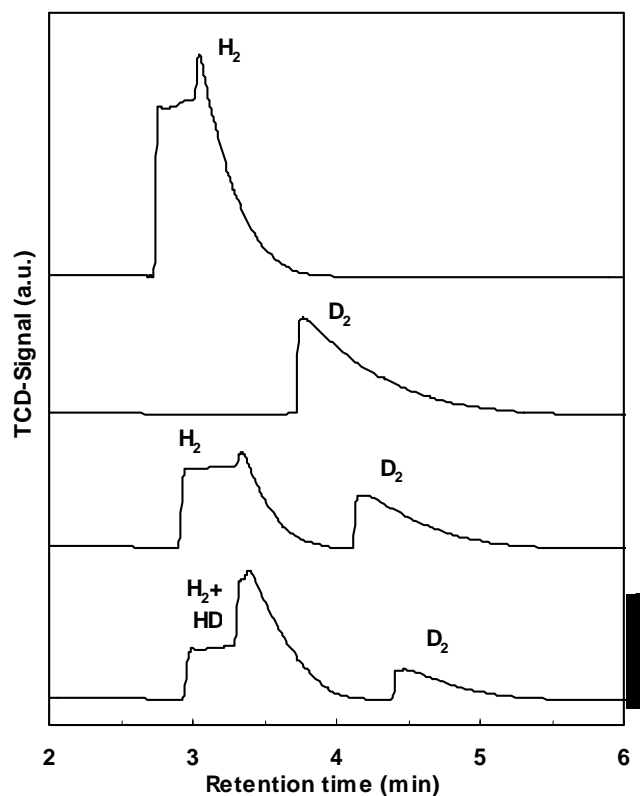


Fig. 5.4.1: μTCD -chromatograms obtained with the 4 m long $\text{Al}_2\text{O}_3 + 2\% \text{MnCl}_2$ column for pure protium (top), pure deuterium (second chromatogram from top), 51.8% H_2 , 1.6% HD and 46.6% D_2 (third chromatogram from top); and 29% H_2 , 47% HD and 24% D_2 (bottom).

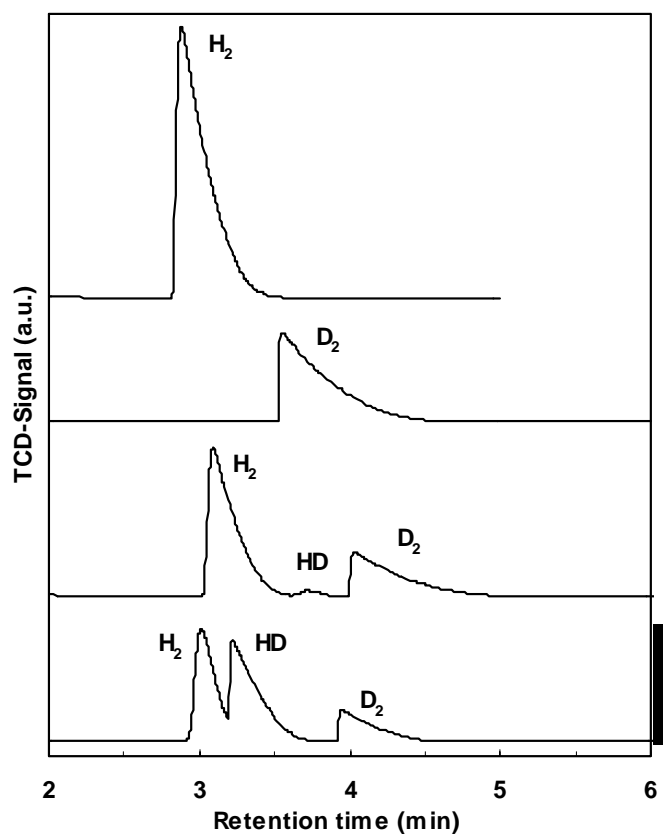


Fig. 5.4.2: μ TCD-chromatograms obtained with the 4 m long $Al_2O_3 + 19\%$ $MnCl_2$ column for pure protium (top), pure deuterium (second chromatogram from top), 51.8% H_2 , 1.6 % HD and 46.6% D_2 (third chromatogram from top); and 29% H_2 , 47% HD and 24% D_2 (bottom).

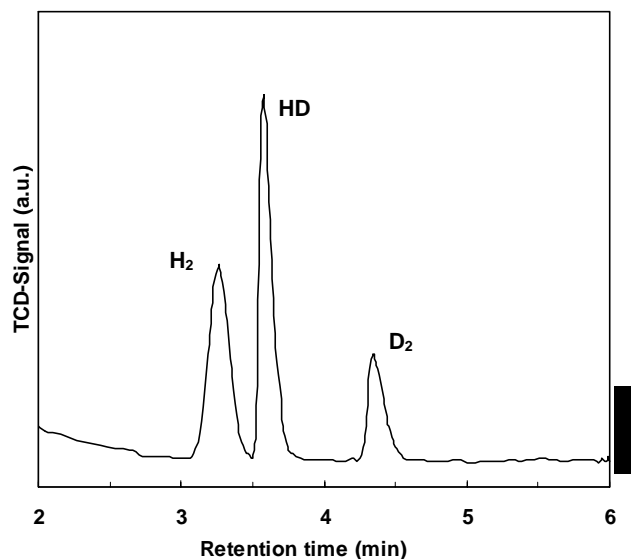


Fig. 5.4.3: μ TCD-chromatogram obtained with the 4 m long $Al_2O_3 + 19\%$ $MnCl_2$ column for a 7% hydrogen (29% H_2 , 47% HD and 24% D_2) and 93% Ne mixture.

5.5) Use of Helium and Neon as carrier gases in micro gas chromatography

When neon and helium are used as carrier gas in connection with thermal conductivity detectors (TCDs), the sensitivity of gas species measured by TCDs changes due to the far lower thermal conductivity of neon in comparison to helium. High sensitivity is obtained when the difference in thermal conductivity between the gas species to be determined and the carrier gas is large.

Helium shows the second highest thermal conductivity only overtaken by hydrogen (H_2). Tritium shows a slightly lower thermal conductivity than helium. In comparison neon has a low thermal conductivity and therefore the difference in thermal conductivity between the hydrogen molecules and neon is larger which means higher sensitivity.

Examples of the different size of the peaks observed for the hydrogen molecules are presented in various chromatograms below. Also the retention time changes due to the different carrier gases. Shorter retention times are observed for helium in comparison to neon.

Fig. 5.5.1 presents two μ TCD chromatograms of a 7% hydrogen gas mixture of 29% H_2 , 47% HD and 24% D_2 in neon. The chromatogram at the top and bottom is measured with the carrier gas Ne and He, respectively. A large Ne peak is only observed with the carrier gas He in the bottom spectrum. No H_2 peak is observed in the bottom spectrum due to the small difference in the thermal conductivities of protium and helium. In the upper chromatogram where Ne is used as carrier gas, the three peaks for H_2 , HD and D_2 are well separated and their areas are large compared to the ones in the bottom spectrum.

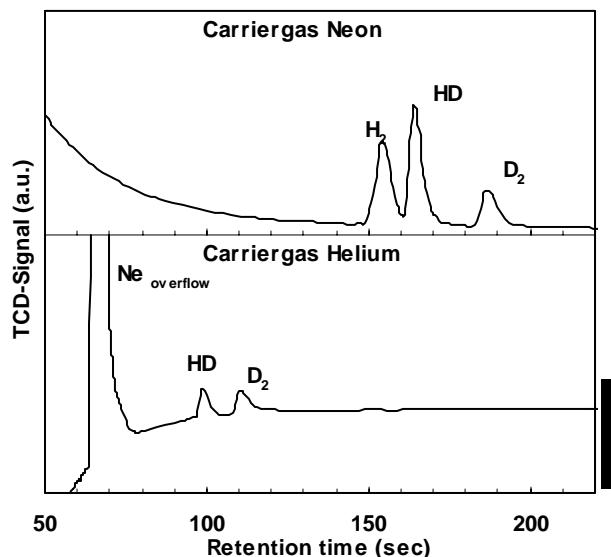


Fig. 5.5.1: Micro gas chromatograms obtained with neon (top) and helium (bottom) as carrier gases for a 7% hydrogen gas mixture of 29% H_2 , 47% HD and 24% D_2 in neon.

Fig. 5.5.2 shows μ TCD chromatograms of the hydrogen gas mixture of 29% H_2 , 47% HD and 24% D_2 with increasing neon content from top to bottom. Although the concentrations of H_2 and D_2 are comparable, in fact the H_2 concentration is slightly larger, the H_2 peak is far smaller than the D_2 one because He is used as carrier gas. When He is the carrier gas, the sensitivity of the hydrogen molecules measured by TCD

increases in the sequence H₂, HD, HT, D₂, DT and T₂. The TCD peak area of tritium is larger than of deuterium even if the injected gas amounts are equal.

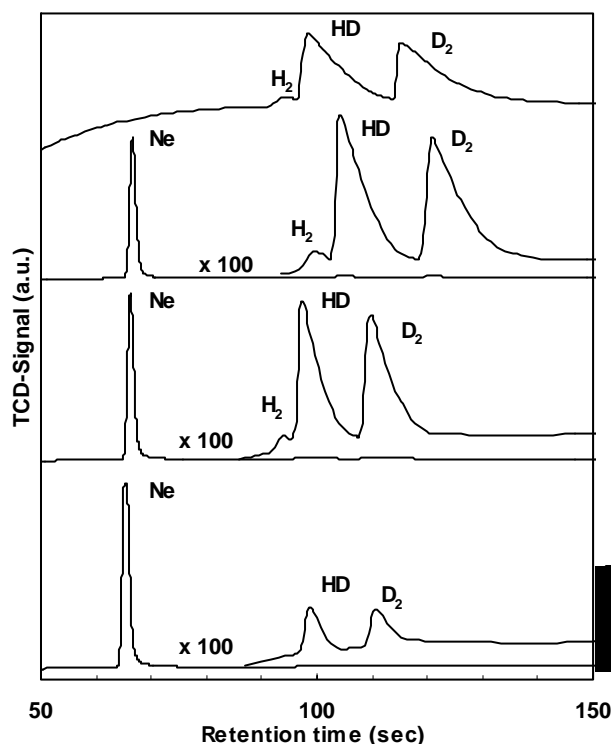


Fig. 5.5.2: Micro gas chromatograms of the Q₂ mixture: 29% H₂, 47% HD and 24% D₂ (top), 43% of the Q₂ mixture with 57% Ne (second from top), 31% of the Q₂ mixture with 69% Ne (third from the top) and 7% of the Q₂ mixture with 93% Ne (bottom). Carrier gas is helium.

For comparison with the previous figure Fig. 5.5.3 presents μ TCD chromatograms of an equilibrated Q₂ mixture of 50% H₂ and 50% D₂ with increasing helium content from top to bottom, but now Ne is used as carrier gas. In this case the sensitivity of a TCD for the hydrogen molecules decreases in the sequence H₂, HD, HT, D₂, DT and T₂. This can be seen when the areas below the H₂ and the D₂ peaks are compared as the H₂ area is slightly larger than the D₂.

Furthermore, the hydrogen peaks are well separated and detected even in the spectrum at the bottom although the Q₂ mixture is only present with 1 % in the residual He gas. When He is used as carrier gas (see bottom spectrum of Fig. 5.5.2) only the HD and D₂ peaks are observed although the amount of the Q₂ mixture injected is seven times larger than in the bottom of Fig. 5.5.3. This again is a clear indication for the higher sensitivity achieved with the carrier gas Ne than with He.

A final comparison is presented in Fig. 5.5.4. Again the H₂ peak area when measured with He as carrier gas, is far too low in the bottom chromatogram with respect to the protium concentration in the gas mixture.

The conclusion of the discussion of the chromatograms shown above is that neon is far better suited for hydrogen analysis than helium.

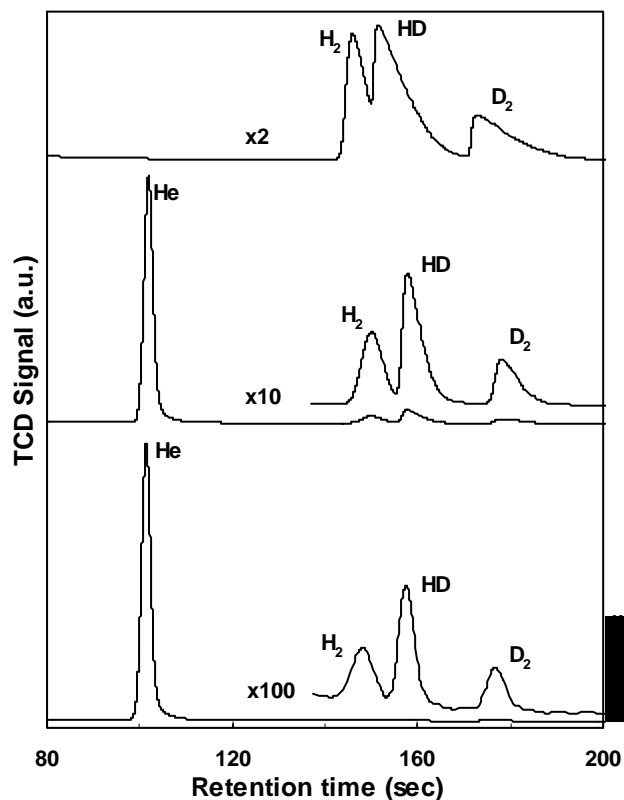


Fig. 5.5.3: Micro gas chromatograms of the equilibrated Q₂ mixture of 50% H₂ and 50% D₂ (top), 12% of the equilibrated Q₂ mixture with 88% He (middle) and 1% of the equilibrated Q₂ mixture with 99% He (bottom). Carrier gas is neon.

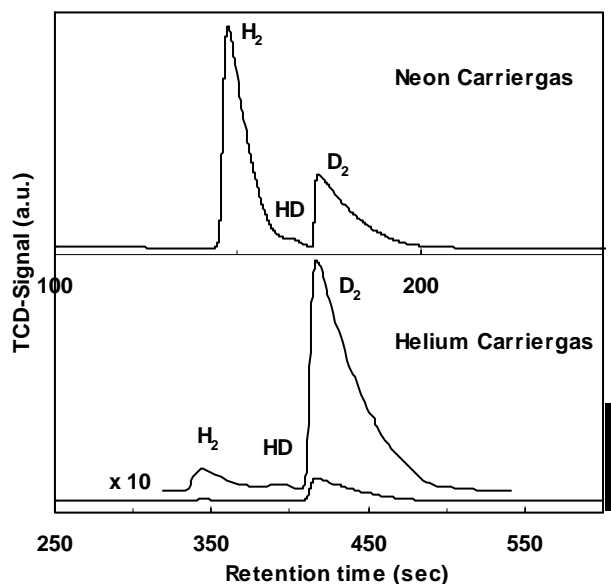


Fig. 5.5.4: Micro gas chromatograms of the Q₂ mixture of 51.8% H₂, 1.6% HD and 46.6% D₂ measured with Ne as carrier gas (top) and with Helium as carrier gas (bottom).

5.6) Influence of the head pressure on the retention time

Fig. 5.6.1 shows the influence of the column head pressure on the retention times of the hydrogen peaks. With higher head pressure the flow rate through the column, which has a constant flow resistance, increases and as a consequence the retention times decrease as seen in Fig. 5.6.1. Therefore, it is important that the head pressure is kept constant if retention times are used for identification of peaks.

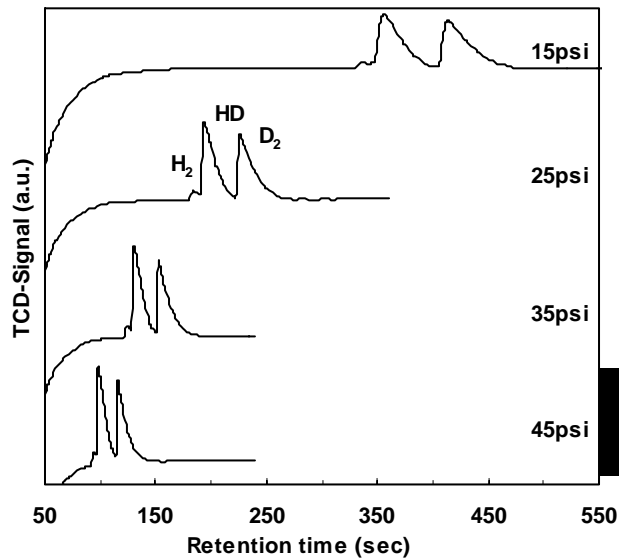


Fig. 5.6.1: Micro gas chromatograms of the Q₂ mixture of 29% H₂, 47% HD and 24% D₂ measured with Helium as carrier gas for various column head pressures between 15 and 45 psi.

6) Gas chromatography proposed for ITER

This section presents the analytical equipment proposed for the ITER Tritium Plant. The proposal is the result of the experience gained at JET in the Active Gas Handling System (AGHS) /1.29, 1.30/, at the Tritium Laboratory Karlsruhe (TLK) /1.2, 1.16/ and at the Tritium Engineering Laboratory (TPL) /1.34, 1.35/ in Japan. The proposal is presented here to demonstrate that the analytical research at the TLK was not only performed to improve the analytical local equipment, but contributed also to the design of the main analytical tools of the Analytical Laboratory (ANS) for ITER.

Furthermore, a comparison between the three main analytical techniques used in tritium handling facilities (mass spectrometry, laser Raman spectroscopy, gas chromatography) revealed clearly that gas chromatography is the simplest one, the one most often used, by far the cheapest of all methods mentioned, demanding only a small amount of space, can be placed fully inside a glove box, does not need any ultra- and high vacuum pumps, does not use any type of window material, which could brake, and is easy to be learnt and to be maintained by the operators. A further advantage is that all the requirements specified for the analytical system of ITER ANS can be dealt by gas chromatographic systems. The main disadvantage is the not clearly specified leak tightness of part of the equipment used in micro gas chromatography. If laser Raman spectroscopy were chosen, further analytical instruments would be required for the detection of noble gases and the quantitative determination of hydrocarbons.

The various analytical tasks required for ITER ANS can not be performed by a single analytical system. Two different types of gas chromatographs, three micro GCs and two conventional packed GCs, are required. If mass spectrometry or Laser Raman scattering were chosen, also a few of these instruments and even others ones would be needed making the cost difference even higher.

In the following the explanations are given using the tag number system developed of the ITER ANS drawings. Furthermore, in the subsequent discussion manual valves are assumed to be open. They are mainly installed for maintenance purposes. Automatic valves are used wherever remote operation of the analytical instruments is required.

6.1) Operation of the micro gas chromatographs used in ANS

The operation of the three micro GCs 1 μ GC-6-7100, μ GC-6-7200 and μ GC-6-7300 is explained below by means of the detailed drawing shown in Fig. 6.1.1 for the micro gas chromatograph μ GC-6-7100. These micro GCs are used only for the analysis of pure helium-hydrogen gas mixtures expected to be handled in the Storage and Delivery System (SDS) and in the Isotope Separation System (ISS) of the ITER fuel cycle.

The gas for analysis is supplied to the injector component of the micro GC-6-7100 by opening the automatic valve VA-6-7105 and expands into the sample loop of the injector. A small continuous gas flow is generated from the connected manifold via the sample loop by the internal pumps PM-6-7115. The internal lines of the injector are purged in this way and the exhaust gases of the internal pump are moved to the upstream pressure regulator PRU-6-7131.

The carrier gas neon flows continuously through the micro-GC-6-7100 via the open manual valve VM-6-7107. The internal pressure regulator reduces the pressure to the necessary head pressure for the columns.

A sample from the sample loop is injected via actuating the internal switching valve. The amount of sample gas injected into the carrier gas by the pressure of the carrier gas just

downstream of the pressure regulator depends on the time the switching valve is operated.

The sample to be analysed is forced by the carrier gas through a capillary column cooled to liquid nitrogen temperature. The carrier gas eluting from the liquid nitrogen cooled column enters the measurement side of the micro TCD, whereas a very similar flow of pure carrier gas (not containing any sample) passes through the reference side of the TCD. Any deviations in the thermal conductivity between the two gas streams are detected and are interpreted as gas species with thermal conductivity different from the one of the carrier gas.

The two outlets of the thermal conductivity detector are combined to one line and the pressure in the TCD is kept constant by a special upstream pressure regulator. The thermal conductivity detector detects helium and the six hydrogen molecules, most of the other gas species - if present in the sample - are trapped in the column and will be released again during warm-up of the column.

Due to the very small gas amounts necessary in micro-GC analysis the exhaust gases of the micro gas chromatographs can be directly sent to simple detritiation system.

The liquid nitrogen dewar is filled with liquid nitrogen via operation of the automatic valve VA-8-7513. When the liquid nitrogen level reaches a certain low height, the valve is opened and liquid nitrogen is added to the dewar until an upper level is reached which causes the valve to close again.

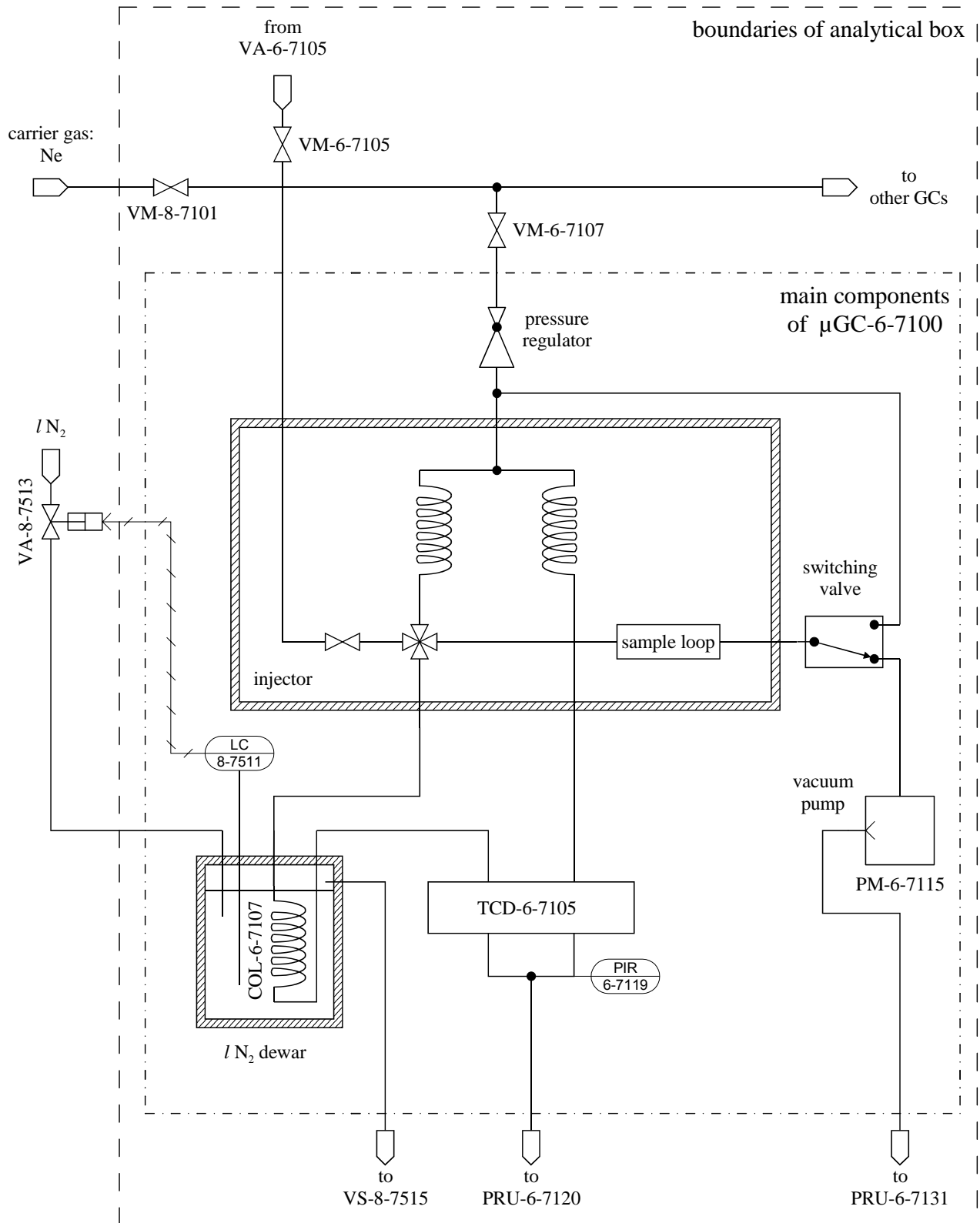


Fig. 6.1.1: Main components of the micro gas chromatograph $\mu\text{GC-6-7100}$ proposed as part of the Analytical System (ANS) for the ITER Tritium plant with connecting pipe work and indications of the next component.

6.2) The operation of the special gas chromatographs used in ANS

The operation of the two special, but conventional GCs GC-7-7400 and GC-7-7500 is explained below by means of the detailed drawing shown in Fig. 6.2.1 for the gas chromatograph GC-7-7400.

6.2.1) The compression loops

The purpose of the compression loops is to compress the samples to a certain pressure before their injection into the GCs by means of the Valco valves VX-7-7458 and VX-7-7478. This compression guarantees the injection of equal sample amounts into the GCs independent of their pressures in the manifolds as long as the set values of the downstream pressure regulators are not modified and the temperature inside the box is not changing.

The compression pressure should be chosen very similar to the head pressure of the GC-unit to avoid any pressure fluctuations and instabilities of detectors. The compression pressure in the two compression loops of the special GC can be modified - if required - by the downstream pressure regulators PRD-7-7453, PRD-7-7455, and PRD-7-7473, PRD-7-7475, respectively, for the two analytical systems.

Naturally, even with the compression loops installed, it is possible to analyse uncompressed samples, that means samples of any pressure. In that case the valves VA-7-7452, VA-7-7454 and VA-7-7472, VA-7-7474, respectively, are kept closed. This possibility permits the injection of small tritium amounts for samples with high tritium concentrations.

A sample to be analysed in GC-7-7400 enters the compression loops after opening the valves VA-7-7405, VA-7-7451 and VA-7-7471. In this way both analytical processes can be used to analyse the same sample. After closing VA-7-7451 or VA-7-7471 the samples in the two compression loops can be compressed by opening valves VA-7-7452 or VA-7-7454 and VA-7-7472 or VA-7-7474.

If only one of the two systems is to be used, the valve to the other system is kept closed (VA-7-7451 or VA-7-7471).

The compression of the gases in the compression loop is preferably done with the type of carrier gas used in the process.

In summary: the compression loop offers a simple method to compress samples to a certain pre-chosen pressure. This allows easier comparison between different chromatograms and gives lower detection limits.

6.2.2) Injection of gas in the sampling volume

The either compressed or uncompressed samples in the sampling volumes of the Valco valves VX-7-7458 and VX-7-7478 are injected into the heated first columns by rotation of the Valco valves.

After the injection, the Valco valves VX-7-7458 and VX-7-7478 are rotated back into their start configuration and the gas in the compression loops is pumped away after opening the valves VA-7-7459 and VA-7-7479 by means of a pump not shown in Fig 6.2.1 which is connected to the line 8-5-7459. To remove any small amount still present from the sample in the long capillary tubes CP-7-7459 and CP-7-7479 with the small inner diameter the inner volumes are flushed extensively with the carrier gas to be used in the next analysis by opening the corresponding valves VA-7-7452 or VA-7-7454 and VA-7-7472 or VA-7-7474.

6.2.3) Separation and detection of He, the six hydrogen molecules and of impurities

The column COL-7-7482 separates He and hydrogen from the other impurities which need more time to pass through the column. All gases are sent through the right side of the TCD-7-7486. After the injection of He and hydrogen via the Valco valve VX-7-7483 into the COL-7-7484 the Valco valve is switched back. The impurities are transferred directly – after their passage through the thermal conductivity detector TCD-7-7486 via VX-7-7483 - to PRU-7-7488 bypassing COL-7-7484. No impurities are absorbed in 77 K cold COL-7-7484 and blocking of the column is excluded.

The hydrogen molecule separation occurs in the liquid nitrogen cooled column COL-7-7484, whereas the separation of N₂, O₂, Ar, CQ₄, CO, etc. happens in COL-7-7482.

The TCD-7-7486 observes hydrogen (Q₂) as one peak, He and impurities in the measurement channel and helium and the six separated hydrogen molecules in the reference channel. To avoid overlapping of the signals from the measurement- and reference channels the column length of the two columns COL-7-7482 and COL-7-7484 must to be chosen correctly. The length of the two columns must be chosen such that the impurities have passed through the TCD before the hydrogen molecules arrive. If the problem of possible overlap (by not correctly chosen column length) of the TCD signals is to be avoided two separate TCD detectors are to be used in the two streams.

The ionisation chamber IC-7-7487 detects the tritiated fractions of the Q₂ gas species (HT, DT, T₂), helps to find the correct assessment of the peaks analysed with the TCD and improves the lower detection limit.

6.2.4) Separation and detection of impurities

The column Col-7-7462 separates the impurities expected in the exhaust gas of a fusion device. Via the 50/50 splitter at the exit of the column the gas stream is split into two equal parts which enter the various detectors.

The Helium ionisation detector HeID-7-7463 detects impurities in the range between 0.1 and 200 ppm, the TCD-7-7465 in the higher concentration ranges above 100 ppm, the FID-7-7467 detects hydrocarbons for concentrations between 0.01 ppm and 100 % and the ionisation chamber XIR-7-7564 tritiated gas species in the range down to approximately 0.01 ppm depending on the amount of the injected sample.

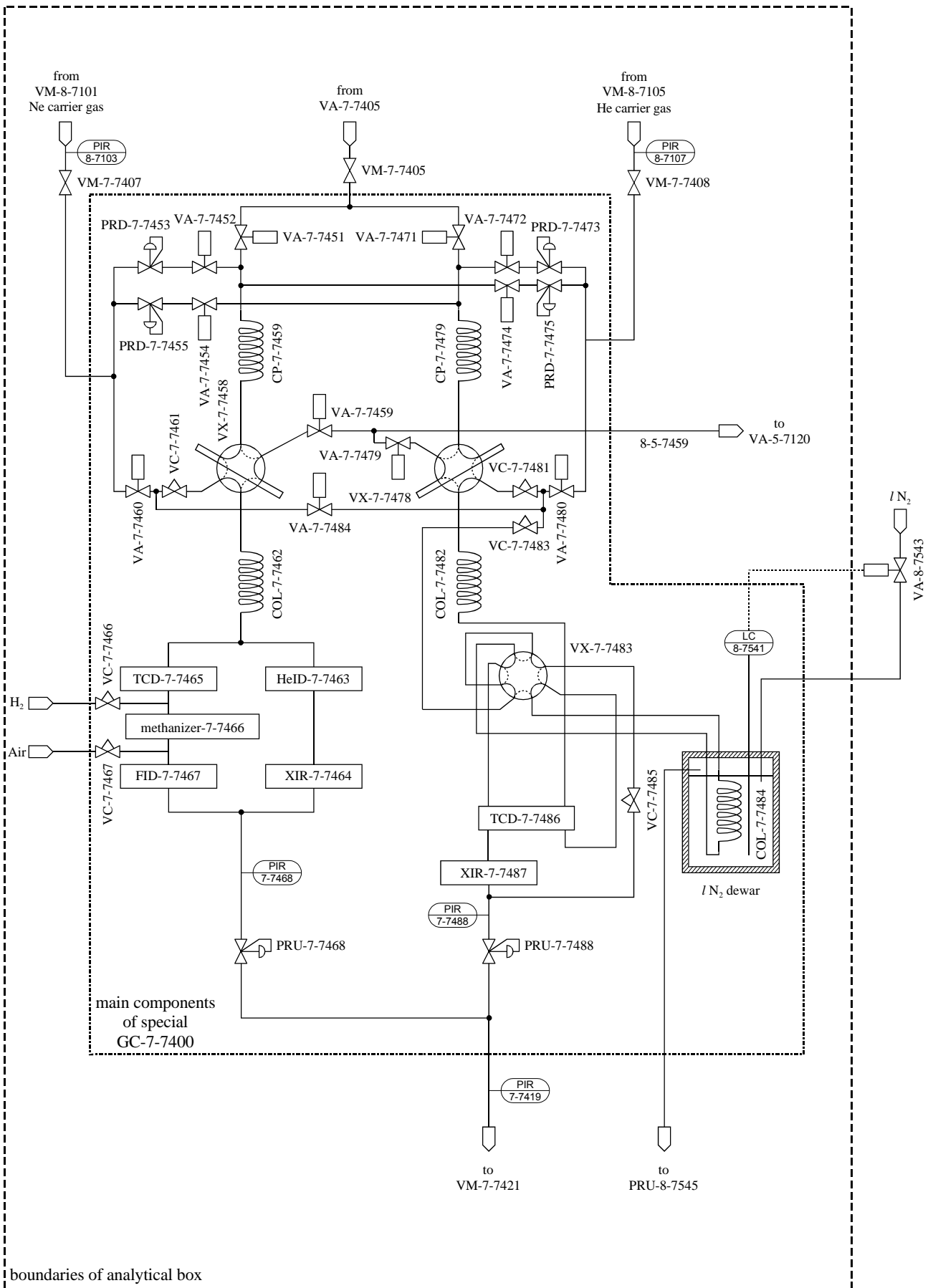


Fig. 6.2.1: Main components of the special gas chromatograph GC-7-7400 proposed as part of the Analytical System (ANS) for the ITER Tritium plant with connecting pipe work and indications of the next component.

7) Possible enhancements for GC1 and GC2 used in TMT

GC1 was and is the workhorse of the TMT and is used for many analytical tasks at the TLK. Together with GC2 both systems can fulfil almost all analytical requests arising in a tritium research facility, but the analysis of a sample by two gas chromatographs is cumbersome. In the following disadvantages, shortcomings and possible enhancements of the existing GC systems are briefly mentioned.

The use of He as carrier gas and of a helium ionisation detector in the present TMT systems GC1 and GC2 causes the following shortcomings:

- Due to the small differences in the thermal conductivity between He and H₂, HD, HT, D₂, DT, T₂, the TCD signals are relatively small when the hydrogen gas species are detected in a He carrier gas in comparison to Ne. An immediate consequence is that for the same injected gas amount the hydrogen species are detected more sensitively with Ne than with He.
- Large amounts of injected protium cannot be quantitatively measured by means of thermal conductivity detectors due to the anomaly of the thermal conductivity of He/H₂ mixtures. This is also true for the TCDs of GC2. A possible solution to avoid this anomaly could be the addition of protium in front of the TCD-B of GC2. This trick is already used in the case of TCD-B of GC1.
- A HeD is a very sensitive detector and only capable of measuring concentrations in the range of approximately 0.1 to 200 ppm. Higher concentrations lead to overflow and quantitative determination of gas species with too high concentrations is not any more possible. For these concentrations other detectors are to be used or other components are to be added, e.g. System 2 of GC1.
- Protium needs to be added in front of the HeD-A to achieve a stable baseline.
- If the exhaust streams of a GC needs to be detritiated the continuous addition of even small protium streams (just in front of the TCD-B or of the HeD-A) is a nuisance as protium must be recovered in various systems and then separated from tritium in special isotope separation systems.
- Due to the use of He as carrier gas in System 1 of GC1, another system with another carrier gas is required to detect helium. This is one of the purposes of System 2 which uses nitrogen as carrier gas. A further advantage of system 2 is that concentrations up to 100% can be determined for O₂, CO and CQ₄.
- With GC1 nitrogen and higher hydrocarbons are only determined quantitatively for concentrations smaller than 200 ppm. For their determination up to 100% the gas chromatograph GC2 is required.

In the flow diagrams of the gas chromatographs GC1 and GC2 shown in Figs. 3.1.1 and 3.2.1 full purging of the compression loop is not possible because compression and evacuation occurs via the same connection point. Better purging is achieved when the vacuum pump is connected to the other end of the compression loop next to the Valco valve. In this way simple purging and evacuation of the whole compression loop in one direction is possible.

GC2 is mainly required to measure higher concentrations of N₂, CO₂ and higher hydrocarbons.

In the following various possible enhancements for GC1 are listed:

- Use of neon as carrier gas instead of He. The benefits are
 - higher sensitivity (lower detection limits) for the hydrogen isotopes,
 - detection of He,
 - no addition of H₂ in front of TCD-B is any more required.
- Installation of a further TCD in front of HeD. This will allow to measure all gas species with concentrations up to 100%.
- The HeD is expected to function also with Ne as carrier gas, but detection of He in the gas mixture by the NeD is not possible. This is not critical as He is anyway moved to column-B and analysed by the TCD-B of GC1.
- Instead of the HeD or NeD a Flame Ionisation Detector (FID) could be installed. A FID is a very sensitive detector for all hydrocarbons and even for CO and CO₂ when a methaniser is used. The main disadvantages of FIDs are the generation of water vapour in the flame, the necessity of heating the exhaust pipes to avoid the appearance of liquid water in the pipe work and its general low leak tightness.

Such an enhanced gas chromatographic system can replace the present GC1 and GC2. Its advantages and disadvantages are

- Higher sensitivity and lower detection limits for the hydrogen isotopes and approximately the same for He with the TCD-B.
- Determination of the gases eluting from column-A with the TCD-A up to 100% (installed directly after column-A) and with the NeD-A (installed instead of HeD-A) in approximately the same concentration range as with the HeD.
- If the NeD is not working as assumed then a FID in combination with a methaniser could be used to detect hydrocarbons, CO and CO₂. The dynamic range of a FID is over six orders of magnitude up to 100%. The gases O₂ and N₂ are only observed by the TCD-A, therefore concentrations of O₂ and N₂ in the range below 200 ppm are not easily detected.
- ³He is observed with the same retention time as ⁴He. Therefore in mixtures with ³He and ⁴He the contribution of ³He can not be distinguished from ⁴He when Ne is used as carrier gas.

The discussion above shows that with the improved GC almost all gas species can be detected better. An exception is ³He. In the past the determination of ³He was not a requirement for most analytical equipments of tritium handling facilities. The analytical results discussed above are achievable with only one gas chromatograph meaning that the number of gas chromatographic runs required is reduced by a factor of 2. In addition, the requirements on GC hardware, on space, on carrier gases are reduced as well as on the time operators have to spend for the analytical runs and the interpretation of the chromatograms.

The TLK experience with the available GCs shows clearly that the gases of interest can be analysed well and that even cross checking between the various GC runs and the obtained results is possible. This gives great confidence in the determinations of the gas compositions, but results into a larger work burden on the operators.

8) Conclusions

Among the analytical techniques (mass spectrometry, laser Raman spectroscopy, gas chromatography, use of ionisation chambers) employed at the Tritium Laboratory Karlsruhe gas chromatography plays a prominent role.

This is partly due to the simplicity of the gas chromatographic separation process, the small space required, the low investment costs in comparison to other methods, the robustness of the equipment and due to the simple analysis, but partly also because all information required for a gas mixture can be simply obtained by performing gas chromatographic analysis alone. This is for example not the case in laser Raman spectroscopy where noble gases can not be characterised by means of vibrational excitations or where the analysis of even simple hydrocarbons such as methane becomes already almost too difficult to perform a quantitative analysis. Not to speak from even higher hydrocarbons with even more possible vibrational excitations to be considered when all three hydrogen isotopes are present. Also mass spectrometry can become too difficult for a quantitative analysis when too many hydrocarbons are present and peaks start to overlap due to the many cracking products. The situation becomes even worse when trimers have to be considered and three hydrogen isotopes are present in the gas mixture and in the hydrogen containing molecules. In addition, the hot filaments can change the equilibrium of the gas mixture to be analysed and cause changes of the composition of the gas mixture.

The conventional gas chromatographs GC1 and GC2 used in the Tritium Measurement Techniques (TMT) System of the Tritium Laboratory Karlsruhe (TLK) and the gas chromatograph GC3 of the experiment CAPER are presented in detail, by discussing their flow diagrams, their major components, many obtained chromatograms, shortcomings and possible improvements. One of the main disadvantages of the conventional gas chromatography is the long retention times required for the analysis of hydrogen gas mixtures. To overcome this disadvantage, micro gas chromatography for hydrogen analysis was developed. Reduction of the retention times by one order of magnitude was achieved. This development requires the modification of conventional micro gas chromatographs and the installation of a special external analytical column for the application of the low temperature required for the separation of the hydrogen molecules. Furthermore, the usefulness of conventional micro gas chromatography for the detection of impurities in gas mixtures similar to the ones to be processed in future power producing fusion devices was demonstrated by the analysis of different impurity gas mixtures. The necessary enhancements and modifications, the special flow diagrams, the obtained chromatograms for various helium-hydrogen isotope and impurity mixtures are also discussed in detail.

The design of the analytical tools of the Analytical System (ANS) of the ITER Tritium Plant is briefly mentioned because it is based to a large extent on the experience gained during the frequent use of gas chromatography at the TLK and on the development of micro gas chromatography in the last years.

Finally, because most analytical equipment can be improved, a few possible enhancements for GC1 are briefly mentioned as well as the use of one enhanced gas chromatographic system instead of GC1 and GC2.

The purpose of this report is to summarise the experience gained with gas chromatography at the TLK during the last years and to present the collected information of major components and of the obtained chromatograms in a simple and comprehensive way. Therefore, it is hoped that the present work may be of use for any scientist interested in analytical problems or for designers of analytical tools such as gas chromatography.

Acknowledgement

This work has been performed within the framework of the Nuclear Fusion Project of the Forschungszentrum Karlsruhe and is supported by the European Communities within the European Fusion Technology Program.

List of Figures

Fig. 3.1.1: Flow diagram of GC1.

Fig. 3.1.2: Compression of a sample (top) and carrier flows during/after the injection of the sample into System 1 and System 2, transfer of He and ΣQ_2 into Col-B (middle) and analysis of impurities with Valco-B switched (bottom).

Fig. 3.2.1: Flow diagram of GC2.

Fig. 3.2.2: Compression of a sample (top) and carrier flows during transfer of the sample to column-A and column-B (middle) and bypassing column-B (bottom).

Fig. 3.2.3: View on a large section of the TMT glove box: On the left side the main electronic equipment is visible, whereas GC1 and GC2 are seen on the left and right side behind the upper window of the TMT glove box.

Fig. 3.2.4: View on the upper part of the TMT glove box with GC1 on the left and GC2 on the right side.

Fig. 3.2.5: View on one side of the TMT glove box.

Fig. 3.3.1: Flow diagram of GC3.

Fig. 3.3.2: Preparation of a sample for injection (top) and carrier flows highlighted during transfer of the sample to column-C and TCD-C (2. picture from top), to column-B and TCD-B (3. picture from top) and to column-A and TCD-A (bottom). ICs are not shown.

Fig. 3.3.3: View on the right end of the CAPER glove box A which contains GC3.

Fig. 3.3.4: Photo of GC3 inside the Caper glove box A.

Fig. 3.3.5: Part of the electronic units to control the gas chromatograph GC3.

Fig. 3.4.1: Flow diagram of the μ GC1. The equipment between the dashed lines shows the external column in a special dewar.

Fig. 3.5.1: Flow diagram of one of the two modules of the μ GC2. The equipment between the dashed lines shows the external column in a special dewar.

Fig. 3.5.2: View on μ GC1 (instrument on right side with flow meter), μ GC2 (on the left side of μ GC1), electronic recorder (on the left side of μ GC2) and gas inlet system with valves, pipe work and mechanical pump in the background.

Fig. 3.5.3: Bird view on the experimental set-up of the micro gas chromatographs μ GC1 and μ GC2 and on the pipe work used for preparation and injection of samples.

Fig. 3.5.4: Agilent μ GC1 with external analytical column placed in liquid nitrogen and freely hanging. The oven for regeneration of the column is visible behind the dewar in the photo on the right side.

Fig. 3.7.1: Connections of calibrated gas mixtures to GC1 and GC2 of TMT.

Fig. 3.7.2: Connections of calibrated gas mixtures for μ GC1 and μ GC2.

Fig. 4.1.1: Area of the D_2 peak as a function of the pressure in the injection loop of GC1.

Fig. 4.1.2: Area of the O_2 peak as a function of the pressure in the injection loop of GC2.

Fig. 4.2.1: H_2 peak areas obtained with TCD-B of GC1 after compression as a function of the pressure in the injection loop of system 1.

Fig. 4.2.2: Helium and hydrogen peak areas obtained with TCD-C of GC1 after compression as a function of the pressure in the injection loop of system-2.

Fig. 4.3.1: TCD-B chromatograms obtained with GC2 as a function of the injection pressure in the compression loop for the 2 vol% gas mixture given in Table 4.1. The peaks at 2.8 and 3.25 minutes are due to H_2 and O_2 , respectively.

Fig. 4.4.1: TCD-B chromatogram of a hydrogen isotope mixture with 49.0% H_2 , 2.3% HD and 48.7% D_2 measured with GC1.

Fig. 4.4.2: TCD-B chromatograms of 99.9999% protium (top), of a 25.4% H_2 , 48.0% HD and 26.6% D_2 hydrogen gas mixture (middle) and of 0.3% HD, 99.7% D_2 gas mixture (bottom) measured with GC1.

Fig. 4.4.3: TCD-B chromatograms of a 48.1% H₂, 1.1% HD and 50.8% D₂ hydrogen gas mixture (top) and of a 25.4% H₂, 48.0% HD and 26.6% D₂ hydrogen gas mixture (bottom) measured with GC1.

Fig. 4.4.4: TCD-B and IC-B chromatograms of the hydrogen-tritium gas mixture given in Table 4.2 and measured with GC1.

Fig. 4.4.5: TCD-B chromatograms of 99.9999% protium (top), of 0.3% HD, 99.7% D₂ (middle) and 0.23% HT, 0.11% DT and 99.66% T₂ (bottom) measured with GC1.

Fig. 4.4.6: One TCB-B (top) and four IC-B chromatograms of a tritium mixture containing 0.23% HT, 0.11% DT and 99.66% T₂ measured with GC1. Top three chromatograms are obtained with compressed samples, second lowest and lowest chromatograms with 5.1 kPa and 600 Pa, respectively.

Fig. 4.4.7: HeD-A chromatogram of the gas mixture given in Table 4.3 and measured with System 1 of GC1.

Fig. 4.4.8: TCD-A and TCD-B chromatograms of the gas mixture given in Table 4.3 and measured with GC2.

Fig. 4.4.9: TCD-A chromatogram of the gas mixture given in Table 4.3 and measured with GC3.

Fig. 4.4.10: HeD signal of the 100 vpm gas mixture listed in Table 4.4 and measured with GC1.

Fig. 4.4.11: TCD-A chromatogram of the gas mixture given in Table 4.3 and measured with GC2 with a slightly modified method (for details see text).

Fig. 4.4.12: TCD-B and IC-B chromatograms of the gas mixture specified in Table 4.5. and measured with GC1

Fig. 4.4.13: HeD-A and IC-A chromatograms of the gas mixture specified in Table 4.5 and measured with GC1.

Fig. 4.4.14: TCD-C and IC-C chromatograms of the gas mixture specified in Table 4.5 and measured with GC1.

Fig. 4.4.15: TCD-B chromatograms of a gas mixture containing 53.1% ³He, 1.3% HT, 0.6% DT and 45.0% T₂ and measured with GC1.

Fig. 4.4.16: IC-B chromatograms of a gas mixture containing 53.1% ³He, 1.3% HT, 0.6% DT and 45.0% T₂ and measured with GC1.

Fig. 4.4.17: IC-B chromatograms of a gas mixture containing 53.1% ³He, 1.3% HT, 0.6% DT and 45.0% T₂, measured with GC1 and processed with PC.

Fig. 4.4.18: TCD-B chromatograms of a gas mixture containing 53.1% ³He, 1.3% HT, 0.6% DT and 45.0% T₂ and measured with GC1.

Fig. 4.5.1 TCD-B and IC-B chromatograms for the gas mixture listed in Table 4.6 and measured with GC1.

Fig. 4.5.2: HeD-A and IC-A chromatograms for the gas mixture listed in Table 4.6 and measured with GC1.

Fig. 4.5.3: TCD-C and IC-C chromatograms for the gas mixture listed in Table 4.6 and measured with GC1.

Fig. 4.5.4: TCD-A and IC-A chromatograms for the gas mixture listed in Table 4.6 and measured with GC2.

Fig. 4.5.5: TCD-B and IC-B chromatograms for the gas mixture listed in Table 4.6 and measured with GC2.

Fig. 4.5.6: TCD-C and IC-C chromatograms of the gas mixture listed in Table 4.6 and measured with GC3.

Fig. 4.5.7: TCD-B chromatogram for the gas mixture listed in Table 4.6 and measured with GC3.

Fig. 4.5.8: TCD-A and IC-A chromatograms for the gas mixture listed in Table 4.6 and measured with GC3.

Fig. 5.1.1: μ TCD-chromatogram of μ GC1 for a gas mixture of 88% He and 12 % hydrogen of equilibrated 50% H/50% D.

Fig. 5.1.2: μ TCD-chromatogram of μ GC1 for a gas mixture of 92% He and 8% hydrogen of equilibrated 50% H/50% D.

Fig. 5.1.3: μ TCD-chromatogram of μ GC1 for a gas mixture of 99% He and 1 % hydrogen of an equilibrated 50% H/50% D.

Fig. 5.1.4: μ TCD-chromatogram of μ GC1 for a gas mixture of 89% He and 11% hydrogen of the mixture of 51.7% H₂, 1.6 % HD and 46.6% D₂.

Fig. 5.1.5: μ TCD chromatograms of a non diluted equilibrated 50% H/50% D hydrogen mixture (top), of an equilibrated 50% H/50% D mixture in 92% He (middle) and in 99% He (bottom).

Fig. 5.1.6: μ TCD chromatograms for a gas mixture with 88% He (top) and 90% He (bottom), balance: equilibrated 50% H/50% D gas mixture.

Fig. 5.2.1: μ TCD-A and μ TCD-B chromatograms of the 80 ppm gas mixture in He (listed in Table 5.2) measured with the HayeSepA column of module a at 35°C (bottom) and the molecular sieve column of module b (top) at 80°C using μ GC2.

Fig. 5.2.2: μ TCD-A and μ TCD-B chromatograms of the 100 ppm gas mixture in H₂ (listed in Table 5.3) measured with the HayeSepA column of module a (bottom) at 100°C and the molecular sieve column of module b (top) at 60°C using μ GC2.

Fig. 5.2.3: μ TCD-A and μ TCD-B chromatograms of the 100 ppm gas mixture in He (listed in Table 5.4) measured with the HayeSepA column of module a (bottom) at 35°C and the molecular sieve column of module b (top) at 80°C using μ GC2.

Fig. 5.2.4: μ TCD-A and μ TCD-B chromatograms of the 2 vol% gas mixture in H₂ (listed in Table 5.5) measured with the HayeSepA column of module a (bottom) at 35°C and the molecular sieve column of module b (top) at 35°C using μ GC2.

Fig. 5.3.1: TCD-A and TCD-B chromatograms of the 1 vol% gas mixture in H₂ (specified in Table 5.6) obtained with the conventional GC2 of the TMT.

Fig. 5.3.2: μ TCD-A and μ TCD-B chromatograms of the 1 vol% gas mixture in H₂ (specified in Table 5.6) measured with the HayeSepA column of module a (bottom) and the molecular sieve column of module b (top) using μ GC2.

Fig. 5.3.3: TCD-A and TCD-B chromatograms of the 2 vol% gas mixture in H₂ (specified in Table 5.5) measured with the conventional GC2.

Fig. 5.3.4: μ TCD-A and μ TCD-B chromatograms of the 2 vol% gas mixture in hydrogen (specified in Table 5.5) measured with the HayeSepA column of module a (bottom) and the molecular sieve column of module b (top) using μ GC2.

Fig. 5.4.1: μ TCD-chromatograms obtained with the 4 m long Al₂O₃ + 2% MnCl₂ column for pure protium (top), pure deuterium (second chromatogram from top), 51.8% H₂, 1.6 % HD and 46.6% D₂ (third chromatogram from top); and 29% H₂, 47% HD and 24% D₂ (bottom).

Fig. 5.4.2: μ TCD-chromatograms obtained with the 4 m long Al₂O₃ + 19% MnCl₂ column for pure protium (top), pure deuterium (second chromatogram from top), 51.8% H₂, 1.6 % HD and 46.6% D₂ (third chromatogram from top); and 29% H₂, 47% HD and 24% D₂ (bottom).

Fig. 5.4.3: μ TCD-chromatogram obtained with the 4 m long Al₂O₃ + 19% MnCl₂ column for a 7% hydrogen (29% H₂, 47% HD and 24% D₂) and 93% Ne mixture.

Fig. 5.5.1: Micro gas chromatograms obtained with neon and helium as carrier gases for a 7% hydrogen gas mixture of 29% H₂, 47% HD and 24% D₂ in neon.

Fig. 5.5.2: Micro gas chromatograms of the Q2 mixture: 29% H₂, 47% HD and 24% D₂ (top), 43% of the Q2 mixture with 57% Ne (second from top), 31% of the Q2 mixture

with 69% Ne (third form the top) and 7% of the Q2 mixture with 93% Ne (bottom). Carrier gas is helium.

Fig. 5.5.3: Micro gas chromatograms of the equilibrated Q₂ mixture of 50% H₂ and 50% D₂ (top), 12% of the equilibrated Q₂ mixture with 88% He (middle) and 1% of the equilibrated Q₂ mixture with 99% He (bottom). Carrier gas is neon.

Fig. 5.5.4: Micro gas chromatograms of the Q₂ mixture of 51.8% H₂, 1.6% HD and 46.6% D₂ measured with Ne as carrier gas (top) and with Helium as carrier gas (bottom).

Fig. 5.6.1: Micro gas chromatograms of the Q₂ mixture of 29% H₂, 47% HD and 24% D₂ measured with Helium as carrier gas for various column head pressures.

Fig. 6.1.1: Main components of the micro gas chromatograph proposed as part of the Analytical System (ANS) for the ITER Tritium plant with connecting pipe work and indications of the next component.

Fig. 6.2.1: Main components of the special gas chromatograph proposed as part of the Analytical System (ANS) for the ITER Tritium plant with connecting pipe work and indications of the next component.

List of Tables

Table 3.1: The columns employed in GC1, GC2 and GC3.

Table 3.2: Bridge currents of the thermal conductivity detectors (TCD) and temperature of the filaments of the TCDs employed in GC1, GC2 and GC3.

Table 3.3: Carrier gas flows through the thermal conductivity detectors (TCDs) and helium ionisation detector (HeD-A), the purge flows through the Valco valves and supply pressure of these gases.

Table 3.4: Details (detectors and columns used, gas species and concentration ranges) of GC1, GC2 and GC3. Abbreviations: HeD: helium ionisation detector, TCD: thermal conductivity detector, IC: ionisation chamber, Col: column, Detec: detector.

Table 3.5: Information of the columns used in μ GC1 and μ GC2.

Table 4.1: Composition of the 2 vol% gas mixture in H₂: 0.98% O₂, 2.14% N₂, 1.97% CH₄, 2.00% CO, 2.04% CO₂, 90.87% H₂

Table 4.2: Hydrogen-tritium gas mixture: 1.7% H₂, 20.2% HD, 0.86% HT, 76.6 D₂, 0.49% DT, 0.15% T₂.

Table 4.3: Composition of the calibrated 1% hydrocarbon gas mixture in He: 1.01% CH₄, 0.99% C₂H₄, 0.98% C₃H₆, 1.99% C₂H₂, 1.96% 1-C₃H₄, 1.00% N-C₄H₁₀, 92.07% He.

Table 4.4: Composition of the calibrated 100 vpm gas mixture in He: 106 vpm CH₄, 106 vpm C₂H₆, 104 vpm C₃H₈, 103 vpm N-C₄H₁₀, 62.6 vpm CO, 53.6 vpm CO₂, 19.3 vpm N₂, balance He.

Table 4.5: Residual gas mixture after absorption of the hydrogen in a cold getter bed: 19 ppm HT, 12 ppm DT, 121 ppm T₂, 16.3 ppm CQ₄, 3.0 ppm CO₂, 0.52 ppm C₂Q₄, 1.36 ppm C₂Q₆, balance: ³He. Approximately 90% of Q in the hydrocarbons are tritiated.

Table 4.6: Composition of the gas mixture measured by means of GC1, GC2 and GC3: ⁴He (91.11%), ³He (3.58%), HD (0.75%), HT (0.41%), D₂ (1.47%), DT (1.71%), T₂ (0.53%), N₂ (0.027%), O₂ (0.002%), CO (0.051%), CO₂ (0.084%), CQ₄ (0.26%), C₂Q₆ (0.013%), C₃Q₈ (0.002%).

Table 4.7: Calibration factors for various compressed gas species and detectors in GC1

Table 4.8: Calibration factors for various compressed gas species and detectors in GC2

Table 5.1: Calibration factors for Micro GC1 for injection pressures of 0.1MPa

Table 5.2: Composition of the calibrated 80 ppm gas mixture in He:

76.9 ppm H₂, 79.0 ppm O₂, 81.1 ppm N₂, 81.5 ppm CH₄, 82.4 ppm CO, 80.6 ppm CO₂, balance He.

Table 5.3: Composition of the calibrated 100 ppm gas mixture in H₂:

19.3 ppm N₂, 106 ppm CH₄, 106 ppm C₂H₆, 104 ppm C₃H₈, 103 ppm C₄H₁₀, 62.6 ppm CO, 53.6 ppm CO₂, balance H₂.

Table 5.4: Composition of the calibrated 100 ppm gas mixture in He:

510 ppm H₂, 90 ppm N₂, 100 ppm CH₄, 100 ppm CO, balance He.

Table 5.5: Composition of the calibrated 2 vol% gas mixture in H₂:

0.98% O₂, 2.14% N₂, 1.97% CH₄, 2.00% CO, 2.04% CO₂, 90.87% H₂.

Table 5.6: Composition of the calibrated 1 vol% gas mixture in H₂:

5.09% He, 1.01% N₂, 0.990% CH₄, 0.987% CO, 1.00% CO₂, 0.964% C₂H₆, 1.04% C₃H₈, 88.919% H₂.

References

- /1.1/ R.-D. Penzhorn, N. Bekris, P. Coad, L. Dörr, M. Friedrich, M. Glugla, A. Haigh, R. Lässer, and A. Peacock: Status and Research Progress at the Tritium Laboratory Karlsruhe, *Fusion Eng.* **49-50**, 753-767 (2000).
- /1.2/ R. Lässer, C. Caldwell-Nichols, L. Dörr, M. Glugla, S. Grünhagen, K. Günther, R.-D. Penzhorn: Analytic of tritium-containing gaseous species at the Tritium Laboratory Karlsruhe, *Fus. Eng. Des.* **58-59**, 411-415 (2001).
- /1.3/ U. Engelmann, M. Glugla, R.-D. Penzhorn, H.J. Ache: *Nucl. Instru. & Methods* **A302**, 345 (1991).
- /1.4/ C.J. Caldwell-Nichols, R.-D. Penzhorn, S. Grünhagen, M. Sirch, J. George: Evaluation of an Omegatron mass spectrometer for use in the plasma exhaust processing of a fusion reactor, *Fus. Eng. Design* **58-59**, 395-399 (2001).
- /1.5/ C. Genty and R. Schott, Quantitative Analysis for the Isotopes of Hydrogen—H₂, HD, HT, D₂, DT and T₂—by Gas Chromatography, *Anal. Chem.* **42** (1970) 7-11.
- /1.6/ G.W. Weems, C.A. Hoffman and A.R. Howard, An Evaluation of a Porapak Q* Column at Cryogenic temperatures for the Separation of Helium-3, Neon, and Hydrogen in Helium-4, *J. Chromatographic Science* **9** (1971) 444-446.
- /1.7/ R. Lässer, M. Glugla, S. Grünhagen, K. Günther, R.-D. Penzhorn and J. Wendel: Use of gas chromatography in the Tritium Laboratory Karlsruhe, *Fusion Science and Technology* **41**, 515-519 (2002).
- /1.8/ S. O'hira, H. Nakamura, S. Konishi, T. Hayashi, K. Okuno, Y. Naruse, R.H. Sherman, D.J. Taylor, M.A. King, J.R. Bartlit and J.L. Anderson, On-line tritium Process Gas Analysis by Laser Raman Spectroscopy at TSTA, *Fusion Technology* **21** (1992) 465-470.
- /1.9/ U. Engelmann, Ramanspektroskopische und massenspektrometrische Untersuchungen der Wasserstoffisotope und isotope substituierter Methane, KfK Report **5116**, Kernforschungszentrum Karlsruhe, December 1992.
- /1.10/ S. O'hira and K. Okuno, Development of Real-time and Remote Fuel Process Gas Analysis System using Laser Raman Spectroscopy, *Fusion Technology* **30** (1996) 869-873.
- /1.11/ D.J. Taylor, M. Glugla, R.-D. Penzhorn: Enhanced Raman Sensitivity using an Actively Controlled External Resonator, *Rev. Sci. Instrum.* **72** (2001) 1970.
- /1.12/ J.A. Mason, N. Bainbridge and J.R. Stencel, Isothermal Calorimetry and Tritium Accountability, *Proc. 18th SOFT, Karlsruhe, Vol. 2* (1994) 1087-1090.
- /1.13/ J.L. Hemmerich, J.-C. Loos, A. Miller, P. Milverton: Advances in thermal derivative control and calorimetry, *Rev. Sci. Instrum.* **67** (1996) 3877-3884.
- /1.14/ M. Glugla, R. Kraemer, T.L. Le, K.H. Simon, K. Günther, J. Wendel and R.-D. Penzhorn, Results from Tritium Operation of the Clean-up Facility CAPRICE, *Proc. 19th SOFT, Lisbon, Fusion Technol. 1996, Vol 2* (1996) 1197-1200.
- /1.15/ M. Glugla, R. Lässer, T.L. Le, R.-D. Penzhorn and K.H. Simon, Experience gained during the Modification of the CAPRICE System to CAPER, *Proc. Of Fusion Engineering and Design, ISFNT-5, Rome, 1999*, to appear.
- /1.16/ R. Lässer, S. Grünhagen and Y. Kawamura: Use of micro gas chromatography in the fuel cycle of fusion reactors, to be published in *Proc. 22nd SOFT, Helsinki, Finland, 2002*.
- /1.17/ W.R. Moore, H.R. Ward: Gas-solid chromatography of H₂, HD and D₂, Isotopic separation and heats of adsorption on alumina, *J. Phys. Chem.* **64**, 832 (1960).

- /1.18/ E.H. Carter, H.A. Smith: The separation of hydrogen, hydrogen deuteride, tritium hydride, deuterium, tritium deuteride, and tritium mixtures by gas chromatography, *J. Phys. Chem.* **67** (1963) 1512.
- /1.19/ J. King: The chromatographic separation of the hydrogen isotopes including tritium, *J. Phys. Chem.* **67** (1963) 1397.
- /1.20/ M.L. Conti, M. Lesimple: Separation of hydrogen isotopes by gas-solid chromatography, *J. Chromatogr.* **29** (1967) 32.
- /1.21/ M. Saeki, T. Hirabayashi, Y. Aratono, T. Hasegawa, E. Tachikawa: Preparation of gas chromatographic column for separation of hydrogen isotopes and its application to analysis of commercially available tritium gas, *J. Nucl. Sci. Technol.* **20** (1983) 50.
- /1.22/ H. Weichselgartner, H. Frischmuth, J. Perchermeier, A. Stimmelmayer: Optimisation of a large-scale gas chromatograph for separation of tritium and DT from other H isotopes, *Nucl. Techn.Fusion* **4** (1983) 687.
- /1.23/ M. Tanase, M. Kato: Enrichment of tritium by a combined gas chromatography-isotopic decomposition process, *Int. J. Appl. Radiat. Isot.* **34** (1983) 687.
- /1.24/ T. Schober, C. Dieker: Gas-handling system of a gas chromatograph for the purity control of tritium gas, *Rev. Sci. Instrum.* **58** (1987) 1116.
- /1.25/ M. Tanase, K. Kurosawa, M. Fujie, H. Sugai, S. Okane, M. Kato: Radio-gas-chromatographic determination of chemical and isotopic purity of tritium gas in tritium production, *Fusion Technol* **14** (1988) 1090.
- /1.26/ R. Vogd, H. Ringel, H. Hackfort, T. Scober, C. dieker: Gas chromatographic separation of hydrogen isotopes on molecular sieves, *Fusion Technol.* **14** (1988) 574.
- /1.27/ C.H. Cheh: Development of a gas chromatographic system for hydrogen isotope separation, *Fusion Eng. Design* **10** (1989) 309.
- /1.28/ J. Wendel, H. Wertenbach, M. Glugla, R.-D. Penzhorn: Quantitative analysis of hydrogen isotopes with mordenite column at 173 K by radio gas chromatography, *Fusion Technol.* **28** (1995) 1090.
- /1.29/ R. Lässer, B. Grieveson, J.L. Hemmerich, R. Stagg, T. Dowhyluk, K. Torr, R. Massey and P. Chambers: The gas chromatographic analysis system in the JET active gas handling plant, *Rev. Sci. Instrum.* **64**, 2449-2458 (1993).
- /1.30/ R. Lässer, A.C. Bell, B. Grieveson, J.L. Hemmerich, R. Stagg and G.V. Atkins: The Analytical Gas Chromatographic System of the JET Active Gas Handling System - tritium Commissioning and use during DTE1, *Fus. Eng. Des.* **47**, 333-353 (1999).
- /1.31/ P. Schira, E. Hutter, G. Jourdan, R.D. Penzhorn, The Tritium Laboratory Karlsruhe: Laboratory design and equipment, *Fusion Eng. Des.* **18**, 19 (1991).
- /1.32/ R.S. Hansen, R.R Frost and J.A. Murphy, The Thermal Conductivity of Hydrogen-Helium Mixtures, *J. Phys. Chem.* **68** (1964) 2028-2029.
- /1.33/ R.-D. Penzhorn, U. Bernd, C. Caldwell-Nichols, S. Grünhagen, E. Kirste, R, Lässer and J. Wendel: Radiochemistry of an equimolar deuterium–tritium mixture or of T₂ with CO, *Fus. Eng. Des.* **49-50**, 927-937 (2000).
- /1.34/ Y. Kawamura, Y. Iwai, T. Yamanishi, S. Konishi and M. Nishi: Analysis of hydrogen isotopes with a micro gas chromatograph, *Fus. Eng. Design* 49-50 (2000) 855-861.
- /1.35/ Y. Kawamura, S Konishi and M. Nishi: Development of a micro gas chromatograph for the analysis of hydrogen isotope gas mixtures in the fusion fuel cycle, *Fus. Eng. Design* 58-59 (2001) 389-394.